ISSN 1063-7826, Semiconductors, 2007, Vol. 41, No. 7, pp. 745–783. © Pleiades Publishing, Ltd., 2007.
Original Russian Text © E.V. Kalinina, 2007, published in Fizika i Tekhnika Poluprovodnikov, 2007, Vol. 41, No. 7, pp. 769–805.

REVIEW

The Effect of Irradiation on the Properties of SiC and Devices Based on this Compound

E. V. Kalinina

Ioffe Physicotechnical Institute, Russian Academy of Sciences, Politekhnicheskaya ul. 26, St. Petersburg, 194021 Russia
e-mail: evk@pop.ioffe.rssi.ru

Submitted October 16, 2006; accepted for publication October 30, 2006

Abstract—Issues related to the production of radiation defects in silicon carbide of various polytypes and with differing conductivity types and concentrations of charge carriers as a result of irradiation with high-energy particles in a wide range of their energies and masses (from electrons to heavy Bi ions) are considered. The effect of irradiation with high-energy particles on the optical and electrical characteristics of the devices based on SiC are also considered, including the devices that operate as detectors of nuclear radiation. Systematic trends (common to other semiconductors and characteristic of SiC) in the radiation-defect formation in SiC are established. The high radiation resistance of SiC is verified; it is shown that this radiation resistance can be increased at increased energies of incident particles and at higher temperatures of operation.

PACS numbers: 61.72.Hh, 61.80.-x, 68.55.Ln, 71.55.Ht, 81.40.Wx

DOI: 10.1134/S1063782607070019

1. INTRODUCTION

Some aspects of the interaction of various types of nuclear radiation with solids with the aim of studying the solid's properties were considered even in the beginning of the previous century. The main directions of these studies consisted in investigation of the color of some minerals, salts [1, 2], and diamond [3], and also the phenomena of aging [4] and modification of the crystal lattice [5] under the effect of radiation of radioactive substances. The experimental data were used to form the basis for the theory of interaction of charged particles with a substance [2, 6].

The development of nuclear reactors and weapons gave rise to an increased interest in studies of the effect of corpuscular and γ-ray radiation on solids. Wigner noted as far back as in 1942 that high-energy neutrons and the fragments formed as a result of fission should be able to displace atoms from their equilibrium positions in the crystal lattice [7]. He stated that an intense bombardment of solids with high-energy heavy-mass particles can give rise to serious technological effects. These considerations led to the accomplishment of a large program of theoretical and experimental studies aimed at determining the origin and magnitude of the expected effects. As a result, the theory of formation of simple point defects (in particular, incorporated atoms and vacant sites in the lattice) as a result of bombardment with high-energy particles was established [8–14]. It became clear that the study of radiation effects can bring about a solution of some fundamental problems in solid-state physics, i.e., new important concepts about the properties of defects in solids and the relation of these defects to the physical and chemical properties of the material.

In the further development of the atomic industry, nuclear-energy engineering, and space technology, the development of radiation-resistant materials and electronic equipment that can operate under the effect of ionizing radiation was required. The issues concerned with the stability of materials' properties under the long-term effect of radiation on these materials and the necessity of indication and dosimetry of radiation types enhanced and expanded the range of studies of the effects of various types of radiation on the properties of solids and devices on their basis. It was determined in the course of these studies that irradiation with high-energy particles and photons brought about relatively stable variations in the electrical, optical, and luminescent properties of a semiconductor material. As a consequence, a new line of studies developed, i.e., the radiation technology of semiconductors; this technology uses various types of ionizing radiation in a wide range of energies and doses. The aim of these studies consisted in specified irradiation of the initial material and fabricated device structures for controlling the main parameters of the material and structures (radiation-caused compensation of the material, introduction of the radiative-recombination centers, and control of the lifetime of nonequilibrium charge carriers) [15, 16]. In order to fabricate the structures doped nonuniformly over the depth, ion-implantation doping was used; this doping provides an effective variation in the semiconductor properties over controlled depths and in local regions [17, 18].

In recent years, the problems of production of radiation-resistant electronic equipment has become increasingly urgent; this equipment includes detectors of high-energy particles, which can operate in extreme conditions, i.e., at high levels of radiation, elevated temperatures, and high chemical activity. These devices are necessary in outer-space electronics, in various nuclear-power installations, and in the control of waste nuclear fuel. In addition, for physical experiments planned to be performed at the next-generation accelerators at CERN (the large hadron collider (LHC) and its modernization, the superlarge hadron collider (SLHC)), devices that can provide a long-term dosimetric monitoring of the situation in the inner channels of nuclear installations are required [19]. Devices with the aforementioned set of characteristics are not produced anywhere in the world and cannot be fabricated on the basis of traditional semiconductor materials (Ge, Si, CdTe, GaAs). The most promising semiconductor for fabrication of the aforementioned devices is SiC, which is at present commercially produced in the form of wafers with the diameter as large as 3 inches. The wide band gap of SiC (2.83–3.23 eV, depending on the polytype) ensures that the corresponding devices can operate at temperatures as high as 900°C [20]. In addition, SiC features high chemical and mechanical strengths, and also high threshold energies for defect production (25–35 eV), which represents a prerequisite for high radiation resistance of a semiconductor [21, 22].

The first studies aimed at gaining insight into the effect of irradiation with neutrons [23, 24] and α particles [25, 26] on the characteristics of SiC and the devices based on this compound showed that it is promising to use this material in the fabrication of high-temperature radiation-resistant devices and detectors of high-energy particles. However, due to the low quality of the initial material, the experimental data on the defect production in this compound and the results of studying the electrical characteristics of SiC-based rectifiers after irradiation were contradictory. In recent years, significant progress has been attained in the growth of high-purity SiC epitaxial layers by the methods of chemical-vapor deposition (CVD) and sublimation selective epitaxy (SSE) with low concentrations of uncompensated donors ($\lesssim 10^{15}$ cm^{-3}) and defects ($\sim 10^{12}$ cm^{-3}) and relatively large values of the diffusion lengths ($L_p \approx 20$ μm) and the lifetimes of minority charge carriers ($\tau_p \approx 1$ μs) [27–29]. This has made it possible to study in more detail the processes of production of radiation defects in SiC [22, 30]. The demands for clarifying some of the basic issues of defect formation in SiC and for development of radiation-resistant electronic devices (including the nuclear-radiation detectors) requires a more intensive and in-depth study of the effect of various types of radiation on the structural, optical, and electrical characteristics of SiC and devices based on this material; this trend has been clearly pronounced in the last decade.

The aim of this review was to present the results of comprehensive studies of the effect of irradiation with various types of particles in a wide range of doses and energies on the structural and electrical properties of SiC in the form of crystals and high-purity epitaxial layers and on the characteristics of device structures based on this material. The results are discussed in the context of present-day notions of the physics of defect formation in multiple-component semiconductors. In Sections 2, 3, and 4 of this review, we consider the results of theoretical and experimental studies concerned with irradiation of various polytypes of SiC (3*C*, 4*H*, 6*H*, and 15*R*) of both the *n*-type and *p*-type of conductivity with slow and fast electrons, neutrons, and light and heavy ions (from H to Bi), respectively. In Section 5, the issues related to the effect of irradiation with various particles on the characteristics of electronic devices and nuclear-radiation detectors based on SiC are considered.

2. IRRADIATION WITH ELECTRONS

It is characteristic of irradiation with electrons that the resulting damage to the crystal lattice is comparatively slight and the chemical composition of the solid remains unchanged, in contrast to the effect of other high-energy particles. In addition, in the case of irradiation with electrons, the concentration of induced defect-related centers is low and is distributed with high uniformity over the sample's bulk, which makes the results of all types of measurements more reliable. As a consequence, irradiation with electrons with a wide range of energies and doses is actively used in the studies of radiation-induced defect formation in semiconductors.

Irradiation with electrons with energies in excess of 1 MeV gives rise to both simple point defects (vacancies, substitutional and interstitial atoms) and their complexes. In contrast, irradiation with electrons with low energies (<1 MeV) makes it possible to determine the configuration of defect-related centers and their behavior under the effect of various factors; it is also possible to determine the threshold energy for defect formation (E_d), i.e., the minimum energy that the particle must transfer to an atom in the semiconductor lattice in order to form a Frenkel defect (a pair consisting of a vacancy and an interstitial atom) [31].

2.1. Studies of the Microstructure

The most informative methods for studying the microstructure of defects and their identification are electron paramagnetic resonance (EPR), optical double magnetic resonance (ODMR), electron spin resonance (ESR), and magnetic circular dichroism of absorption (MCDA). The following methods are very sensitive to the vacancy-containing defects: positron annihilation spectroscopy (PAS); slow positron implantation spectroscopy (SPIS); Rutherford backscattering (RBS);

photoluminescence (PL), especially at low temperatures, ~1.7 K (LTPL); and cathodoluminescence.

2.1.1. Irradiation with high-energy electrons. In the first studies concerned with irradiation of SiC with high-energy electrons, the Lely crystals were used; these crystals exhibit high concentrations of both charge carriers and defects, which gave rise to appreciable discrepancies in the results obtained. However, according to the measurements by the EPR, ESR, and PAS methods, the main radiation defects in various SiC polytypes were isolated neutral silicon vacancies V_{Si} or negatively charged silicon vacancies V_{Si}^- and complexes with these vacancies [32–34]. In addition, the threshold dose for amorphization of SiC in the case of irradiation with electrons was found to be equal to 10^{22}–10^{23} cm^{-2} [35].[1]

The appearance of defects identified with neutral V_{Si} vacancies and complexes that include these vacancies was also observed later in spectral dependences of the ODMR signals and the ESR, PAS, PL, and Hall measurements in the case of irradiation of high-purity epitaxial layers of *n*-3*C*-, *n*-6*H*-, and *n*-4*H*-SiC ($N_d - N_a \lesssim 10^{16}$ cm^{-3}) with electrons with energies of 1–2.5 MeV and doses of 10^{17}–10^{18} cm^{-2} [36–38]. The positron lifetimes of ~190 and ~210 ns were attributed to the V_{Si} vacancy and defect complexes that involve this vacancy [39–42]. According to theoretical data [43], these complexes can be represented by divacancies. It was assumed that the defect-related complexes that involve the V_{Si} vacancy introduce deep levels into the SiC band gap. It was also noted that the intensity of PL spectra decreased sharply if the samples were irradiated with electrons with a dose higher than 10^{17} cm^{-2}, which was attributed to the appearance of nonradiative defect-related centers [44]. In the case of heat treatment of irradiated samples, a partial annealing of the V_{Si} vacancies was observed at 200°C, which was accounted for by capture of interstitial atoms by these vacancies [38]. The complete annealing of the V_{Si} vacancy centers was observed at the temperatures of 750–900°C, while the complexes involving these vacancies were annealed out at 1200–1400°C [40–42]. In addition, it was mentioned [44, 45] that charged vacancies V_{Si}^{2+} can be present; according to the theoretical data, the levels of these vacancies are located in the band gap near the valence-band top (Fig. 1) [44].

Subsequent studies using the PAS method showed that the temperature of annealing of radiation defects formed as a result of irradiation with electrons depends on the SiC polytype [46]. The CVD layers of the *n*-3*C*-, 4*H*-, and 6*H*-SiC polytypes were irradiated with electrons with energies of 0.5–2 MeV and doses of (3–6) × 10^{17} cm^{-2} and were then annealed at temperatures as high as 1700°C in vacuum or Ar atmosphere. Vacancies V_{Si} and some vacancy-containing complexes were revealed in all polytypes; however, the temperatures at which these complexes were annealed out were different for different polytypes. The annealing temperature increased as the degree of hexagonality of SiC increased (by 0% for 3*C*, 33% for 6*H*, and 50% for 4*H* polytypes) from 1000 to 1700°C, respectively (Fig. 2) [46]. The two-stage annealing of the V_{Si} vacancies at temperatures of 200 and in excess of 700°C observed for all polytypes was similar to that reported in [38] and was accounted for by recombination of a vacancy with an interstitial defect and for migration of the V_{Si} vacancies, respectively.

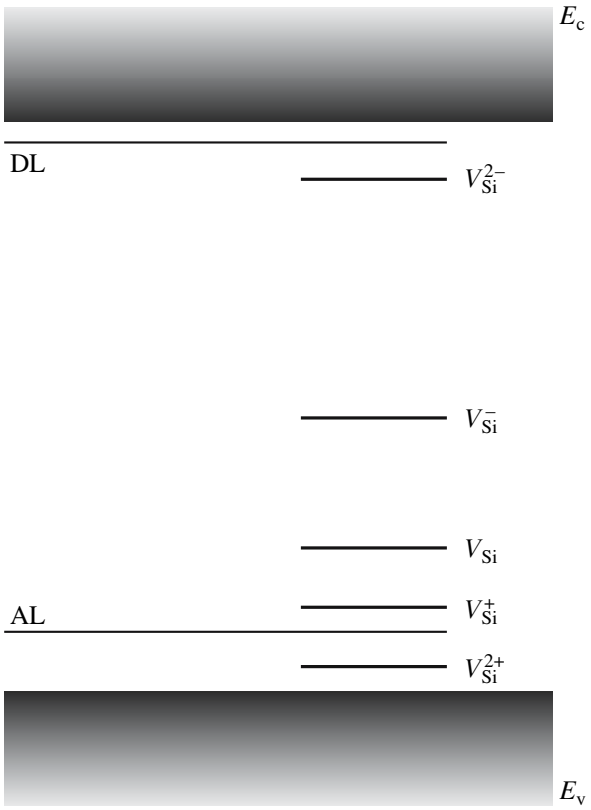

Fig. 1. Schematic representation of positions of the energy levels for silicon vacancies in the SiC band gap; these positions were confirmed by both theoretical calculations and experimental data. DL stands for donor level, and AL stands for acceptor level [44].

The effect of the electron dose on the characteristics of the radiation-defect centers was noted in the case of electron irradiation of *n*-6*H*-SiC epitaxial layers with $N_d - N_a = 1.4 \times 10^{16}$ cm^{-3} [47]. According to the PAS measurements, an increase in the radiation dose (to higher than 10^{19} cm^{-2}) gave rise to the V_{Si}–V_{Si} complex defects. The defects involving V_{Si} and identified with the V_{Si}–V_C divacancies or the V_{Si}–Si_C complexes were observed previously in the case of the ODMR measurements [48]. In addition, it was established that the amorphization dose decreases as the concentration of

[1] In what follows, the terms "dose" (for light incident particles) and "fluence" (for heavier particles) are considered as equivalent.

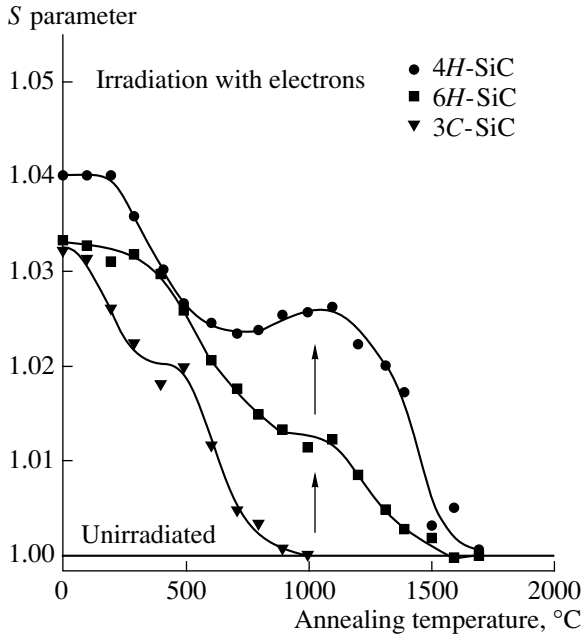

Fig. 2. Dependences of value of the *S* parameter (PAS) on the annealing temperature of the *n*-3*C*-, *n*-4*H*-, and *n*-6*H*-SiC samples irradiated with 2-MeV electrons with a dose of 3×10^{17} cm^{-2} [46].

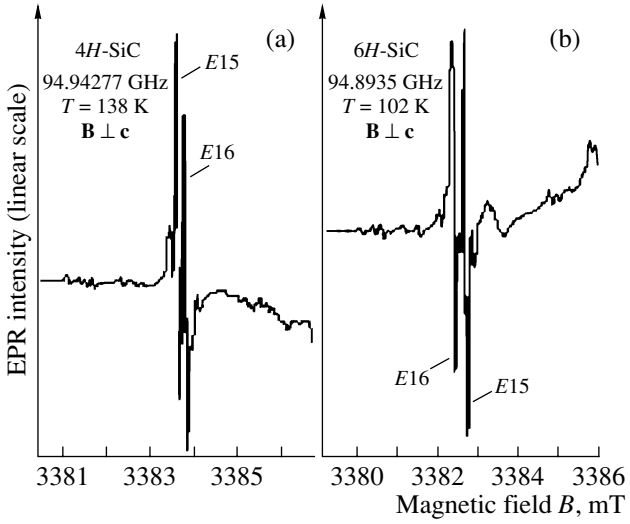

Fig. 3. The EPR spectra of the *E*15 and *E*16 defect-related centers; the spectra were measured for (a) *p*-4*H*- and (b) *p*-6*H*-SiC epitaxial layers irradiated with 2.5-MeV electrons [54].

impurity in the samples is decreased [47]. In the case of $N_d - N_a = 1.4 \times 10^{16}$ cm^{-3}, the above dose was 1.8×10^{19} cm^{-2} and, according to the data of X-ray diffractometry, an increase in the SiC lattice parameters *a* and *c* (expansion) was observed by the relative values of 6.4×10^{-5} and 6.9×10^{-5}, respectively.

The appearance and temperature-related behavior of carbon vacancies in the case of irradiation of SiC with fast electrons was studied mainly in the *p*-type samples. In the case of irradiation of *p*-3*C*-, *p*-4*H*-, and *p*-6*H*-SiC ($N_a - N_d = 10^{16}$–10^{17} cm^{-3}) with electrons with the energies of 1–3 MeV and doses of 10^{18} cm^{-2}, positively charged V_C^+ vacancies (the *T*5 centers) were detected by the ESR, PAS, EPR, and PL methods [37, 49–51]. These V_C^+ defects with the positron lifetime of ~153 ns were annealed out at temperatures of 150–200°C, whereas the silicon vacancies V_{Si} were stable at temperatures as high as 750°C [50, 51]. It is also worth noting that the complexes including the V_{Si} vacancies were also more stable (the annealing temperature of ~1200°C) than the V_C vacancies whose annealing temperature is 400°C [52].

Irradiation of *p*-4*H*-SiC and *p*-6*H*-SiC with electrons at elevated temperatures (~400°C), in which case the carbon vacancies become the most mobile species, made it possible to use the high-frequency (~95 GHz) EPR measurements to reveal the various defect-related centers *E*11–*E*16 [53–56]. These centers were identified as follows: *E*11 is identified with the V_C–H complex; *E*12 is identified with the V_{Si} vacancy; *E*13 is identified with the V_C–2H complex; *E*14 is identified with the $V_C^+ - V_C^+$ complex; *E*15 is identified with the V_C^+ vacancy (the *T*5 center); and *E*16 is identified with the Si_C^+ center (Fig. 3). It was also found that relaxation of the *E*16 center depends heavily on temperature and that this center can be a donor in *p*-SiC; i.e., the *E*16 center can act as a compensating defect in obtaining semi-insulating SiC. The position of the V_C^+ defect was determined on the hexagonal and quasi-cubic sides of the SiC sublattice [57–59]. Measurements of the EPR conducted at 4–300 K and at the orientations of the magnetic field parallel to the crystallographic planes (1120), $(1\bar{1}00)$, and (0001) in SiC revealed three nonequivalent positions of the V_C^+ defect in the SiC lattice [60]. One of these positions (K_y3) is located at the hexagonal side and two other defects (K_y1 and K_y2) are located at the quasi-cubic side.

The use of photo-EPR measurements in the studies of *p*-4*H*-SiC irradiated with 2.5-MeV electrons with a dose of 2×10^{18} cm^{-2} with subsequent heat treatment at temperature as high as 1600°C made it possible to reveal both previously observed defects V_C^+ and Si_C^+ and new defect-related centers [61]. The center with the energy $E > 1.15$ eV that was observed previously in *n*-6*H*-SiC and is referred to as the *P*6/*P*7 [62] center was identified with a thermally stable V_C–C_{Si} pair whose appearance is accounted for by a transformation of the V_{Si} vacancy at temperatures of 600–800°C. The donor-type defect with the energy level at $E_v + 1.47$ eV was associated with complexes that included the

V_{Si} vacancy [63]. The appearance of the vacancy-type defect complexes V_C–C_{Si} and V_{Si}–Si_C was theoretically predicted in [43, 64]. It was concluded that the stable V_C–C_{Si} defect most likely manifests itself in *p*-SiC samples, while the complexes with the V_{Si} vacancy appear with a higher probability in the *n*-SiC samples.

The effect of the quality of the initial material on the radiation-defect formation in the *n*-4*H*-SiC and 6*H*-SiC samples irradiated with 2.2-MeV electrons with a dose of 7×10^{16} cm^{-2} was studied using the EPR and PAS methods [65]. It was shown that the number of the V_{Si} and V_C vacancies and also the number of vacancy-containing complexes formed as a result of irradiation are independent of the nitrogen concentration and the number of vacancies and vacancy-containing clusters in the initial samples. It was shown when studying the temperature behavior of radiation defects in irradiated samples in the course of isochronous annealing at temperatures as high as 1450°C that the V_{Si} vacancies transform into the V_C–C_{Si} defect complexes with a lower mobility at a temperature close to 1000°C, which is consistent with the data reported in [61, 33]. In the temperature range of 1200–1400°C, the V_{Si} vacancies, which are more mobile than the defect complexes, migrated and temporarily formed divacancies; the latter were then trapped by vacancy-containing clusters that were present in the initial samples [66, 67].

The origin of radiation defects in the *n*-6*H*-SiC samples irradiated with 2.5-MeV electrons with a dose of 1.6×10^{18} cm^{-2} and then annealed at temperatures as high as 1200°C was studied in more detail using a combination of methods: EPR, MCDA, and LT PL [68]. In consistency with the aforementioned results [38], the V_C^+ and V_{Si} defects are annealed out partially at 150–300°C and completely at 600–750°C. Annealing of the V_{Si} vacancy center was accompanied by the appearance of the V_C–C_{Si} defect complex even after annealing at 150°C; this complex was annealed out at temperatures of 900–1050°C. The process of formation of the V_C–C_{Si} complex was envisaged as a result of transition of a C atom to the V_C vacancy, which is consistent with previous assumptions [62]. The energy barrier for transformation of V_{Si} into the V_C–C_{Si} complex is lower for a *p*-type sample and was determined theoretically as equal to ~2.2 eV [69]. New defect-related centers were observed after heat treatment at temperatures higher than 750°C; these centers were hypothetically identified with cluster complexes that involve antisite defects, i.e., $V_CC_{Si}(Si_CC_{Si})$ or $V_CC_{Si}(Si_C$–$C_{Si})$ [70]. At temperatures higher than 900°C, these complexes disappeared and gave rise to new V_{Si} vacancies. It was noticed that the disappearance of the defect complexes was accompanied by an increase in the concentration of the well-known D_1 defects (the peak at 2.6 eV in the LT PL spectra) [71]. The temperature-related behavior of the defect complexes suggested that the so-called D_1 PL has its origin in a complex with antisite defects (Si_CC_{Si})

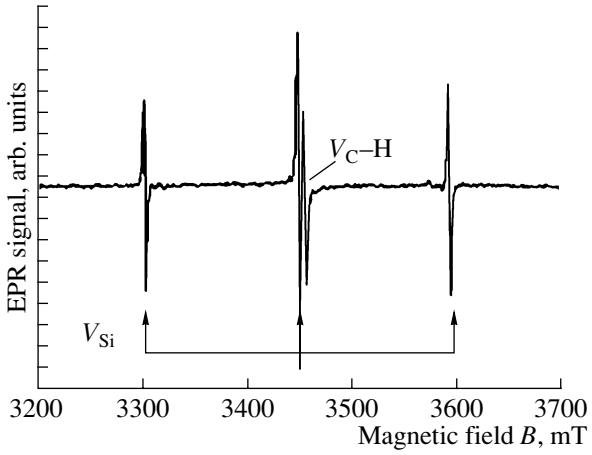

Fig. 4. The EPR spectrum measured at 300 K for the *n*-6*H*-SiC crystals irradiated with 300-keV electrons with the doses of 5×10^{17}–10^{18} cm^{-2} [78].

[72]. The appearance of clusters with antisite defects was predicted theoretically in [73] and was attributed to an increased mobility of a substitutional atom C in comparison with the mobility of a Si atom. It is noteworthy that the diversity of charge states of vacancies, as observed experimentally in SiC by many researchers, was explained theoretically in [74], where the main spin states that correspond to the centers under consideration are considered.

2.1.2. Irradiation with low-energy electrons. Irradiation with low-energy electrons made it possible to reveal an additional diversity of configurations and charge states of radiation defects. For example, production of the Frenkel pairs in the form of V_{Si}^-–Si_i and V_{Si}^{3-}–Si_i was observed in the EPR measurements (at 4–300 K) of the 3*C*-, 4*H*-, and 6*H*-SiC crystals of the *n*- and *p*-type conductivity after irradiation with electrons with energies of 300–900 keV and doses of 5×10^{17}–3×10^{19} cm^{-2} [75, 78]. However, the other defect-related centers in the samples with one conductivity type differed from those in the samples with the other conductivity type. In all samples with the *n*-type conductivity, the centers containing the negatively charged V_{Si}^{3-} and V_{Si}^{2-} vacancies and also the V_C–H complexes were detected [78] (Fig. 4). It was assumed [78] that the V_{Si}^{3-} and V_{Si}^{2-} vacancies introduce levels into the band gap that are close to the conduction band, which is consistent with the data reported in [44]. The presence of the V_C^+ vacancies and V_C–2H complexes was detected in irradiated *p*-SiC samples [75, 78]. It is worth noting that hydrogen was actively involved in the defect formation, which was attributed to a high concentration of H atoms that are mobile at room temperature. The appearance of interstitial hydrogen atoms and related vacancy-containing complexes was predicted theoreti-

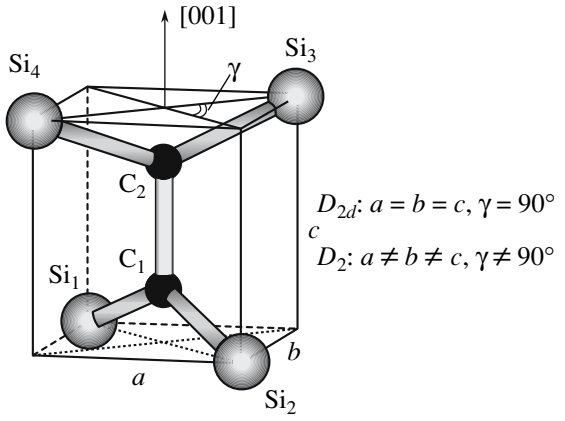

Fig. 5. A model of a dumbbell-like configuration of a split interstitial C–C in 3*C*-SiC located on the side of the carbon sublattice [85, 86].

cally [79] for 3*C*-SiC with the *n*- and *p*-type of conductivity. It was assumed [79] that an interstitial H atom is a shallow-level donor in *p*-SiC and compensates acceptors. The energy of formation of interstitial H_2 is high in *n*-SiC; therefore, H forms the complexes V_{Si}–H and V_C–H that act as traps for electrons and holes, respectively.

The dependence of the radiation-defect formation on the energy of incident electrons in the range of 0.3–2.5 MeV for the crystals and epitaxial layers of 3*C*- and 6*H*-SiC with the *n*-type and *p*-type of conductivity was studied in [77, 80–82]. The results of the PAS measurements showed that the lowest electron energy ($\gtrsim$300 keV) is required for the formation of V_C vacancies with the positron lifetime of $\lesssim$160 ns. An increase in the energy of incident electrons gave rise to silicon vacancies in various charge states (V_{Si}, V_{Si}^{-}, V_{Si}^{2-}, and V_{Si}^{3-}) and then to defect-related centers, presumably in the form of divacancies (V_{Si}–V_{Si} or V_C–V_{Si}). It was concluded that, irrespective of the polytype and conductivity type of SiC, an increase in the energy of incident electrons brings about a diversity in the types of radiation defects and also an increase in their concentrations and in the sizes of defects with involvement of vacancies. However, in this case, the thermal stability of vacancy-related centers depended on the conductivity type of SiC [83]. It was noted that the vacancy-related defect centers in the *p*-SiC samples were annealed out at lower temperatures (~700°C) compared to the annealing of similar defects in the *n*-SiC samples (at 850°C).

Irradiation of SiC with low-energy electrons also makes it possible to study the models of interstitial defects, the mobility of these defects, and their interrelation with other defects and atoms. For example, irradiation of the 3*C*-, 4*H*-, 6*H*-, and 15*R*-SiC epitaxial layers with the *n*- and *p*-type conductivity with electrons (with energies of 90–300 keV) in a transmission electron microscope (TEM) made it possible to identify the defect-related center D_1 detected previously in the 3*C*, 4*H*, and 6*H* polytypes of SiC [71, 84]. The samples were enriched with the ^{13}C isotope, which made it possible to use the LT PL measurements (at 7 K) to identify the observed optical centers with dumbbell-like split interstitial atoms C–C (Fig. 5) [85, 86]. These centers were formed of interstitial carbon atoms in the samples irradiated with electrons with an energy lower than 150 keV. Theoretical calculations showed that the centers with this configuration have the lowest (second only to the carbon vacancy [87–89]) formation energy. However, for the 4*H*-SiC polytype and the same energy of incident electrons, an unsplit interstitial center of only a single type observed; as a result, it was concluded that the polytype under consideration is more resistant to radiation than the 6*H*-SiC polytype. If the energy of incident electrons exceeded 150 keV, another center was observed in all polytypes; this center was presumably identified either with a C–Si complex with the dumbbell-like configuration or with the split (C–C)C interstitial on the carbon side in the neutral state for the *n*-4*H*-SiC compound [90].

The most important parameter in the estimation of the radiation resistance of a semiconductor material is the value of the energy required for displacement of an atom from its crystal-lattice site, i.e., the threshold defect-formation energy (E_d). Irradiation of a material with low-energy electrons represents one of the most effective methods for determination of the value of E_d. The theoretical values of the energy E_d in SiC reported in various publications differed only slightly and were either equal to 27.5 eV for both the Si and C atoms [91] or equal to 24 and 35 eV [92] (20 and 30–35 eV [93, 94]) for the C and Si atoms, respectively. In addition, an anisotropy of these quantities was considered as in the case of other semiconductors irradiated with high-energy particles [95].

The above values of E_d were smallest for the C atoms displaced in the $[1\bar{1}00]$ direction and Si atoms displaced in the $[000\bar{1}]$ direction [92].

The threshold displacement energies E_d were determined in the case of irradiation of the *n*-6*H*-SiC crystals with TEM electrons with the energies of 200 and 300 keV and with simultaneous analysis of the diffraction patterns [96]; these energies were found to be equal to ~18 and ~43 eV for the C and Si atoms, respectively. It was also found that the displacement energy of a Si atom is higher in the 3*C*-SiC polytype than in the 6*H*-SiC polytype [77]. The values of the threshold displacement energy E_d for the C and Si atoms, equal to ~20 and ~30 eV, were recommended for calculations of the damage level (dpa, displacements per atom) observed in SiC subjected to irradiation [97].

An anisotropy of the threshold displacement energy E_d in SiC was verified experimentally [98] in

the case of irradiation of the 4*H*- and 6*H*-SiC samples of the *n*- and *p*-type conductivity with low-energy electrons. According to the PL data, a significant anisotropy is observed for the values of E_d in the [0001] and [000$\bar{1}$] directions; the smallest values were 20 and 24 eV for the C and Si atoms, respectively.

In the case of irradiation of semiconductors with low-energy electrons, it also becomes possible to determine precisely the incident-electron energy required for the formation of vacancies. This energy was determined in the case of irradiation of the high-purity 4*H*- and 6*H*-SiC crystals and epitaxial layers of the *n*- and *p*-type conductivity in a TEM with electrons with the energies of 50–300 keV in a wide range of doses (10^{16}–10^{20} cm^{-2}) [98–100]. The carbon atoms were displaced at the electron energies higher than 90 keV; a certain spread in this value, depending on the direction of the electron-beam incidence ((0001) or (000$\bar{1}$)) was observed [98]. In order to displace the Si atoms and for the V_{Si} vacancies to appear, irradiation with electrons with energies of 200–300 keV was required. In this case, the Si atoms were displaced irrespective of the electron-beam direction in relation to the crystallographic axes in the samples.

2.2. Studies of Electrical Properties of the Samples Irradiated with Electrons

Diverse centers related to radiation defects formed as a result of irradiation with electrons introduce a wide variety of energy levels into the SiC band gap; the parameters of these levels are determined most easily from the capacitance and current deep-level transient spectroscopies (*C*-DLTS and *I*-DLTS).

The results of studying the deep-level centers that appeared in the *n*-6*H*-SiC crystals and in epitaxial layers and p^+–*n* junctions based on these crystals with the concentrations of uncompensated donors 5×10^{14}–8×10^{17} cm^{-3} as a result of irradiation with electrons in a wide range of doses (5×10^{13}–10^{18} cm^{-2}) with energies of 1.5–5 MeV are reported in [39, 101–106]. The temperature-related behavior of the deep-level centers was studied in relation to annealing of the irradiated samples at temperatures as high as 1600–1700°C. According to the data obtained, more than ten radiation-induced levels were detected in the energy range of 0.15–1.65 eV from the conduction-band bottom in 6*H*-SiC. The most characteristic were the levels with the ionization energies of 0.18, 0.38/0.44, 0.51, 0.68/0.70, 1.15/1.25, and 1.5 eV (measured from the conduction-band bottom E_c); the corresponding centers were considered as the traps for holes (Fig. 6) [106]. The center with E_c – 0.38/0.4 eV (ED_3 in Fig. 6), known as the E_1/E_2 center [102], was thermally stable and annealed out at a temperature of 1600°C [106]. The origin of this center was assumed as related to a divacancy (V_C–V_{Si}) or to a complex containing the V_{Si} vacancies

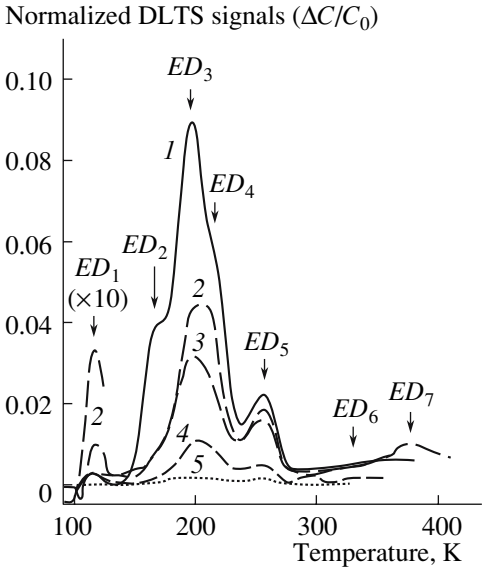

Fig. 6. A normalized DLTS spectrum of an *n*-6*H*-SiC sample irradiated with 1.7-MeV electrons with the dose D = (*1*) 9.04×10^{15}, (*2*) 4.52×10^{15}, (*3*) 3.38×10^{15}, (*4*) 1.13×10^{15}, and (*5*) 2.26×10^{14} cm^{-2} [106].

[39]. According to another approach, the center with the level at E_c – 0.38/0.4 eV is considered as a system of two negatively charged *U* centers, each of which introduces two levels into the band gap (an acceptor level and a donor level) [105]. In accordance with this concept, the level with energy E_c – 0.38 eV is considered as an acceptor level, while the level at E_c – 0.44 eV is considered as a donor level. The center with the level at E_c – 0.5 eV has a temperature-independent cross section for capture of charge carriers (2×10^{-15} cm^2), is thermally unstable (disappears as a result of heating to 250°C), and is identified with either the V_C^+ vacancy or the vacancy–impurity complex [101, 106]. The deep center with the level at E_c – (0.68–0.71) eV is identified with the well-known Z_1/Z_2 center [102, 103]. The deep centers with the levels at E_c – (1.15–1.25) eV and E_c – 1.5 eV, detected in high-temperature measurements, are hypothetically identified with structural defects in the form of complexes that involve vacancies [101].

Special features of the radiation-induced defect formation in the case of irradiation with electrons in relation to the SiC polytype were considered in publications [107–116], where the experimental data obtained for the *n*-4*H*-SiC polytype were compared with the known results for the *n*-6*H*-SiC polytype. The *n*-4*H*-SiC epitaxial layers with concentrations $N_d - N_a$ = 2×10^{14}–2×10^{16} cm^{-3} and p^+–*n* junctions based on these layers were irradiated with electrons with energies of 0.2–15 MeV and doses of 5×10^{13}–10^{17} cm^{-2}. In some of the studies, the samples were annealed at temperatures as high as 900–2000°C after irradiation [107, 110, 116]. The deep-level transient spectroscopy

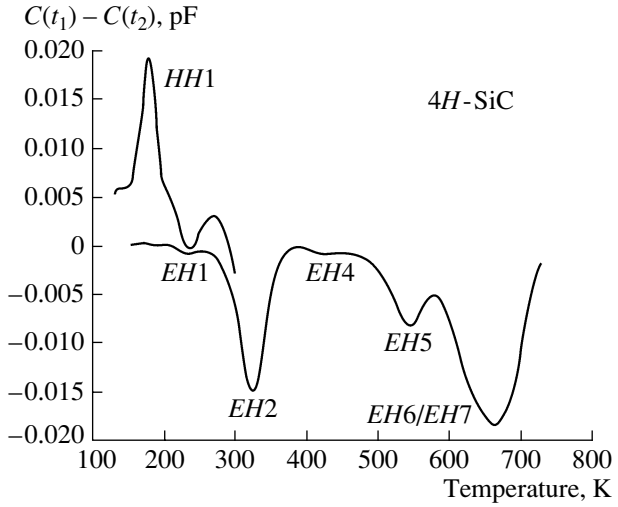

Fig. 7. The DLTS spectrum for a 4*H*-SiC sample irradiated with 2.5-MeV electrons with a dose of 2.5×10^{14} cm^{-2} [107].

(DLTS) was used to obtain a wide variety of acceptor-type centers that were similar to those observed in *n*-6*H*-SiC and featured the energy levels at 0.39, 0.45, 0.5, 0.68/0.7, and 1.13 eV below the conduction-band bottom (Fig. 7). The center with the level $E_c - 0.39$ eV (the E_1/E_2 center) is thermally unstable in *n*-4*H*-SiC (in contrast to what takes place in *n*-6*H*-SiC) and anneals out at temperatures of 360–400 K. This center was identified with the C_i interstitial defect in *n*-4*H*-SiC; this defect was annealed out at a temperature of 400 K [114]. The Z_1/Z_2 center with the level at $E_c - 0.68/0.7$ eV exhibits relatively large values of the cross section for the electron capture (1.3×10^{-14}–1.3×10^{-13} cm^2) and is thermally stable. These centers partially anneal out at a temperature of 1300°C; however, the presence of this defect with concentration amounting to 25% of the initial value was detected even after annealing at 2000°C. It was concluded that the defect under consideration is formed as a result of diffusion of simple defects, in particular, vacancies V_{Si}, substitutional atoms Si_C and C_{Si}, or complexes involving these defects [107, 110, 116]. However, Castaldini et al. [114] noted a low thermal stability of the Z_1/Z_2 center. It was annealed out at anomalously low temperatures (400–470 K) and was considered as either an intrinsic defect or a complex involving an intrinsic defect and the N or H atoms [111–114]. These data verify the previously noted activity of the H atoms in the formation of radiation defects [75, 78, 79]. According to another version, the Z_1/Z_2 center with the level at $E_c - 0.68/0.7$ eV is considered as a system of two negatively charged *U* centers [108] in analogy with the center with the level at $E_c - 0.38/0.4$ eV in *n*-6*H*-SiC [105]. It was concluded that these negative *U* centers had the same structure in *n*-4*H*-SiC and *n*-6*H*-SiC since they exhibit many common properties; in particular, these centers are annealed out at temperatures of $\gtrsim$1400°C. The new defects observed in *n*-4*H*-SiC were those with the level at $E_v + 0.35$ eV; these defects were considered as traps for holes and appeared after heat treatment at temperatures of 350–400°C. The new defects also included the acceptor center with the level at $E_c - 1.65$ eV (the *HH*1 and *EH*6/*EH*7 features in Fig. 7) [107, 116]. The *EH*6/*EH*7 center, with a comparatively large cross section for capture of electrons (~10^{-13} cm^2) irrespective of temperature, is thermally stable, is annealed out at a temperature of ~2000°C, and was attributed to the presence of V_C vacancies or structural defects of a complex type.

The dependence of the radiation-induced defect formation on the conductivity type was studied using the *p*-6*H*-SiC epitaxial layers with $N_a - N_d = 6.6 \times 10^{18}$ cm^{-3}; the layers were irradiated with 1.7-MeV electrons with the doses of 2.26×10^{14} cm^{-2} and 1.13×10^{15} cm^{-2} [117]. Two new deep centers with the levels located at $E_v + 0.55$ eV (*H*2) and $E_v + 0.78$ eV (*H*2) were detected; these centers were annealed out at the temperatures of 500 and 200°C, respectively. The cross sections for the capture of holes were equal to 1.23×10^{-11} cm^2 and 1.35×10^{-13} cm^2 for the *H*1 and *H*2 centers, respectively. These centers are of the donor type. Taking into account their different temperature-related behavior, it was concluded that these centers are related to two different defects of unknown origin. According to the EPR and ESR measurements for the *p*-6*H*-SiC and 4*H*-SiC samples, these centers can be identified with the V_C^+ vacancies and complexes that involve these vacancies [50–52].

The common result of the above studies presumably consists in the fact that, irrespective of the polytype and the conductivity type, the appearance of all defects in SiC does not require an additional heating of the samples after irradiation with electrons. An increase in the dose of incident electrons brings about an increase in the radiation-defect concentration until this concentration levels off, and also a decrease in the rate of accumulation of the defect-related centers, which is also characteristic of other semiconductors irradiated with high-energy particles [15]. The increase in the concentration of radiation defects is accompanied by a broadening of the DLTS spectra, which suggests that the energy bands of defects are formed within the SiC band gap. The centers with the levels located in the vicinity of the conduction-band bottom do not affect to any significant extent the degree of compensation of the doping impurity, which manifests itself in the capacitance–voltage (*C*–*V*) characteristics. It is established that the highest level of thermal stability is represented by the defect-related centers E_1/E_2 (with the level at $E_c - 0.4$ eV) in 6*H*-SiC, and also the Z_1/Z_2 centers (with the level at $E_c - 0.6/0.7$ eV) and the *EH*6/7 centers (with the level at $E_c - 1.5/1.6$ eV) in 4*H*-SiC with large cross sections for the capture of charge carriers (these cross sections are temperature-independent).

3. IRRADIATION WITH NEUTRONS

Since fission neutrons with a broad spectrum of energies from 0 to 15 MeV (with a mean energy of 2 MeV) can penetrate deep into matter, the distribution of the formed radiation defects is uniform over the sample's bulk [118]. This circumstance ensures the fact that the results of studying the radiation-defect formation in the case of irradiation of SiC with neutrons are exact and reliable. The interest in studying the effect of irradiation with neutrons on the structural properties of SiC increased after it was reported that nuclear transmutational doping of this compound with phosphorus ^{31}P (from the ^{30}Si atoms) can be attained using irradiation of this semiconductor with thermal neutrons [119]. However, the transmutational doping in the case of irradiation with nuclear neutrons is always accompanied by the appearance of radiation defects.

Previously, the DLTS, ESR, EPR, and the electron and nuclear double resonance (ENDOR) data on the characteristics of radiation-defect centers were obtained as a result of irradiation with reactor neutrons of the SiC crystals and epitaxial layers of the 3*C*, 4*H*, 6*H*, and 15*R* polytypes with the concentration of the majority charge carriers of $\gtrsim 10^{16}$ cm^{-3} [120–122]. Some of these centers were identified with vacancies in different charge states (V_{Si} and V_{Si}^{-}) [121, 122]. It was found that approximately 90% of the defects are annealed out at a temperature of 350°C [120] in the course of annealing of radiation defects formed as a result of irradiation of 3*C*-SiC diodes. This has made it possible to conclude that SiC-based devices can operate at elevated temperatures when exposed to radiation. In the case of irradiation of the *n*-6*H*-SiC and 15*R*-SiC crystals with reactor neutrons with high fluences (>10^{20} cm^{-2}), the threshold radiation dose (~10^{21} cm^{-2}) that gives rise to amorphization was determined [123].

An improvement in the structural quality of SiC made it possible to increase the number of observed radiation defects appearing as a result of irradiation with neutrons, and also to study the dependences of these defects on the characteristics of the initial material. For example, in the case of irradiation of the *n*- and *p*-4*H*- and 6*H*-SiC crystals with neutrons with the energy of >0.1 MeV and the fluence of 6×10^{16} cm^{-2}, studies using the ESR method at 77 K revealed a broad spectrum of defect-related centers in various charge states [52, 124]. The temperature-related behavior of radiation defects was studied in the temperature range of 100–1500°C. The defect-related centers *K*1–*K*6 and *K*11–*K*14 were observed; these centers were annealed out at different temperatures and were identified with various defect configurations. The centers annealed out at temperatures of 800°C (*K*1 and *K*2) were identified with the V_{Si}^{-} vacancy and the V_{Si}–V_{Si} divacancy, respectively (Fig. 8). The *K*3 center was stable at temperatures as high as 200°C, like the defect observed in *n*-6*H*-SiC irradiated with electrons; this defect was associated

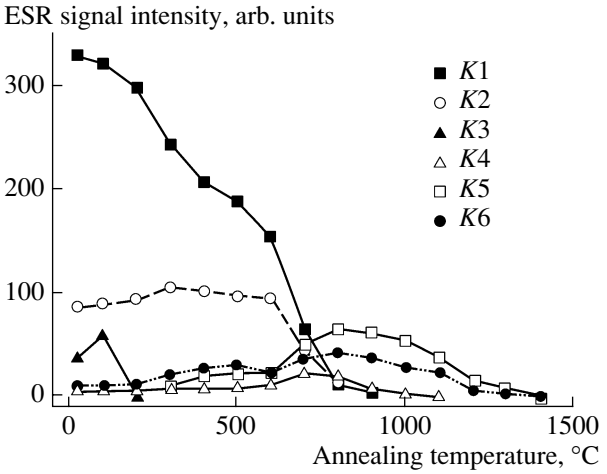

Fig. 8. The ESR spectra of the *K*1–*K*6 defect-related centers at various annealing temperatures; the spectra were measured for the *n*-6*H*-SiC samples irradiated with neutrons with energies higher than 0.1 MeV and with the fluence of 6×10^{16} cm^{-2} [124].

with recombinations of vacancies [38]. The thermally stable *K*4–*K*6 centers appeared after annealing of the *K*1 and *K*2 centers at 800°C and were annealed out at temperatures higher than 1300°C. The temperature-related behavior of these centers as their concentration increased in the temperature range of 800–1300°C was attributed [52] to interaction of impurities with the V_{Si} vacancies in the defect complexes. One of these complexes can be the center with the $(V_C–C_{Si})^{2+}$ structure; this center appeared after annealing of the V_{Si} vacancies at a temperature of 600°C, according to the data of MCDA and MCDA–EPR obtained at 1.5 K [68, 125]. This defect was denoted as the *P*6/*P*7 center in the case of irradiation with electrons [62]. The *K*11 and *K*12 centers that are stable at temperatures as high as 300–400°C were identified with the V_C vacancies, while the centers *K*13 and *K*14 that are thermally stable at temperatures as high as 1200°C were thought of as complex defect centers. It was concluded that the energy positions and temperature-related behavior of all defects in SiC are identical for the samples irradiated with both electrons and neutrons. A study of the EPR spectra showed that the concentrations of these defects increased in proportion to the radiation dose, while the positions of their energy levels were pinned in the vicinity of the midgap [126].

An increase in the fluence of incident neutrons to 10^{20}–10^{21} cm^{-2} brought about not only an increase in the concentrations but also the fact that the defects became more complex and larger. The centers with deep energy levels and the annealing temperatures of 1500–2000°C were revealed as a result of EPR measurements of the *n*-6*H*-SiC crystals irradiated with neutrons. These centers were considered first as the multiple-vacancy V_{Si}–$3V_C$ or V_C–$4V_{Si}$ clusters [127] and later

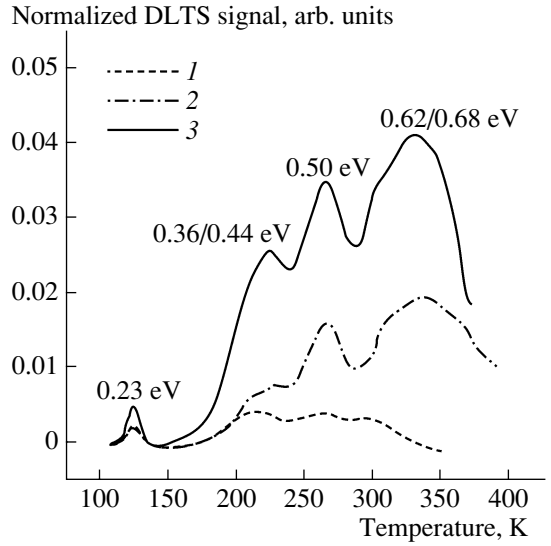

Fig. 9. Normalized DLTS spectra of the centers observed in *n*-6*H*-SiC after irradiation with neutrons with the fluences of (*1*) 5×10^{13}, (*2*) 2.5×10^{14}, and (*3*) 1.0×10^{15} cm^{-2} [130].

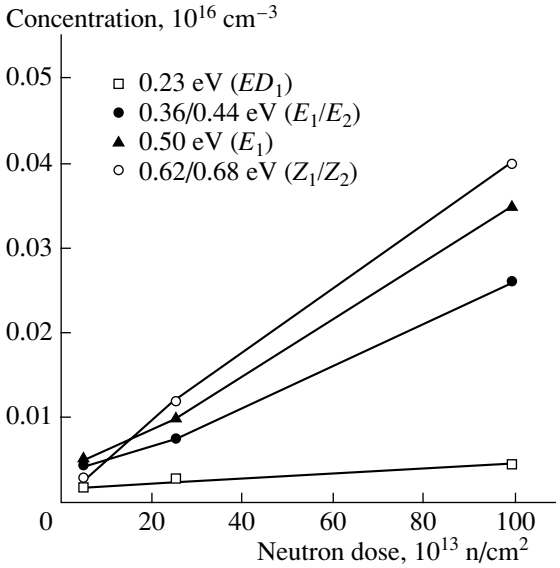

Fig. 10. Concentrations of deep-level centers in relation to the dose of irradiation of epitaxial CVD *n*-6*H*-SiC layers with neutrons [130].

as the V_{Si}–V_C divacancies and the V_{Si}–$3V_C$ and $(C_2)_{Si}$ complexes, or the $(C_2)_{Si}$–Si_C and V_{Si}–C_N pairs [128]. It was assumed that some of these centers introduce deep levels into the band gap; these levels were previously related to the so-called D_I and D_{II} defects that were identified with the V_{Si}–V_C divacancies and the interstitial carbon center $2C_i$ [71, 129].

The structural diversity of radiation defects introduced in the case of irradiation with neutrons gives rise to a broad spectrum of deep levels in the SiC band gap. According to the DLTS measurements, there are defects with the activation energies of 0.23, 0.31/0.44, 0.5, and 0.62/0.68 eV measured from the conduction-band bottom in *n*-6*H*-SiC irradiated with neutrons with the fluences of 5.1×10^{13}–10^{15} cm^{-2} (Fig. 9) [130]. All the levels were of the acceptor type and were associated with the ED_1, E_1/E_2, E_i (RD_5), and Z_1/Z_2 centers, respectively; these centers were identified in the case of irradiation of *n*-6*H*-SiC with electrons [102, 106]. The dominant center was the Z_1/Z_2 center with the energy level at E_c – 0.62/0.68 eV; this center is always present in SiC after irradiation with electrons and is of the acceptor type (the D_1 center) [71, 102, 103]. This center was annealed out at 900°C and its nature was related to either the V_{Si} vacancies or the defect complexes $(Si_CC_{Si})_2$ [102]. The centers with the levels E_c – 0.23 eV and E_c – 0.5 eV were annealed out at a temperature of 350°C and their structure was identified with that of the V_C vacancies. The center with the highest thermal stability was the E_1/E_2 center (with the level at E_c – 0.31/0.44 eV) with the electron-capture cross section ~10^{-14} cm^2 and the annealing temperature of 1400°C; this center was identified with the V_C–C_{Si} defect, as in the data reported by Lingner et al. [125]. It was found that concentrations of all defects increased as both the fluence and energy of neutrons were increased (Fig. 10).

It was found possible to extend the range of observed deep levels produced by irradiation with neutrons in SiC by increasing the temperature of the DLTS measurements (from 100 K to 700 K) and by using the *p*–*n* junctions [131]. The Schottky diodes and the p^+–*n*–n^+ diodes formed by ion-implantation doping by Al in the CVD 4*H*-SiC layers with the concentration of $(5–8) \times 10^{15}$ cm^{-3} were irradiated with 1-MeV neutrons with fluences of $(1.2–6.4) \times 10^{16}$ cm^{-2}. The DLTS measurements of initial CVD layers revealed the presence of a single deep center Z_1 with the activation energy of 0.62 eV and the concentration of (2–3) × 10^{13} cm^{-3} (Fig. 11, curve *1*). After irradiation of the diode structures with the neutron fluence of 1.2×10^{14} cm^{-2}, the DLTS measurements (at 80–400 K) revealed that, in addition to an increase in the concentration of the Z_1 centers, another deep center NI_2 with the energy of 0.68 eV appeared (curve *2*). As the neutron fluence was increased to 3.1×10^{14} cm^{-2}, the centers with the levels located at E_c – 0.37 eV and E_c – 0.74 eV appeared simultaneously with an increase in the concentration of the Z_1 centers (Table 1). Thus, an increase in the fluence of incident neutrons brought about an increase in the types and concentrations of the defects in SiC, as was also concluded in [126, 130]. Heat treatment of the samples at a temperature as high as 700 K brought about (in addition to an appreciable decrease in the concentrations of the NI_1 and NI_2 centers) an appearance of centers with deep levels at 0.92 and 1.56 eV (the NI_3 and NI_4 centers) that were also observed after irradiation of *n*-6*H*-SiC with electrons [101]. The parameters of all detected deep levels are listed in Table 1; the total concentration of the corresponding defects was equal to

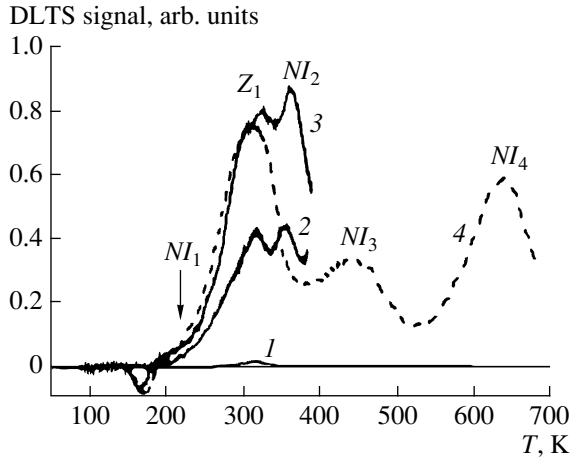

Fig. 11. The *C*-DLTS spectra of (*1*, *2*) Schottky diodes and (*3*, *4*) p^+–*n* junction doped by Al using ion implantation; the spectra were measured (*1*) before irradiation and (*2*, *3*) after irradiation with neutrons with the fluence of (*2*) 1.2×10^{14} cm^{-2} and (*3*) 3.1×10^{14} cm^{-2}. Spectra *1*–*3* were measured at temperatures no higher than 400 K, while spectrum *4* was measured after heating of the sample to 700 K [131].

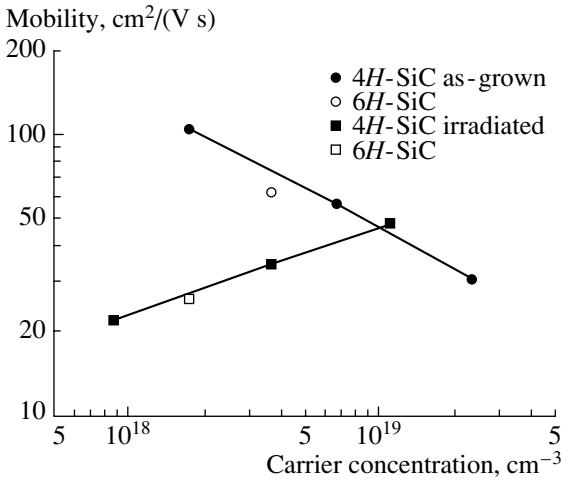

Fig. 12. Mobility of charge carriers in initial SiC samples and samples irradiated with neutrons in relation to the carrier concentration in the initial samples [132].

$\sim 2 \times 10^{15}$ cm^{-3} after the second irradiation and became comparable to the initial concentration of electrically active donors in the CVD layer, $(5–8) \times 10^{15}$ cm^{-3}. Taking into account the aforementioned insignificant decrease in the concentration of uncompensated donors in the epitaxial CVD layer (according to the measurements of the *C*–*V* characteristics) as a result of irradiation of the samples with neutrons, we may assume that only a fraction of the deep-level centers are compensating centers.

The effect of introduced radiation defects on the electrical characteristics of the initial material was considered in the case of the *n*-6*H*-SiC crystals irradiated with reactor neutrons with energies higher than 0.1 MeV and the fluence of 6×10^{16} cm^{-2} with subsequent annealing in the temperature range of 373–823 K in the Ar atmosphere [132]. As can be seen from Fig. 12, the charge-carrier mobility in irradiated samples increased as the $N_d - N_a$ concentration was increased in the initial samples, whereas the opposite pattern was observed for the initial samples. Thus, as the degree of purity of the sample is increased, the effect of radiation on the charge-carrier mobility becomes more pronounced (the mobility decreases more rapidly). Annealing of irradiated samples showed that the charge-carrier concentration remained unchanged at temperatures as high as 823 K, while the charge-carrier mobility increased in two stages, at the temperatures of 300 and 500 K (Fig. 13). A decrease in the mobility in the initial samples as a result of irradiation was attributed to the introduction of additional acceptor-type scattering centers. After annealing, the concentration of these centers became lower, which brought about an increase in the

Table 1. Parameters of deep level detected in epitaxial 4*H*-SiC CVD layers after irradiation with neutrons with various fluences

Irradiation no.	Center	$E_c - E_i$, eV	σ_n, cm^2	N, cm^{-3}
Initial sample	Z_1	0.63 ± 0.01	10^{-14}	$(2–3) \times 10^{13}$
First (D_1)	Z_1	0.63 ± 0.01	10^{-14}	4×10^{14}
	NI_2	0.68 ± 0.01	10^{-14}	4×10^{14}
Second (D_2) (before annealing)	NI_1	0.37 ± 0.01	10^{-16}	5.5×10^{13}
	Z_1	0.69 ± 0.01	10^{-14}	5.5×10^{14}
	NI_2	0.74 ± 0.03	5×10^{-15}	5.8×10^{14}
Second (D_2) (after annealing at 700 K)	NI_1	0.37 ± 0.01	10^{-16}	$<10^{13}$
	Z_1	0.68 ± 0.01	10^{-14}	5.3×10^{14}
	NI_2	0.74 ± 0.03	10^{-14}	$<10^{13}$
	NI_4	0.92 ± 0.1	5×10^{-15}	$\sim 2 \times 10^{14}$
	NI_5	1.56 ± 0.02	5×10^{-13}	8×10^{14}

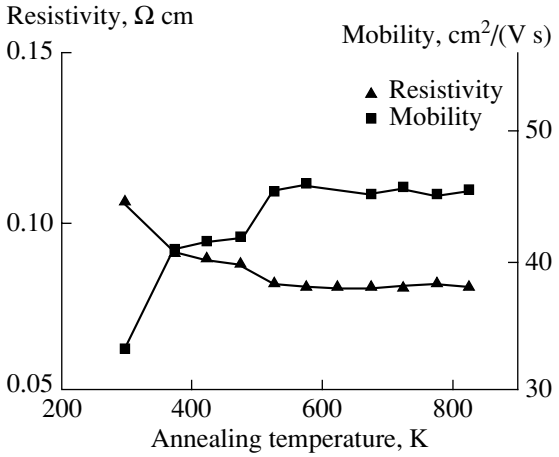

Fig. 13. The mobility and resistivity of neutron-irradiated SiC sample in relation to the annealing temperature [132].

charge-carrier mobility. This circumstance indicates that it is possible to recover the SiC electrical characteristics (degraded as a result of irradiation with neutrons) using elevated annealing temperatures.

The high degree of penetration of neutrons through a material provides not only a uniform distribution of radiation defects over the bulk of the material but also a uniform doping of SiC with P atoms in the case of neutron-induced nuclear transmutation of ^{30}Si atoms at high irradiation fluences. The early EPR studies showed that irradiation of *n*-6*H*-SiC crystals with reactor neutrons gave rise to P atoms that either occupied the lattice sites P_{Si} or formed a complex with a vacancy [133, 134]. According to theoretical data, this complex was treated as the P_{Si}–V_C center [135]. This theoretical prediction was confirmed experimentally in the case of EPR measurements of the *p*- and *n*-4*H*-SiC and *p*- and *n*-6*H*-SiC crystals and epitaxial layers irradiated with reactor neutrons with fluences of 3×10^{18}–7.7×10^{20} cm^{-2} with subsequent heat treatment at temperatures as high as 1850–2000°C [136–139]. The appearance of a neutral donor P atom in the *p*-6*H*-SiC epitaxial layers as a result of neutron-induced transmutation of ^{30}Si atoms was supported by the LT PL and ICTS measurements [136]. The layers with the phosphorus concentration of 3×10^{14} cm^{-3} were obtained in the *n*-4*H*-SiC epitaxial CVD layers with the carrier concentrations of 2×10^{14}–2×10^{15} cm^{-3} as a result of irradiation with thermal neutrons with a fluence of 3×10^{18} cm^{-2} with subsequent annealing at 2000°C [137]. It became possible to detect the appearance of a *p*–*n* junction in the course of nuclear transmutation of ^{30}Si atoms into ^{31}P atoms after irradiation of epitaxial CVD *p*-6*H*-SiC layers with the maximum neutron fluence of 7.7×10^{20} cm^{-2} [138]. Appreciable structural changes in irradiated SiC were observed in the case of such high neutron fluence. According to the XRD data, the dislocation density was 2.2×10^{10} cm^{-2}. It was noted that the dislocation density in the samples increased superlinearly with increasing irradiation dose. Heat treatment of irradiated samples at a temperature of 1850°C initiated annealing of point defects and rearrangement of dislocations. According to the TEM measurements, irradiation of 6*H*-SiC crystals with ultrahigh neutron fluences ($E > 0.1$ MeV) of ~1.5×10^{22} cm^{-2} brought about amorphization of the samples [140]. When the samples were annealed, the crystallization occurred inhomogeneously in the volume of the irradiated layer and was completed as a result of annealing in the temperature range of 1150–1250°C. In this case, the amorphous 6*H*-SiC layer could recrystallize into a defect-containing layer of the 3*C*-SiC polytype.

As follows from the aforesaid, all trends that took place in the case of irradiation of SiC with electrons were also observed when SiC was irradiated with neutrons. However, the defects formed in SiC irradiated with neutrons exhibit a more complex structure than in the case of irradiation with electrons. At high neutron fluences, the transmutation of ^{30}Si atoms into ^{31}P atoms can occur with simultaneous conductivity-type inversion; also, the formation of amorphous layers is possible with subsequent recrystallization to the 3*C*-SiC polytype.

4. IRRADIATION WITH IONS

Irradiation with ions is used both with the aim of studying the radiation-induced defect formation and in the course of production of device structures doped controllably with depth and locally over the area (using the method of ion implantation). In the case of irradiation of SiC with accelerated ions, a wide range of defects and structural imperfections are formed; these defects and imperfections not only worsen the transport properties of electrons and holes but also retard the activation of implanted impurities. Therefore, in the case of formation of device structures using ion implantation, it is necessary to reduce the concentration of radiation-induced defects, which is accomplished by subsequent high-temperature annealing or by irradiation of a heated target. A special feature of irradiation of semiconductors with accelerated ions is nonuniform distribution of radiation defects over the range of particles, which hinders their study.

4.1. Irradiation with Protons

Protons represent the main fraction of cosmic radiation (approximately 85%); therefore, the issues related to the effect of these lightest ions on the structural and electrical characteristics of semiconductor materials are of practical interest. A variation in the properties of semiconductors under the effect of proton radiation can occur as a result of several processes: radiation-effect production, formation of new impurities as a result of nuclear reactions (radiation-induced modification), and accumulation of hydrogen atoms [10, 141–143]. If the

proton energies are as high as 50 MeV, a large number of primarily displaced atoms can be expected owing to elastic scattering by the atoms and nuclei of the material. At proton energies higher than 50 MeV, the process of transmutation doping of semiconductors is possible due to nuclear reactions [144]. The nonuniform distribution of defects in depth of the material along the ion range brings about a production of simple defects in the initial portion of the range; clusters of defects are formed or electrons are captured with transformation into a hydrogen atom at the end of the range [145].

These theoretical data were experimentally confirmed by performing ESR and EPR studies for crystals and epitaxial layers of the *n*- and *p*-type 3C-, 4*H*- and 6*H*-SiC irradiated with protons [146–149]. At the chosen conditions of irradiation with protons (the energy of 2–12 MeV and the fluence of ~10^{16} cm^{-2}), the range of ions exceeded the thickness of the epitaxial layers or crystals, which provided the uniform distribution of radiation defects in the volume of the crystals under study. Simple defects with various charge states V_{Si}, V_{Si}^{-}, V_{Si}^{2-}, V_C, and V_C^{+} were detected, similar to what was observed in SiC in the case of irradiation with low-energy electrons [78, 82]. According to EPR measurements, V_{Si} vacancies were located on different sides of the lattice (hexagonal or cubic) and their concentration increased with increasing fluence of incident protons (Fig. 14) [148]. Since the vacancy concentration exceeded the concentration of doping impurity ($N_d - N_a = 2 \times 10^{17}$ cm^{-3}) at high radiation fluences, it was assumed that, along with V_{Si} vacancies, the V_C vacancies were formed as a result of irradiation and introduced donor levels into the band gap. In addition, the number of formed V_{Si} vacancies was smaller than the theoretical value [145], which was attributed to recombination of vacancies with interstitial atoms even at room temperature. The annealing temperature for the V_C and V_C^{+} vacancies was 150°C [146, 147], while simple radiation defects were completely annealed out at 1100°C [148]. The V_{Si} vacancies in various charge states were considered as the acceptor-type defects that brought about the conversion of *n*-4*H*-SiC and *n*-6*H*-SiC with $N_d - N_a = 2 \times 10^{17}$ cm^{-3} to the insulator state if the proton-radiation doses exceeded 2×10^{16} cm^{-2}. Measurements of absorption coefficients at 10 K were used to determine two ionization levels for the V_{Si} vacancies in negatively charged states with energies $E_c - 0.6$ eV (V_{Si}^{-}, V_{Si}^{2-}) and $E_c - 1.1$ eV (V_{Si}^{-}, V_{Si}); these levels were associated with the Z_1/Z_2 centers and the deep *R* center, respectively [148, 149].

The effect of proton fluences on the concentration of the formed radiation defects was studied in the case of irradiation of epitaxial *n*-4*H*-SiC CVD layers (with the charge-carrier concentration of ~10^{15} cm^{-3}) with protons with doses of 10^{11}–10^{13} cm^{-2} and energies of 2.9 and 6.5 MeV; these energies ensured the formation of

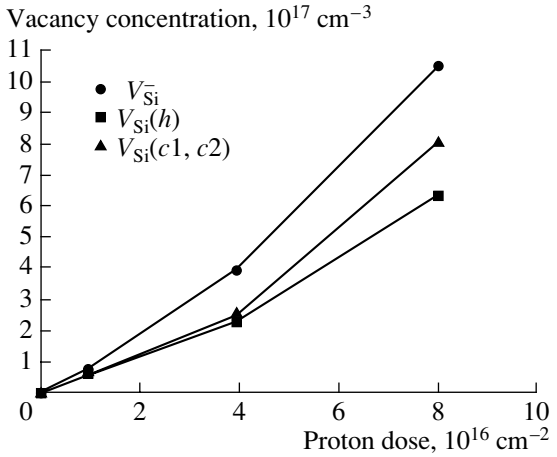

Fig. 14. Concentration of negatively charged and neutral silicon vacancies on the (*h*) hexagonal and (*c*1, *c*2) sides in *n*-6*H*-SiC in relation to the fluence of incident 12-MeV protons [148].

simple defects in the bulk of the samples under study [115, 150–152]. The measurements by the methods of DLTS and MCTS (minority carriers transient spectroscopy) revealed a wide spectrum of acceptor-type radiation defects with energy levels in the range E_c – (0.18–1.09) eV, including the well-known center with the energy level at $E_c - 0.68/0.7$ eV (the Z_1/Z_2 center). In addition, three other centers were identified, with energy levels located at 0.35, 0.44, and 0.79 eV above the valence-band top and with capture cross sections in the range of 5×10^{-14}–8×10^{-13} cm^2; these centers acted as traps for holes. The center with the level at E_c – 0.4 eV was annealed out at temperatures of 100–400°C, according to different versions. The deep center with the level at $E_c - 0.86$ eV and the capture cross section of 7×10^{-12} cm^2 was stable at temperatures as high as 1700°C, while the deep level at $E_c - 1.09$ eV was attributed to the radiation defect with the divacancy structure V_C–V_{Si}. All other centers were annealed out at temperatures no higher than 1700°C, except for the center with the level at $E_v + 0.35$ eV; this center did not disappear even at 1700°C and was more thermally stable than the Z_1/Z_2 center. The concentrations of all deep-level centers increased as the proton fluences were increased, similarly to the data obtained in the case of irradiation of SiC with electrons [106, 115]. However, due to the difference in the generation rate of radiation defects (caused by the difference between the masses of protons and electrons), the number of centers with deep levels was larger in the case of irradiation with protons due to their larger mass. In addition, it was concluded that the concentration of the Si and C interstitial atoms formed as a result of irradiation was on the order of 10^{15} cm^{-3} and that a significant fraction of these defects recombined with vacancies and formed stable defect con-

figurations that gave rise to deep-level recombination centers affecting the lifetime of free charge carriers [153].

In the case where the incident protons were completely stopped in the bulk of the samples under study, the PAS measurements indicated that more complex defect-related centers appeared. The positron lifetimes of ~200, 257, and 280 ps were determined in the *n*-4*H*-SiC and *n*-6*H*-SiC crystals and epitaxial layers irradiated with 5-MeV and ~200-keV protons with fluences of 10^{15}–10^{16} cm^{-2} [154–157]. These lifetimes were associated with the radiation-defect centers with the V_C–V_{Si} divacancy structure or complexes in the form of vacancy clusters $(V_C–V_{Si})_2$ and $(V_C–V_{Si})_3$ [154–157]. In this case, annealing of radiation defects occurred in several stages. Annealing of simple defects took place at temperatures of 150–200°C, in which case the V_C and V_{Si} vacancies could recombine. The subsequent annealing stages at temperatures of 600–900°C and higher than 1000°C were accounted for by annealing of complex defects. It was found that the size of clusters increased as the annealing temperature was increased to 1300°C, which was attributed to transfer of vacancies from small clusters to larger clusters that are more favorable energetically [156, 157]. Complete annealing of radiation defects was observed at a temperature of 1400°C; however, it was noted that the features of annealing of various defects depended heavily on the protons' fluence, the charge-carrier concentration, and the conductivity type of the samples [155].

The effect of the proton energy on the characteristics of radiation defects in 4*H*- and 6*H*-SiC was studied by the DLTS method using Schottky diode structures and *p*–*n* junctions obtained by the sublimation or CVD methods [158]. The samples were irradiated with protons with energies of 150 keV, 8 MeV, and 1 GeV and with fluences of 10^{14}–2×10^{16} cm^{-2}. In the case of 4*H*-SiC samples, a deep center with the level at E_c – 1.5 eV, a large cross section for electron capture (2×10^{-13} cm^2), and the concentration of 5×10^{15} cm^{-3} was detected. A similar center was observed in *n*-6*H*-SiC and *n*-4*H*-SiC irradiated with electrons and neutrons, respectively [101, 131]. For this center, the rate of its introduction in relation to the proton energy was determined; this rate was found to be 0.17, 70, and 700 cm^{-1} for the energies of 1 GeV, 8 MeV, and 150 keV, respectively. Thus, an increase in the proton energy brought about a decrease in the rate of radiation-defect generation, which led to a decrease in their concentration. Therefore, one should expect that irradiation of SiC with high-energy protons should bring about an increase in the critical value of the irradiation dose [159] and, consequently, an increase in the radiation tolerance of the devices based SiC. These premises are consistent with the results of calculations (using the TRIM software package) of the defect formation in SiC under the effect of irradiation with 8-MeV protons [160].

The possibility of obtaining insulating layers in the SiC bulk in the case of proton radiation was studied using the *n*-6*H*- and *n*-4*H*H-SiC crystals, epitaxial layers, and *p*–*n* junctions fabricated on the basis of the above structures using the sublimation or CVD methods [161–163]. The materials and structures were irradiated with 100-keV and 8-MeV protons with fluences in the range from 10^{14} to 6×10^{17} cm^{-2}. At low energies of incident ions, the method of atomic-force microscopy (AFM) was used to establish that amorphous layers are formed at a depth corresponding to the projected range of protons (0.65 μm) in amorphous layers after irradiation of the samples with fluences of 3×10^{17} cm^{-2}. Probably, in the case of this dose of protons, the critical concentration of multiple-vacancy complexes (~2×10^{20} cm^{-2}) required for realization of the (single crystal)–(amorphous state) phase transition was attained [164]. The formation of the defect complexes was also verified by the temperature dependence of the PL spectra measured at 77 K [159]. After irradiation, the PL peaks observed in the initial samples virtually disappeared and appeared again only after annealing at 800°C. The complete recovery of the intensity of the PL spectra was observed after annealing at 1500°C, which is characteristic of the annealing temperatures for vacancy complexes in SiC. According to the EPR measurements, some of the defect-related centers can be treated as V_C–V_{Si} divacancies; simple V_C vacancies are also present. According to the DLTS measurements, these defects introduced the deep levels with energies of E_c – 0.5 eV (V_C) and E_c – 0.7 eV and E_c – (1.1–1.22) eV (V_C–V_{Si}). The complete annealing of radiation defects was observed upon a temperature increase to 1500 K as the resistivity of the samples decreased according to an exponential law [163]. In this case, the maximum activation energy of the samples' resistivity (ε_A) was observed at the maximum radiation dose of 2×10^{16} cm^{-2} and was close to the deep-center energy level at E_c – (1.1–1.22) eV; the concentration of this center increases as the radiation dose is increased (Fig. 15). It was noted in [163] that, as a result of irradiation of 6*H*-SiC with protons, the charge-carrier concentration decreased compared to the initial value at a temperature of 300 K and increased at a temperature of 650 K as the radiation fluence was increased. At the same time, in the case of the 4*H*-SiC samples at room temperature and higher temperatures of measurements, the concentration of uncompensated donors decreased as the radiation fluence was increased.

Thus, in the case of irradiation of SiC with protons, characteristic features of the radiation-defect formation inherent to other semiconductors irradiated with ions were revealed. The simple V_C and V_{Si} vacancies in various charge states are formed at initial portions of the ions' range; these vacancies are annealed out at approximately 150°C. At the final portion of the protons' range, clusters with vacancies and divacancies are formed; these clusters are annealed out at temperatures higher than 1300°C. Irradiation with protons gives rise to levels at E_c – 0.4 eV, E_c – 0.7 eV (the Z_1/Z_2 center), and E_c – 1.6 eV (the *EH*6.7 center), similar to the case

of irradiation with electrons and neutrons. However, compared to irradiation with electrons, the number of deep-level centers is larger in the case of irradiation with protons since the proton mass is larger. By varying the conditions of irradiation with protons, one can control the formation of insulating layers in the SiC bulk. As the proton energy is increased, one can expect the radiation resistance of devices based on SiC to increase.

4.2. Irradiation of SiC with Ions of Medium Masses

The following important results have been obtained in early studies concerned with the effect of irradiation of SiC with ions of medium masses on the radiation-defect production:

(i) It was shown that the main defects introduced by implantation of He, Ne, N, Al, Ge, Ar, Ag, and I ions into SiC are vacancy-type defects, i.e., vacancies, divacancies, and complexes involving both vacancies and impurities [103, 165, 166]. The concentrations of these vacancy-related centers decrease as the sample's temperature is increased during irradiation, owing to an increase in the rate of recombination of interstitial atoms with vacancies; this increase is caused by an increase in the mobility of both interstitials and vacancies [167, 168].

(ii) In the SiC samples of the 3*C*, 4*H*, 6*H*, and 15*R* polytypes irradiated with electrons and ten types of ions, the D_1 center was detected (the peak at ~2.6 eV in the luminescence spectrum); this center was annealed out at temperatures higher than 1700°C [165]. This center was attributed to divacancy (the plausible model is V_C–V_{Si}) and is considered as a compensating center in the case of the obtaining of implanted *p*-SiC.

(iii) The center with the lines at 4202–4210 Å was also detected in the LT PL spectrum [169] of the 4*H*- and 6*H*-SiC samples irradiated with more than ten types of ions; this center is referred to as the D_{11} defect. The D_{11} center is stable at temperatures as high as or higher than 1700°C; its position in the LT PL spectrum is independent of the type of ions.

(iv) It was also noted that the concentration profile of radiation defects extends to a depth that appreciably exceeds the range of implanted ions [168, 170].

(v) Annealing of radiation defects at temperatures no higher than 1800°C does not bring about a complete recrystallization of the implanted layer; the polytype conversion from 6*H*-SiC to 3*C*-SiC is observed in the case of irradiation with Ge ions at $T > 1300$°C [171].

(vi) The critical implantation doses that bring about amorphization of the 6*H*-SiC layers irradiated at 300 K are equal to 10^{14} and 8×10^{14} cm^{-2} for the Ge and Al ions, respectively [171, 172].

4.2.1. Irradiation at low temperatures of the target. Irradiation of SiC with various ions made it possible to reveal the effects of different factors on the basic quantity in studying radiation-defect formation in semiconductors, i.e., the displacement energy of atoms (E_d),

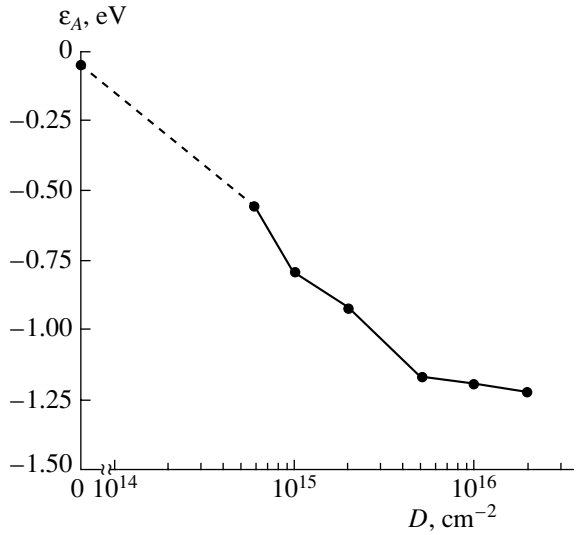

Fig. 15. Dependence of the activation energy (ε_A) for the resistance of the Schottky diodes formed on sublimation-grown 4*H*-SiC epitaxial layers on the dose of irradiation with 12-MeV protons [163].

which was previously determined in the case of irradiation with low-energy electrons.

The value of E_d for Si atoms was determined from the RBS measurements of bulk *n*-6*H*-SiC crystals irradiated with He, C, and Si ions with the energies of 390–550 keV [173]. The ions' doses were varied in a wide range so that the parameter characterizing the displacement of atoms at the peak of the defect concentration ranged from 0.008 to 0.42 dpa (displacement per atom), which corresponded to the region of transition from the formation of isolated simple defects to the formation of amorphized layers. In the case of irradiation with He ions, the threshold displacement energy for Si atoms in *n*-6*H*-SiC was determined to be equal to $E_d = 30$–35 eV, which is consistent with the theoretical value [93, 94]. It was established that this experimental value decreased as either the mass of incident ions or their dose was increased (Fig. 16). This dependence was attributed to the fact that the defect cascades produced by heavier ions contain more structural imperfections and also to the fact that it is easier to form imperfections in a system where these imperfections already exist. The threshold radiation dose for amorphization in the case of irradiation with C ions was found to be equal to 2×10^{15} cm^{-2}.

Later, the defect-formation energies for the Si and C sublattices in the *n*-6*H*-SiC crystals were compared in the case of irradiation with low-energy (50-keV) He ions with doses of 7.5×10^{14}–2.5×10^{16} cm^{-2} at temperatures of 100 and 300 K [174]. Irradiated samples were annealed at temperatures of 200–1200°C. The evidence (obtained previously in the case of irradiation with electrons [69, 97]) that the displacement threshold energy is lower in the C sublattice than in the Si sublat-

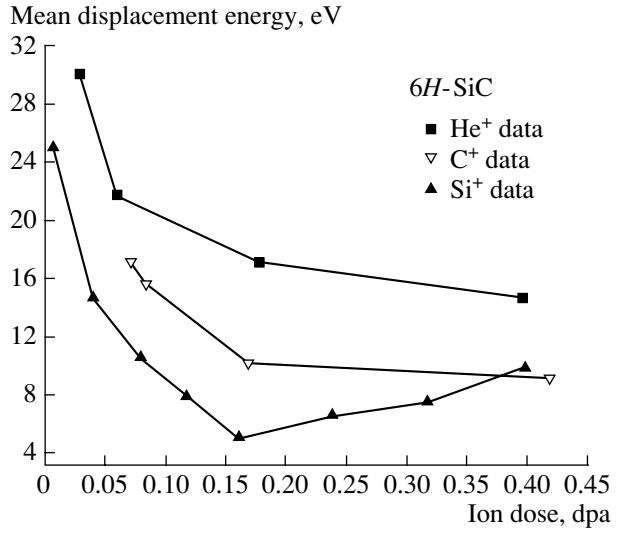

Fig. 16. Mean displacement energy in the Si sublattice in 6*H*-SiC crystals in relation to the dose of irradiation with the He, C, and Si ions in dpa (displacement per atom) units [173].

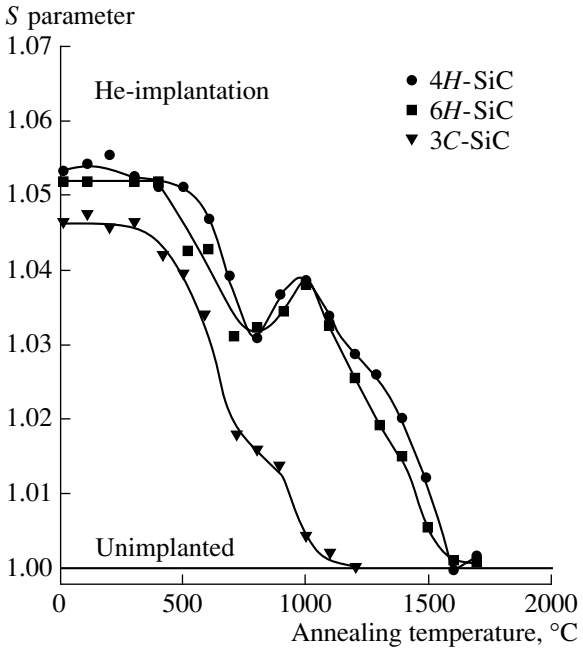

Fig. 17. Temperature dependence of the normalized *S* parameter (PAS) for the 3*C*-, 4*H*-, and 6*H*-SiC epitaxial *n*-type layers irradiated with He ions [46].

tice was verified. In addition, the activation energy for C atoms in the processes of migration and recombination is also lower than for Si atoms, which possibly brought about [69, 97] the annealing of carbon-related defects even during irradiation. Annealing of defects in irradiated samples proceeded with a higher rate in the case of irradiation with higher doses, so that the defects were annealed out at 1200°C after irradiation with a dose of 10^{16} cm^{-2}. The dose of 2.5×10^{16} cm^{-2} of irradiation with 50-keV He ions at 100 K was considered as limiting for the transition to the amorphous state; this dose increased as the temperature of the samples was increased from 100 to 300 K during irradiation. However, in the case of irradiation of the *n*-6*H*-SiC crystals with 3.5-MeV He ions with the doses of 10^{16}–10^{17} cm^{-2}, the RBS measurements did not indicate that there are any amorphous regions formed [175]. In addition, it was shown that the radiation-defect concentration increased as the defect-introduction rate (the particles' flux) was increased with the dose remaining unchanged. Comparing these data with those obtained previously [173], we may assume that, as the energy of incident particles is increased, the critical irradiation dose giving rise to amorphization of the implanted layer increases.

The effects of the polytype structure and the conductivity type on the defect formation in 4*H*- and 6*H*-SiC in the case of irradiation with He ions was studied and compared using the PAS and DLTS methods [176]. The ions' energy was 1 MeV and the total dose was 8×10^{12} cm^{-2}; this dose was attained steplike in order to form a boxlike profile. The CVD ~5-μm-thick layers of two polytypes with the *n*- and *p*-type conductivities with charge-carrier concentrations of ~5×10^{15} cm^{-3} were irradiated. For both polytypes and both conductivity types, the average positron lifetime was found equal to 210 ps, which is close to the positron lifetimes as measured by the PAS method in the SiC samples irradiated with electrons [38] and protons [154]; these lifetimes were associated with the formation of vacancy-type radiation defects.

However, subsequent studies performed in the case of irradiation of the 3*C*-, 4*H*-, and 6*H*-SiC epitaxial layers ($N_d - N_a = 5 \times 10^{15}$–$10^{16}$ cm^{-3}) with He ions showed that the temperature behavior of the *S* parameter (in the PAS data) related to the vacancy-type defects is different for these polytypes (Fig. 17) [46]. The annealing temperature of the defects characterized by the *S* parameter increased as the degree of hexagonality in the SiC structure increased, and attained a maximum value of 1700°C for the 4*H*-SiC polytype. The first stage of annealing of radiation defects at 500–700°C was attributed to the disappearance of isolated vacancies, similar to their behavior in the SiC samples of various polytypes and conductivity types in the case of irradiation with electrons [39, 61]. An increase in the value of the *S* parameter in the *n*-4*H*- and *n*-6*H*-SiC polytypes in the temperature range of 800–1000°C was related [39, 61] to the formation of the vacancy-involving complexes as a result of the mobility of these vacancies. Such temperature dependence of the PAS parameters in the course of annealing were not observed in the SiC samples irradiated with electrons [46], which was accounted for by a high concentration and diversity of radiation defects that appear as a result of irradiation with heavier He ions. After the irradiated samples were annealed at

700°C, the DLTS measurements revealed in 6*H*-SiC the defects E_1/E_2 and Z_1/Z_2 with the ionization energies of 0.42–0.46 and 0.66–0.72 eV, respectively. In the 4*H*-SiC polytype, the Z_1/Z_2 and $RD_{1/2}$ centers were revealed, with the ionization energies of 0.59–0.65 and 0.66–0.74 eV, respectively. On the basis of comparison of the temperature behavior of the *S* parameters and the deep-level concentrations, these levels were identified with vacancy-type defects. For example, the E_1/E_2 levels in 6*H*-SiC and Z_1/Z_2 levels in 4*H*-SiC observed in the case of irradiation with electrons were related to complexes based on the V_{Si} vacancies [39].

Similar defect-related centers E_1/E_2 and Z_1/Z_2 in *n*-6*H*-SiC and Z_1/Z_2 and $RD_{1/2}$ in *n*-4*H*-SiC were observed in the case of irradiation of these polytypes with 2-MeV protons with the fluence of 10^{13} cm^{-2}, with He ions (with steplike irradiation with energies of 30–950 keV and total fluence of 8×10^{12} cm^{-2}), and with 2-MeV electrons [177]. Irradiated samples were annealed first at a temperature of 1000°C in vacuum and then at a temperature of 1700°C in Ar atmosphere. It follows from the measurements by the DLTS and PAS methods that the formation of the observed deep-level centers depends on the type of incident particles. For example, in the samples irradiated with the H and He ions, the Z_1/Z_2 center (with the level at $E_c - 0.65$ eV in 4*H*-SiC) appeared only after annealing at 600°C, whereas this center was formed at room temperature in the case of irradiation with electrons. The annealing of this center with a further increase in temperature also proceeded differently for different incident particles, which was shown by the example of the 4*H*-SiC polytype (Fig. 18). Formation of all defect-related centers was attributed [177] to vacancy-involving complexes. It was concluded that the types of the vacancy-related defects were the same for all three SiC polytypes under consideration, but the ways of formation of these defects and transformation of them in the course of annealing were different.

In order to gain deeper insight into the defect formation in the case of ion-implantation doping, the DLTS measurements were carried out for the *n*-4*H*-SiC samples irradiated with the He and B ions with low doses, so that the compensation effect was excluded [178]. The high-purity epitaxial CVD layers with the charge-carrier concentration of ~10^{15} cm^{-3} were irradiated with 1.7-MeV He ions with the dose of 2×10^9 cm^{-2} and with 5-MeV B ions with doses of 10^7–8×10^7 cm^{-2}, so that the maximum in the concentration was formed at a depth of ~4 μm. The samples irradiated with He were then annealed at temperatures of 700 and 1000°C in vacuum, while the B ions were implanted either at room temperature or at temperatures of 400 and 500°C. The DLTS measurements were carried out in the temperature range of 80–700 K using the Au and Ni Schottky barriers. It was noted that compensating defects were introduced in the case of irradiation with He ions;

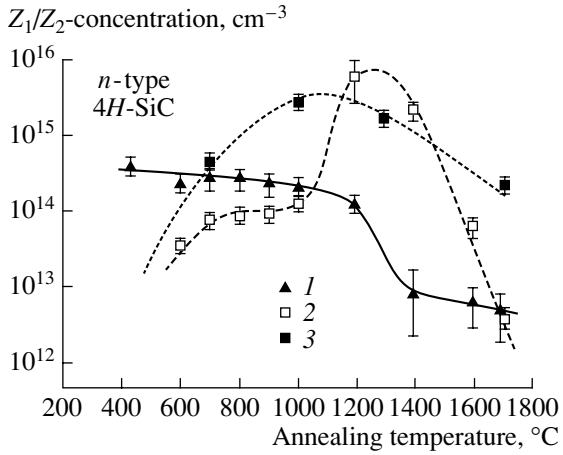

Fig. 18. Dependences of the concentration of Z_1/Z_2 defects in 4*H*-SiC; this defect appeared as a result of irradiation with (*1*) electrons, (*2*) He ions, and (*3*) protons [177].

these defects were partially annealed at temperatures of 700 and 1000°C. In the case of irradiation with B ions, there was a center with the level at $E_c - 0.7$ eV, which was close to the energy position of the level of the well-known Z_1/Z_2 defect considered as an acceptor center [101, 102]. It was found that the concentration of the centers with the level at $E_c - 0.7$ eV increased as the end of the range of B ions was approached, increased linearly with an increase in the radiation dose, and increased as the irradiation temperature increased to 400°C. In addition, a center with the energy level at $E_c - 1.6$ eV and a large cross section for capture of electrons (9×10^{-12} cm^2) was revealed at higher temperatures of measurements; the energy position of this center was independent of temperature.

The effect of annealing on the behavior of radiation defects formed in the *n*-6*H*-SiC samples as a result of irradiation with He^+ ions was studied by the DLTS and LT PL methods [179]. High-purity epitaxial CVD 5-μm-thick layers with the charge-carrier concentration of 4×10^{15} cm^{-3} were irradiated with He^+ ions successively with the energies from 30 to 650 keV in order to form the boxlike profile at a depth as large as 1.6 μm. The radiation doses were chosen so that the concentrations of the vacancy-type defects were 2×10^{16}, 8×10^{16}, and 2×10^{17} cm^{-3}. Irradiated samples were annealed with a steplike increase in temperature to 1700°C. The DLTS measurements revealed two defect-related centers with the ionization energies of 0.42/0.46 and 0.64/0.7 eV that were close to the energy positions of the well-known E_1/E_2 and Z_1/Z_2 defects' levels. The E_1/E_2 center was identified [179] with the well-known defect D_1 (the LT PL peak at 2.6 eV), which was annealed out at temperatures higher than 1700°C [165]. The line at 4349 Å in the LT PL spectrum was attributed to a defect that had the same nature as the Z_1/Z_2 center and was annealed out at ~1400°C. The centers E_1/E_2

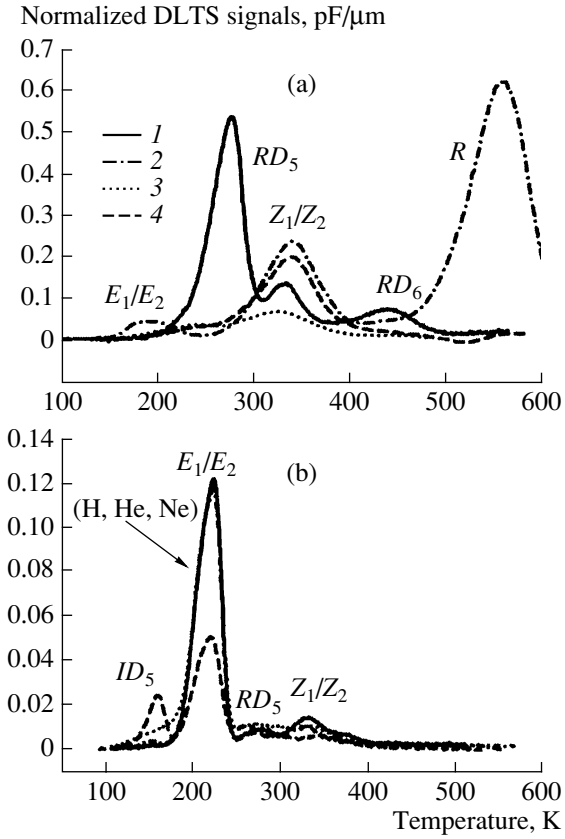

Fig. 19. Normalized DLTS spectra of the *n*-6*H*-SiC samples irradiated with the (*1*) H, (*2*) He, (*3*) Ne, and (*4*) Ar ions and then annealed for 30 min at (a) 800 and (b) 1400°C [182].

(0.38/0.44 eV) and Z_1/Z_2 (0.64/0.75 eV) with similar temperatures of annealing $\gtrsim$1600°C were identified using the DLTS measurements for the CVD layers of *n*-6*H*-SiC irradiated with He ions; these layers were 5 μm thick and had the charge-carrier concentration of 10^{16} cm^{-3} [180, 181]. The samples were irradiated with He ions with the energies increased successively from 55 to 840 keV in order to form the boxlike profile to a depth of 2 μm. Centers with the ionization energies of 0.5 and 0.53 eV, annealed at 300 and higher than 1400°C, respectively, were revealed. It was found that the E_1/E_2 defect (with activation energy of 0.38/0.44 eV) appeared after heating of the samples to 500°C and was annealed out at a temperature of 1600°C. This defect was identified [180, 181] with the well-known center D_1. The defect Z_1/Z_2 was annealed out at 1400°C; it is noteworthy that, as the annealing temperature was increased, the increase in both the activation energy of this center [E_a(700°C)) = 0.65 eV and E_a(1200°C) = 0.74 eV] and the cross section for electron capture [σ(700°C) $\approx 10^{-17}$ cm^2 and σ(1200°C) $\approx 10^{-16}$ cm^2] were observed. It was concluded that the annealing temperatures for the E_1/E_2 and Z_1/Z_2 centers observed in *n*-6*H*-SiC in the case of irradiation with He ions were higher than in the case of irradiation of similar samples with electrons and neutrons. The nature of all defects was related to vacancies bonded to dislocations.

The high thermal stability of the E_1/E_2 centers in 6*H*-SiC and of the Z_1/Z_2 centers in 4*H*-SiC was also observed in comparative DLTS studies of the radiation defects produced by irradiation of the samples with electrons (2 MeV), protons, and He, Ne, and Ar ions with subsequent annealing at temperatures of 800–2300°C [182]. The radiation doses were varied for different particles, which was done with the aim of ensuring that the concentration of the vacancies introduced was the same (10^{18} cm^{-3}) in all cases. It was shown that the types of introduced defects, their concentrations, and temperature behavior depend on the mass of the incident particles. For example, the E_1/E_2 defect in 6*H*-SiC appeared only after annealing at 1400°C of the samples irradiated with the H, Ne, and Ar ions, whereas the Z_1/Z_2 center in 4*H*-SiC appeared immediately after irradiation with electrons without any subsequent annealing. The latter behavior was also observed by Weidner et al. [177]. The defect concentrations decreased as the annealing temperature was increased. The centers with the highest thermal stability (the E_1/E_2 centers in 6*H*-SiC and Z_1/Z_2 centers in 4*H*-SiC) annealed out at temperatures higher than 1700°C (Fig. 19).

The role of the D_1 defect in the formation of implanted *p*-SiC was studied by the DLTS and LT PL methods in the case of irradiation of the *n*-4*H*-SiC epitaxial layers with the Al and B ions (the layers had the charge-carrier concentration of 10^{16} cm^{-3}) [183]. In order to obtain the boxtype profile to a depth of 0.6 μm, the samples were irradiated steplike in the energy range of 40–400 keV for Al ions and in the range of 40–300 keV for B ions with the total dose equal to 5×10^{14} cm^{-3}. After implantation, the samples were annealed at temperatures of 1400–1700°C. A line located at 4272 Å was observed in the LT PL spectrum for both types of ions after annealing at a temperature of 1400°C; this line was related to the appearance of the D_1 defects, as in the case of irradiation of SiC with electrons [71]. This center did not disappear even after annealing at 1700°C, although the concentration of the activated Al impurity increased sharply with the activation energy E_a = 160–165 meV. It was concluded [71] that the D_1 center does not play the role of a compensating center in the formation of implanted *p*-SiC, which is in disagreement with the opinion of Patrick and Choyke [165]. The positron lifetime of 216 ps observed after implantation of both types of ions was attributed to the appearance of divacancies V_C–V_{Si}. After heat treatments, the positron lifetime was 147–148 ps, which was associated with the vacancy-type defects related to the carbon vacancies V_C [37, 39].

The Z_1/Z_2 center (with the level at E_c – 0.71 eV) was also identified with the V_C–V_{Si} divacancy in the *n*-6*H*-SiC samples ($N_d - N_a = 2 \times 10^{15}$ cm^{-3}) implanted with 2-MeV He ions with the dose of 10^{11} cm^{-2} and then annealed in the range of temperatures of 200–

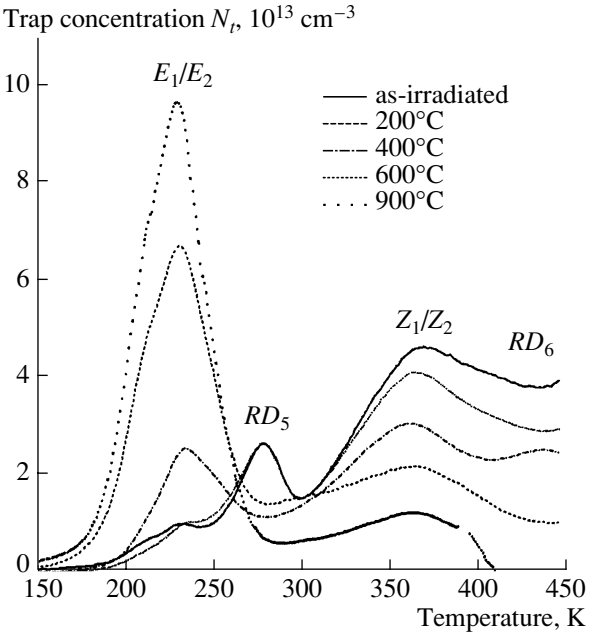

Fig. 20. The DLTS spectra of the *n*-6*H*-SiC samples irradiated with 2-MeV He ions with the dose of 10^{11} cm^{-2} after annealing at the temperatures indicated [184].

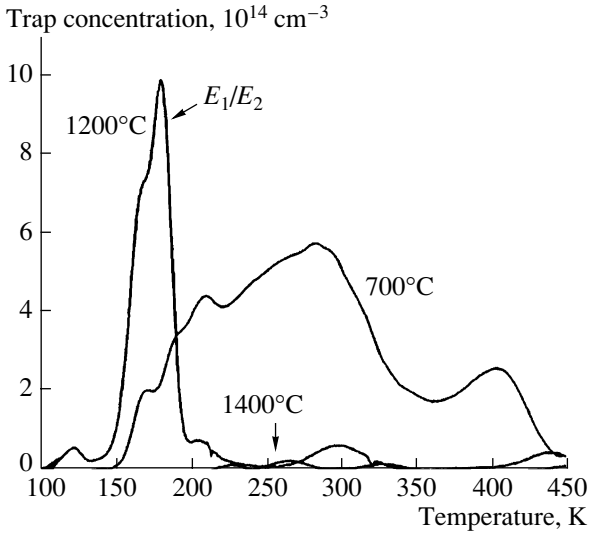

Fig. 21. The DLTS spectra measured for an *n*-6*H*-SiC epitaxial layer irradiated with 10-MeV C ions with the dose of 10^{11} cm^{-2} [185] and then annealed at the temperatures indicated.

900°C [184]. Studies of the DLTS and PAS spectra revealed the defects E_1/E_2 (the level at $E_c - 0.4$ eV), RD_5 (the level at $E_c - 0.51$ eV), and RD_6 (the level at $E_c - 0.82$ eV). The Z_1/Z_2 center appeared after an annealing at 400°C. The concentrations of all defects decreased as the annealing temperature was increased, except for the E_1/E_2 center. Its concentration increased as the annealing temperature was increased to 900°C (Fig. 20). It was assumed [184] that the vacancy-type defects (V_C) are annealed out at 600°C.

The same defects E_1/E_2 (with the level at $E_c - 0.4$ eV), RD_5 (with the level at $E_c - 0.51$ eV), and Z_1/Z_2 (with the level at $E_c - 0.67$ eV) were also revealed in the DLTS measurements in the CVD epitaxial *n*-6*H*-SiC layers irradiated with C ions [185]. The samples were irradiated with C ions with the dose of 10^{11} cm^{-2} and the energy of 10 MeV; this energy ensured the complete penetration of the epitaxial layer by the particles and the formation of uniformly distributed radiation defects in this layer. In this case, the concentration of introduced vacancies was 2×10^{16} cm^{-3}, according to calculations based on the TRIM software package. After irradiation, the samples were annealed in the Ar atmosphere. All defects were annealed out at a temperature of 1200°C, except for the E_1/E_1 center that annealed at 1400°C (Fig. 21). The E_1/E_2 defect was identified with the V_{Si} vacancy or with complexes on the basis of this vacancy, similarly to conclusions advanced in the case of irradiation of SiC with electrons [39, 110], and was considered responsible for quenching of the luminescence line at 423 nm in the spectrum of room-temperature PL.

Formation of deep-level defects as a result of irradiation of SiC with 8-MeV Si ions with doses of 10^9–10^{12} cm^{-2} was observed by the methods of scanning capacitance microscopy (SCM), TEM, and DLTS (at 150–450 K) [186]. The 4-μm-thick *n*-6*H*-SiC layers with the electron concentration of 2.4×10^{16} cm^{-3} were irradiated. A single deep level (at $E_c - 1.38$ eV) of defects with the concentration of 1.6×10^{13} cm^{-3} was detected in the band gap of initial samples. After irradiation, this level disappeared, but four new levels appeared; these levels were located at 2.17, 1.34, 1.23, and 0.91 eV below the conduction-band bottom and had the concentrations of 2.5×10^{15}, 7.4×10^{14}, 4.4×10^{14}, and 7.1×10^{13} cm^{-3}, respectively (Fig. 22). The radiation-defect level at $E_c - 2.17$ eV was considered as compensating for energy levels of major impurities.

The effect of irradiation with ions with various masses on the defect formation in SiC was studied in the case of irradiation of 6*H*-SiC crystals with 2-MeV Au ions at a temperature of 170 K and with 550-keV Si ions at a temperature of 190 K [187]. After irradiation with various doses, the samples were annealed at a temperature as high as 800 K. A comparison of the results of simulation of the defect-formation processes by the method of molecular dynamics with experimental data obtained by the RBS method made it possible to suggest [187] that isolated point defects and extended clusters composed of interstitial and substitutional defects are formed as a result of irradiation of SiC with Au ions. These defects were not completely annealed out at 800 K, which was attributed [187] to partial amorphization of SiC in the course of irradiation, or to the forma-

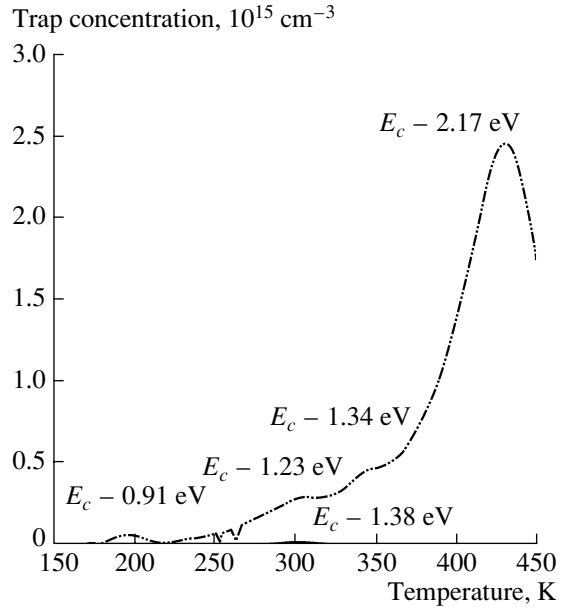

Fig. 22. The DLTS spectrum measured for the *n*-6*H*-SiC layer irradiated with 8-MeV Si ions with the dose of 10^{12} cm^{-2} [186].

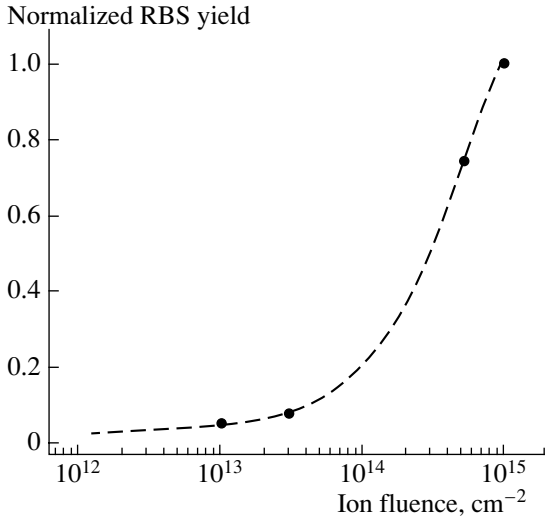

Fig. 23. Dependence of the damage degree in the *n*-4*H*-SiC epitaxial layers on the dose of Al ions implanted with the energy of 100 keV at 25°C [188].

tion of clusters in the cascade process of defect formation in the course of annealing. In the case of irradiation with Si ions, isolated vacancies and also interstitial and substitutional defects appeared; these defects were annealed out at 300 K owing to an increased migration rate of defects in a nonequilibrium system. The number and size of the clusters composed of substitutional atoms were much larger in the case of irradiation with Au ions than in the case of irradiation with Si ions. Thus, an increase in the mass of incident ions brought about an increase in the number of types of radiation defects; also, the concentration and size of these defects increased.

An increase in the radiation dose can also bring about an increase in the variety of radiation defects and in the concentration and size of these defects. This statement was confirmed by the data obtained in the experiments with irradiation of the *n*-6*H*- and *n*-4*H*-SiC epitaxial layers with Al ions with the energies of 100–150 keV and doses of 10^{12}–5×10^{16} cm^{-2} at 25°C (Fig. 23) [56, 188]. According to the PAS, EPR, and RBS data, monovacancies and divacancies were formed in the case of doses lower than 10^{13} cm^{-2}. At the doses equal to approximately 10^{13} cm^{-2}, positrons were annihilated mainly at divacancies that were grouped in clusters as the dose was increased to 10^{14} cm^{-2}. At doses exceeding 10^{14} cm^{-2}, the structure started to transform to the amorphous state; as a result, it was impossible to identify the defects, which is consistent with the data reported in [172]. According to the EPR data, phase inclusions appeared in this case; hypothetically, these inclusions were considered as stable graphite nanoclusters that were not annealed out even at 1100°C [56].

Other types of defects were detected as a result of PAS measurements of the 6*H*-SiC samples irradiated with P ions, so that the resulting P concentrations exceeded the solubility limit [189]. The CVD layers with the charge-carrier concentration of 3.5×10^{15} cm^{-3} were irradiated with 200-keV P ions with the dose of 5×10^{16} cm^{-2} at 300 K, which gave rise to the layer implanted to a depth of ~250 nm. After irradiation, the samples were annealed isochronously in the temperature range of 100–1700°C for 20 min at each temperature in Ar atmosphere. An amorphous layer extending to a depth of 180 nm was detected at the surface after irradiation. At a larger depth, there was a layer for which the positron lifetime was 266 ps; this layer was associated with the V_C–V_{Si} divacancies. An analysis of the PAS measurements indicated that there are radiation defects at a depth of 700 nm, which is much larger than the projected range of the ions R_p. Annealing of the implanted layer occurred in three stages. As the annealing temperature was increased to 600°C, a relaxation in the amorphous layer occurred, while at higher temperatures, the *S* parameter decreased owing to migration of monovacancies (such as V_{Si}) to the surface of the sample. A further increase in the annealing temperature to 1000°C brought about an increase in the *S* parameter in the range of 0.5–0.54 and an increase in the positron lifetime to 250 ps, which was attributed to the appearance of cluster-type defects composed of more than ten V_C–V_{Si} divacancies over the entire depth of the implanted layer. An annealing at 1700°C brought about the transition from the amorphous state to the crystalline state with an insignificant decrease in the value of the *S* parameter and shift of the defect-profile curve

towards the surface. The decrease in the value of the *S* parameter at this stage of annealing was related [189] to the possible polytype transformation from 6*H*-SiC to 3*C*-SiC, as with the data obtained in the case of irradiation with Ge ions [171]. A similar conclusion concerning the possible transformation of polytypes in the case of annealing of amorphized implanted layers was advanced in the case of the Hall measurements and Raman spectroscopy in the *p*-SiC samples irradiated with high doses of P ions with the aim of formation of *n*-type layers [190]. The *p*-4*H*-SiC epitaxial layers with the hole concentration of 5×10^{15} cm^{-3} were consequently irradiated with P+ ions successively with the energies of 10–280 keV in order to form a boxtype profile to the depth of 300 nm. The radiation doses were 10^{13}–5×10^{16} cm^{-2}, which corresponded to the phosphorus concentration of 3.3×10^{17}–8×10^{20} cm^{-3}. Irradiated samples were annealed isochronously at temperatures of 1200–1700°C. An almost complete annealing of defects occurred at a temperature of 1700°C in the case of concentrations of implanted atoms lower than 3×10^{18} cm^{-3} (the dose lower than 10^{14} cm^{-2}); in this situation, the concentration of activated charge carriers was 1.93×10^{18} cm^{-3}. Irradiation of the samples with phosphorus atoms giving rise to their concentration of 2.3×10^{20} cm^{-3}, which is considered as the solubility limit for phosphorus [191, 192], brought about the formation of an amorphous layer that was not recovered to the crystalline state even after annealing at 1700°C. The Raman measurements demonstrated that the 4*H*-SiC polytype can be transformed into the 3*C*-SiC polytype and that the stacking faults can be formed if the concentration of implanted atoms exceeded the solubility limit.

The effect of a decrease in the initial depth of radiation defects introduced as a result of high-dose implantation of Al ions into 4*H*-SiC [189] was also detected by the RBS/C method [193]. The *n*-4*H*-SiC epitaxial layers ($N_d - N_a = 10^{15}$ cm^{-3}) were irradiated with 100-keV Al ions at 25°C with a dose of 5×10^{16} cm^{-2} and were then annealed for 15 s at 1700°C. According to the results of calculations and the SIMS (secondary-ion mass spectrometry) data, the depth of the profile of implanted ions was 120 nm, while the maximum of structural damage was located at a depth of 85 nm. According to the RBS/C data, the implantation gave rise to an amorphous layer at a depth of $\gtrsim$200 nm, which exceeded the width of the region where primary defects were generated; this width was calculated using the TRIM software package (Fig. 24). It was assumed [193] that this discrepancy is related to the effect of saturation of the generation rate of radiation defects in the case of irradiation of SiC with ions with the dose that corresponds to the threshold for transition to the amorphous state, as was observed previously for irradiation of SiC with electrons [101]. It is noteworthy that heat treatment brought about partial recrystallization of the amorphous layer to a depth of ~50 μm from the internal boundary of this layer. The thickness of the implanted-layer amorphous part remaining after annealing virtually coincided with the width of the region of generation of primary defects; according to the conclusions advanced in [167], this remaining amorphous layer consisted of clusters that involved two–five V_C–V_{Si} divacancies, which is also in good agreement with the data reported in [189]. In the case of implantation of Al ions into 6*H*-SiC [167], the RBS/C measurements also indicated that the depth of the defects' profile was smaller than the projected range R_p. However, according to the PAS measurements, the depth of location of defects after implantation appreciably exceeded the value of R_p for Al ions, which suggested that the RBS/C and PAS methods detect different types of defects. The RBS/C measurements detect the defects related to interstitial C atoms C_i, whereas the PAS data are related to the vacancy-type defects (V_{Si}).

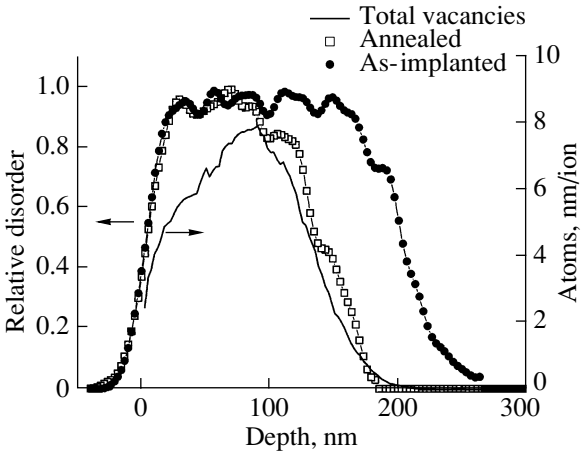

Fig. 24. The function of generation of primary defects (the total number of vacancies) calculated using the TRIM software package (solid line) and also the defects' profile in the 4*H*-SiC CVD layer after Al implantation and after subsequent annealing [193].

Radiation defects that are located at a depth exceeding the projected range R_p of implanted ions and were detected using the PAS method [168, 170] were also observed in the case of irradiation of the *n*-4*H*-SiC epitaxial layers with B, N, and Al ions [194]. The samples were irradiated at 300 K with the B, N, and Al ions with the doses of 4×10^{14}, 5×10^{13}, and 9×10^{11}–6×10^{13} cm^{-2}, respectively; the ion energies were chosen so as to provide the same projected range $R_p \leq 0.11$ μm for all types of ions. It was shown that the depth of location of radiation defects much exceeded the value of R_p and the tails of the distributions of radiation defects extended to larger depths for heavier ions. The formation of these tails was attributed to the effect of channeled ions during irradiation [194]. Previously, in the case of irradiation of *n*-6*H*-SiC with high-energy B, Al, and Ga ions, it was shown that the channeling depth depends on the mass of ions and increases as the mass increases [195]. This effect was attributed to an

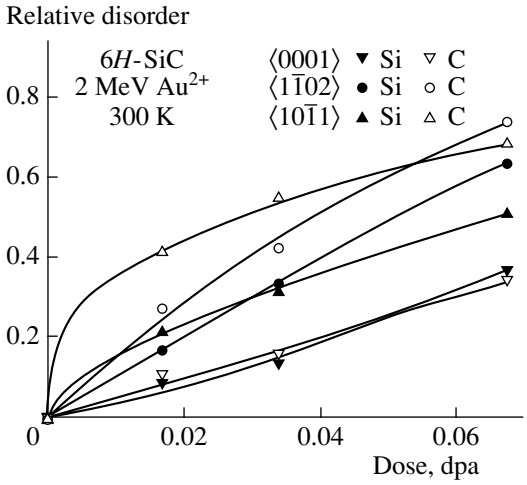

Fig. 25. Relative damage in the C and Si sublattices along the ⟨0001⟩, ⟨1 $\bar{1}$ 02⟩, and ⟨10 $\bar{1}$ 1⟩ directions as a function of the dose of irradiation with Au ions of the *n*-6*H*-SiC crystals at 300 K [196].

increase in the contribution of nuclear stopping to the total stopping power as the mass of ions is increased, which brought about channeling to larger depths. According to the PAS measurements, the defects formed in the vicinity of the R_p peak are identified with the V_C–V_{Si} divacancies, whereas the V_{Si} vacancies act as the main traps for positrons at the tails of the radiation-defect distribution [194]. In this case, the depth of location of the radiation-defect tails did not increase when the radiation doses were increased to the values that ensured the transition to the amorphous state.

The depth of channeling of implanted ions depends to a great degree on the orientation of the SiC crystallographic axes with respect to the direction of the incident-ion beam [196]. The *n*-6*H*-SiC crystals were irradiated at an angle of 60° to the normal to the (0001) plane with 2-MeV Au ions with doses of 2.9×10^{12}–1.2×10^{13} cm^{-2} at 300 K. The distribution of defects along the [0001], [1 $\bar{1}$ 02], and [10 $\bar{1}$ 1] directions was studied by the RBS and NRA/C methods. Along the [0001] direction, the same degrees of damage due to channeled ions were observed for the Si and C sublattices. Accumulation of damage proceeded linearly as the radiation dose was increased (Fig. 25). However, the amount of damage along the [1 $\bar{1}$ 02] and [10 $\bar{1}$ 1] axes in the Si and C sublattices was larger and increased sublinearly with the radiation dose. In these directions, the largest amount of damage was observed in the C sublattice owing to a lower threshold displacement energy (E_d) for C atoms. Annealing of structural damage at a temperature of 570°C also occurred more efficiently in the case of defects aligned along the [0001] direction.

In the case of irradiation of *n*-4*H*-SiC crystals with Al ions, a pronounced channeling of these ions was observed in the [11 $\bar{2}$ 0] direction with the penetration depth that exceeded by 45 times the projected range R_p [197]. The surface of the crystals was oriented in the (0001) and (11 $\bar{2}$ 0) planes. It was concluded that, in the fabrication of devices to be subjected to irradiation, it is reasonable to choose the material with the (0001) orientation. In order to reduce the effect of channeling, it was suggested to arrange the crystals with the (0001) orientation normally to the incident beam of particles.

4.2.2. Irradiation of a heated target. As shown above, irradiation with ions gives rise to a broad spectrum of radiation defects. High-temperature heat treatments are necessary for studying the origin of these defects and also for decreasing their concentration and activating the impurity in the case of using ion implantation for production of device structures. However, these heat treatments can give rise to secondary defects, transformation of polytypes with formation of stacking faults, and erosion of the implanted-layer surface. One of the methods for reducing the concentration of defects introduced in the course of irradiation of SiC with ions is implantation into a heated target.

The effect of a decrease in the concentration of defects introduced into SiC as a result of irradiation with ions in the temperature range of 25–600°C was studied on the example of the behavior of the well-known defect D_{11} observed in the PL spectra at 2 K [198]. The *n*-4*H*- and *n*-6*H*-SiC samples were irradiated with C and Si ions with the energies of 110 and 200 keV, respectively; these energies ensured that the projected range R_p was the same for both ions (R_p = 2000 Å). The doses of implantation were 1.4×10^{13} and 4.3×10^{12} cm^{-2} for the C and Si ions, respectively; this choice of doses ensured that there was the same quantity of generated vacancies for both types of ions. It was found that the concentration of the D_{11} defects increased as the implantation dose was increased. This defect was stable at temperatures as high as 1500°C and was identified with the lines at 3850 Å for 4*H*-SiC and at 4200 Å for 6*H*-SiC in the PL spectrum. It was also shown that, as a result of heating of the samples of both polytypes to temperatures as high as 600°C during irradiation, the intensity of the PL line corresponding to the D_{11} defect was higher in the case of irradiation with C ions. This finding was accounted for by the formation of defects that involved interstitial C atoms due an increase in the mobility of these atoms (in contrast to Si interstitials) as a result of heating of the samples. These conclusions are consistent with previous inferences in [169].

Previously [167, 168], it was found that different types of radiation defects are formed in *n*-6*H*-SiC irradiated with Al and N ions, depending on the implantation temperature in the range of 200–1000°C. The samples were irradiated with Al ions with energies of 180–500 keV and doses of (2–4) $\times 10^{14}$ cm^{-2} or first with

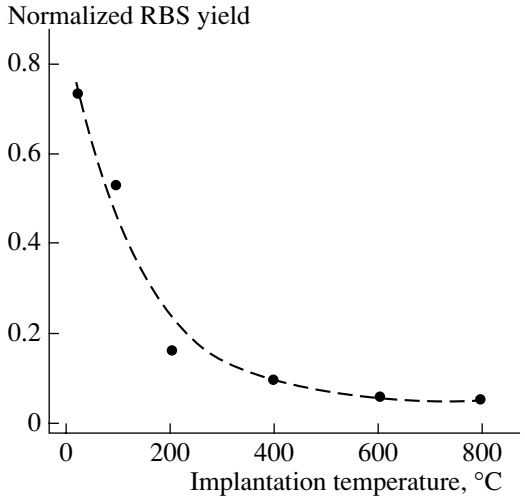

Fig. 26. Dependence of the degree of damage in the *n*-4*H*-SiC layers implanted with 100-keV Al ions with the dose of 5×10^{14} cm^{-2} on the implantation temperature [188].

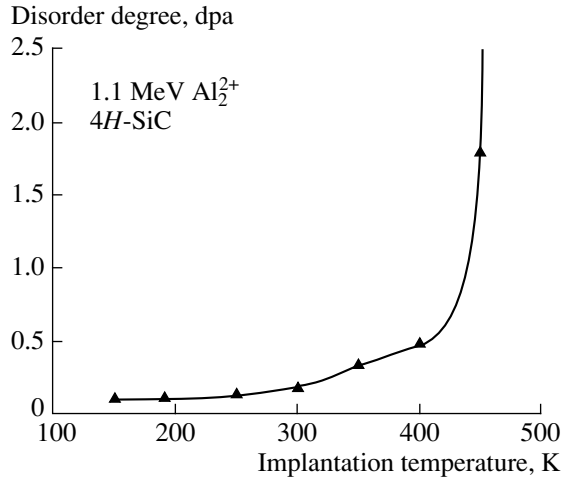

Fig. 27. Dependence of the dose required for obtaining the amorphous layer with the relative disorder of 0.9 on the temperature of the sample during irradiation with Al ions [201].

N ions with energies of 65 and 120 keV and doses of 5×10^{16} and 1.3×10^{17} cm^{-2} and then with Al ions with energies of 100 and 160 keV and doses of 5×10^{16} and 1.3×10^{16} cm^{-2} [168]. The studies by the PAS, RBS, and SPIS methods at the irradiation temperature as high as 200°C showed that amorphous layers and vacancy clusters whose size exceeded the size of five V_C–V_{Si} divacancies were formed. An increase in the irradiation temperature brought about a decrease in the degree of damage in the implanted layer with simultaneous shift of radiation defects to the sample's surface; the V_C–V_{Si} divacancies were considered as the main defects. These defects and their transformations were accounted for [168] by enhanced recombination of interstitial atoms and vacancies caused by an increase in their mobility with increasing temperature. The lowest concentration of the vacancy-type defects was observed in the case of irradiation at 400°C [199].

Later, in the case of irradiation of the *n*-4*H*-SiC epitaxial layers with 100-keV Al ions with the dose of 5×10^{14} cm^{-2} at the substrate temperature of 25–800°C, the studies by the PAS and RBS methods confirmed that the number of defects decreases as the sample's temperature during irradiation is increased (Fig. 26) [188, 200]. A rapid decrease in the concentration of radiation defects was observed as the target was heated even to 100°C. Based on the temperature dependences of the parameters *S* and *W* obtained by the PAS method, it was concluded that this decrease is caused by the formation of vacancy-containing clusters. The low temperature of annealing of radiation defects (100°C) was accounted for by an increased mobility of vacancies in implantation as a result of the nonequilibrium state of the system. As the temperature of the samples during irradiation is increased, two processes are in effect: annihilation of defects (recombination of interstitial atoms and vacancies) and accumulation of defects as the clusters' size increases. The smallest number of defects was observed at a temperature of 400°C, in which case the process of annihilation of defects (the recovery process) still dominated over the processes of their accumulation. As the temperature of the samples was increased to 800°C, the sizes of the clusters increased and could exceed the sizes of five monovacancies.

The effect of recovery of the structure in the case of irradiation of the *n*-4*H*-SiC epitaxial layers (with the electron concentration of 1.5×10^{15} cm^{-3}) with Al ions in the temperature range of 150–450 K was studied using the RBS/C, NRA/C, and TEM methods [201]. The samples were irradiated with 1.1-MeV double-charged Al ions with the doses of 1.4×10^{13}–4.0×10^{15} cm^{-2}, in which case both isolated defects and buried amorphous layers were formed. According to the studies, a drastic increase in the irradiation dose required for amorphization of the implanted layer was observed as a result of heating of the target to the critical temperature of 450 K (Fig. 27). In this case, the annihilation process brought about a suppression of the process of accumulation of radiation defects, so that an increase in the implantation dose by a factor of 20 (compared to the dose in the case of implantation at 150 K) was required to introduce the same number of defects. This finding indicates that it is possible to increase the radiation resistance of devices based on SiC at increased temperatures of operation.

Since the process of annihilation of radiation defects introduced as a result of irradiation with ions is thermally activated, the sample's temperature during irradiation also appreciably affects the production rate of defects, which, in turn, also governs the defect-formation process [202]. As noted above, the concentration of introduced radiation defects depends on the balance between their generation and annihilation rates. Therefore, if the introduction rate of defects is fairly low, they

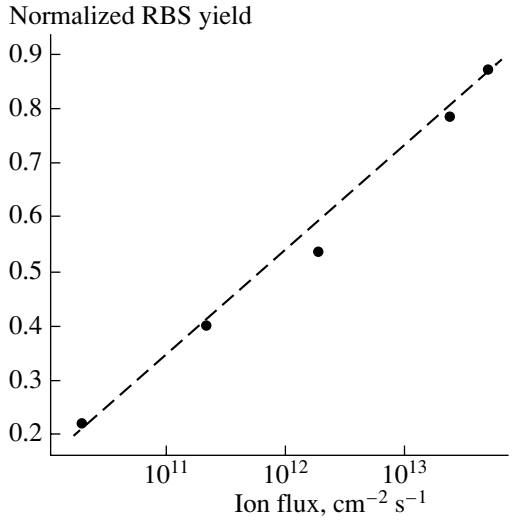

Fig. 28. Dependence of the degree of damage on the dose rate of irradiation of the *n*-4*H*-SiC crystals with 100-keV Si ions with a dose of 5×10^{14} cm^{-2} [188].

have a chance to annihilate, especially in the case where implantation is performed into a heated target (dynamic annealing). In this situation, the defect density can never attain the value that corresponds to the amorphization threshold. The phenomenon of dynamic annealing was studied by the RBS method for the *n*-4*H*-SiC crystals irradiated with 100-keV Si ions with a dose of 4×10^{15} cm^{-2} introduced with different rates in the range of 1.9×10^{10}–4.9×10^{13} cm^{-2} s^{-1} [188, 203]. The samples were heated to 200°C during irradiation. It was shown that an increase in the dose rate (the dose-rate effect) brought about an increase in the radiation-defect concentration; the onset of amorphization was observed at the dose rate of 10^{13} cm^{-2} s^{-1} (for the dose of 4×10^{15} cm^{-2}) (Fig. 28). Divacancies were believed to be the main types of radiation defects in the experimental conditions under consideration. The activation energy for dynamic annealing was determined and was found to be equal to 1.3 eV for temperatures in the range of 25–150°C. This energy ensured that the number of displaced Si atoms in the SiC samples irradiated at 100°C was smaller by a factor of 4 than at 25°C. These results indicate that the rate of introduction of defects into SiC is lower at elevated temperatures.

4.3. Irradiation with Heavy High-Energy Ions

Numerous studies of the effect of irradiation with light particles (electrons, protons, and neutrons) on the nature of defects in SiC made it possible to reveal the systematic trends in the radiation-defect formation in this material [101, 131, 158]. However, studies of the mechanisms of defect formation in SiC in the case of irradiation with high-energy heavy ions (i.e., with atoms with a mass number larger than 80 and the energies higher than 100 MeV) are also of considerable interest; indeed, the results of irradiation with these ions simulate structural damage produced by the fission fragments. In this case, under the conditions of high and ultrahigh levels of ionization energy losses and a high rate of radiation-defect generation, various types of radiation defects can be formed. The latter phenomenon is also favored by the nonuniform distribution of radiation defects along the ions' tracks, which gives rise to both point and extended defects, and also to latent tracks. The most plausible cause of the generation of the latter defects is the formation of an amorphous phase that is located in the region of the track and has density lower than the density of the crystal lattice. The high thermal–elastic stresses originating in the region of the track can also profoundly affect the defects' formation [204].

The first PAS studies of the defect formation in SiC crystals of the 3*C*, 6*H*, 4*H*, and 15*R* polytypes that had the *n*- and *p*-type conductivity and were irradiated with heavy ions were carried out using the 124-MeV Xe ions [205, 206]. The crystals with the impurity concentrations of 2×10^{17}–10^{20} cm^{-3} were first irradiated with Xe ions with fluences in the range of 5×10^{10}–5×10^{14} cm^{-2} and then isochronously annealed at temperatures as high as 1000°C in air and as high as 2300°C in the atmosphere of Ar. It was found that, at the fluence of 5×10^{11} cm^{-2}, the long-lived component of the positrons' lifetime attained its saturation with the value of 220–230 ns, which was related to the formation of complexes with divacancies, similar to the data obtained in the case of irradiation of SiC with electrons [38, 39], protons [154], and Al and B ions [183]. Annealing of the samples irradiated with fluences lower than 5×10^{13} cm^{-2} proceeded at a single stage in the temperature range of 1400–1600°C, in which case positrons were annihilated at the vacancy-related defects of the same type (dark circles in Fig. 29). However, annealing of the samples irradiated with the fluence higher than 5×10^{13} cm^{-2} occurred in two stages with the involvement of a negative annealing (empty circles in Fig. 29). The fluence of 5×10^{13} cm^{-2} was believed to be the critical value; i.e., when it was exceeded, the irradiated system became unstable in the course of annealing, which brought about clusterization of primary defects in the temperature range of 500–1000°C. These vacancy-containing clusters can bring about the degradation of electronic properties of the devices that are based on SiC and operate at temperatures higher than 500°C.

A similar value of the lifetime of positrons (225 ns) was determined from the results of PAS studies for the radiation defects formed as a result of irradiation of the *n*-6*H*-SiC crystals with 246-MeV Kr ions with the fluences of 10^{10}–10^{14} cm^{-2} [207]. The values of the *S* parameter and the positron lifetime increased as the fluence was increased to 10^{13} cm^{-2}; with a further increase in the fluence, the above characteristics leveled off, so that the positron lifetime became equal to 225 ns. This lifetime was close to the value that was determined

for the *n*-4*H*-SiC crystals (216 ns) irradiated with Al and B ions and was associated with the vacancy-containing defects of the V_C–V_{Si} type [183].

The effect of the fluence of Xe ions on the defect formation in SiC was also studied using the *p*-6*H*-SiC crystals with the charge-carrier concentration of 1.4×10^{17} cm^{-3} [208]. The samples were irradiated with 5.5-GeV Xe ions with the fluences of 10^9–10^{14} cm^{-2}, which ensured that radiation defects were formed uniformly over the entire volume of the sample since the projected range of Xe ions was $R_p \approx 400$ μm. The Hall measurements revealed an increase in the samples' conductivity as the fluence was increased to 10^{12} cm^{-2}, which was accounted for by the introduction of point radiation defects that introduce levels into the band gap. The formation of point defects in similar experimental conditions was confirmed by the TEM and HRTEM data [209]. An increase in the fluence of Xe ions to 10^{15} cm^{-2}, as well as annealing of irradiated samples at temperatures as high as 1373 K brought about the formation of extended defects that were considered as dislocation loops located in the basal or prismatic regions. An increase in the fluence also gave rise to a decrease in the conductivity of samples after irradiation; also, as a result of measurements of optical absorption, the band gap was found to decrease to 2.62 and 1 eV as a result of irradiation with the doses of 2×10^{13} and 10^{14} cm^{-2}, respectively. A similar pattern was observed in the case of irradiation of SiC with electrons and was attributed to the appearance of tails of the states in the vicinities of the edges of the corresponding bands at a high level of structural damage [210]. It was concluded that all defects were produced owing to elastic scattering conditions; no amorphous layers were formed in the case of ionization losses lower than 2.19 keV/nm. Also, the formation of latent tracks along the range of heavy ions in the case of irradiation of *n*-6*H*-SiC crystals at 300 K with 72-MeV iodine ions with a dose higher than 10^{17} cm^{-2} [211] and with 710-MeV Bi ions with the fluence of 10^{12}–10^{13} cm^{-2} [212]. Thus, in the above cases as well, the defects were formed by the mechanism of elastic scattering, and the formation of amorphous layers was not observed until the levels of ionization losses were no higher than 15 keV/nm (I) and 34 keV/nm (Bi).

In order to gain insight into the mechanism of amorphization in the case of irradiation with heavy ions, dependences of the threshold dose giving rise to amorphization on the temperature for irradiation of the *n*-6*H*-SiC crystals with electrons, Si ions, and Xe ions were compared (Fig. 30) [140]. The rate of introduction of defects was the same for all of the above types of incident particles and was equal to 2×10^{-3} dpa/s. It was shown that, as the mass of incident particles was increased, the threshold dose required for transition to the amorphous state decreased at all irradiation temperatures under consideration. For each type of ions, there exists a critical irradiation temperature above which the threshold dose for amorphization increases drastically. In addition, for each type of ions, the threshold dose

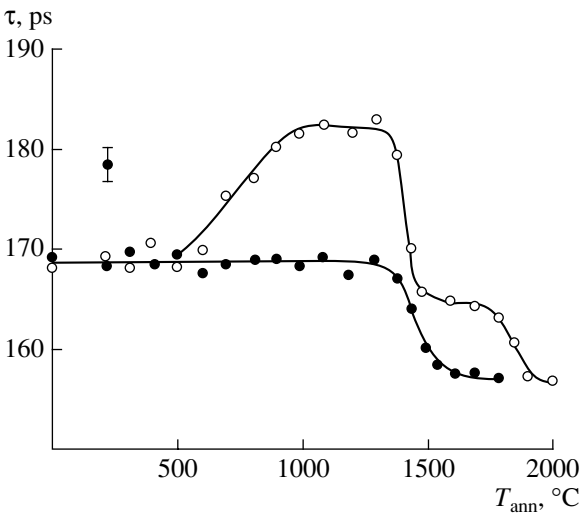

Fig. 29. Dependences of the mean positron lifetime τ on the temperature of isochronous annealing T_{ann} of the samples irradiated with Xe ions with fluences lower than 5×10^{12} cm^{-2} (closed circles) and lower than 5×10^{13} cm^{-2} (open circles) [205].

required for amorphization increased as the implantation temperature was increased. Since irradiation with heavy ions gives rise to extended defect formations (clusters), it is believed [140] that the process of amorphization sets in within these clusters and at higher temperatures than for the samples irradiated with electrons, in which case amorphization is caused by simple defects.

The use of *n*-4*H*-SiC epitaxial layers of higher purity made it possible to perform optical and electrical studies of these layers irradiated at 300 K with 246-MeV Kr ions with the fluences of 5×10^9–5×10^{10} cm^{-2} [213]. The electrical characteristics were studied using Schottky barriers made of Cr that were deposited onto the 26-μm-thick epitaxial SiC CVD layers with the charge-carrier concentration of $(4–5) \times 10^{15}$ cm^{-3}; these layers were grown on low-resistivity substrates. The temperature dependences of the resistance of the CVD layer before and after irradiation were determined in the temperature range of 293–695 K. The depth of the concentration profile for implanted Kr ions was 22 μm according to the calculations performed using the TRIM software package (Fig. 31) [145]. Therefore, all obtained data are referred to the changes that occur in the 26-μm-thick SiC layer as a result of irradiation. It was established that irradiation brought about quenching of the 3.189-eV exciton-related line in the PL spectrum measured at 77 K and an increase in the intensity of the broad band with the peak at ~2.7 eV. At the same time, the lines corresponding to the defects typical of the samples irradiated with light particles were not observed in the PL spectrum. This finding indicated [145] that there are different mechanisms of the effects of electrons and fast heavy particles on the

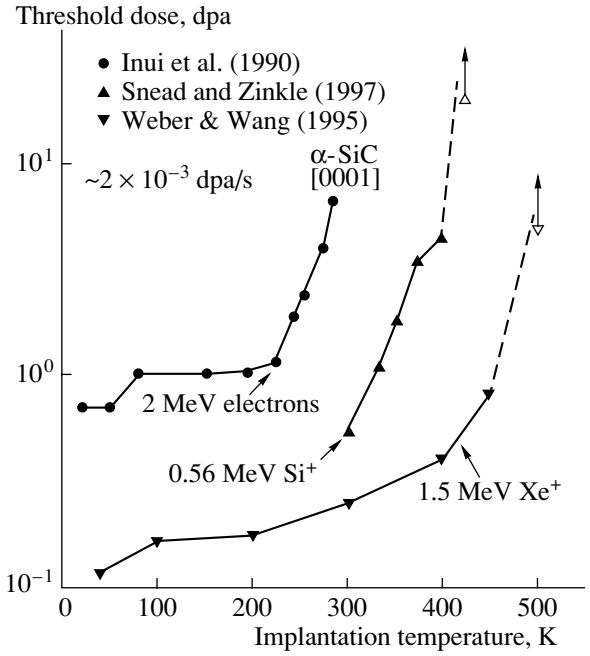

Fig. 30. Dependences of the threshold dose for amorphization on the temperature of irradiation for the *n*-6*H*-SiC crystals irradiated with electrons and with the Si and Xe ions [140].

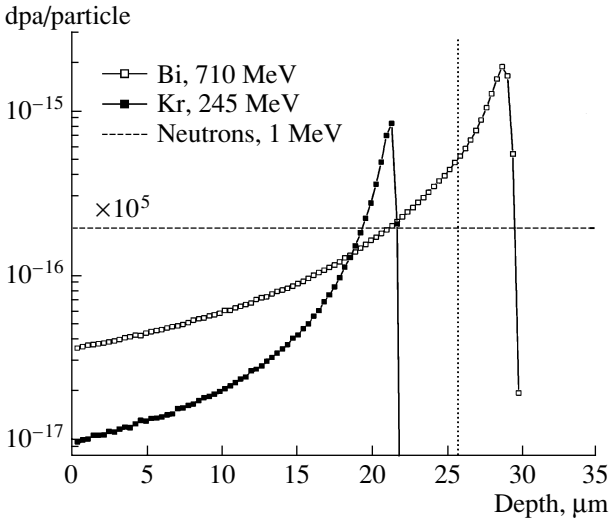

Fig. 31. Distribution of primary radiation defects calculated using the TRIM software package in *n*-4*H*-SiC in the case of irradiation with neutrons and the Kr and Bi ions with the energies of 1, 246, and 700 MeV, respectively [145].

SiC crystal lattice. According to the *C*-DLTS and *I*-DLTS measurements, the main radiation defects in the CVD layer at a depth as large as 5 μm from the surface were the deep centers with the levels at 0.43, 0.66, and 0.76 eV below the conduction-band bottom E_c, as was also observed in the case of irradiation with electrons, protons, He ions, and neutrons. The centers with the levels at E_c – 0.43 and E_c – 0.76 eV were annealed out as a result of heating of the samples to a temperature of 620 K, while the concentration of deep centers with the level at E_c – 0.66 eV (Z_1/Z_2) increased as the fluence of the Kr ions was increased. By comparing the variations in the concentrations of charge carriers and the Z_1/Z_2 centers before and after irradiation, it was concluded that this deep-level center is not a compensating center, which is consistent with the data reported in [165].

In the case of irradiation of the aforementioned CVD *n*-4*H*-SiC layers with 710-MeV Bi ions with the fluences of 1.4×10^9–10^{13} cm^{-2}, radiation defects with the parameters similar to those obtained in the case of irradiation with Kr ions were detected [214]. An intense broad band peaked at 2.7 eV attributed to the well-known D_1 center was observed in the PL spectrum. DLTS measurements were conducted using Cr Schottky diodes in the temperature range of 80–400 K, or at 80–700 K, on the ion-implantation-doped Al p^+–n junctions formed in these layers. The profiles of primary radiation defects obtained using the TRIM software package amounted to 28.8 μm along the track of the 710-MeV Bi ions in SiC (Fig. 32). Taking into account that the thickness of the CVD layer was equal to 26 μm, we may state that the results observed in the case of irradiation with Bi ions represent the processes occurring in the epitaxial layer. As shown in Fig. 32, irradiation of 4*H*-SiC with neutrons and Kr and Bi ions gave rise to the defect-related levels in the upper half of the band gap at the positions of E_c – 0.37/0.43 eV, E_c – 0.68 eV (Z_1/Z_2), E_c – 0.74 eV, E_c – 0.92 eV, and E_c – 1.47/1.56 eV. Some of the levels (E_c – 0.43 eV and E_c – 0.74 eV) were annealed out at 700 K. The parameters and concentrations of all detected deep-level centers for the initial and irradiated samples are listed in Table 2. Heating of the samples after irradiation brought about various changes in the resistance of the epitaxial CVD layers in relation to the type and dose of incident particles. In Fig. 33, we show the temperature dependences of resistance of the CVD layer irradiated with the Bi ions and neutrons (curves *1* and *2*, respectively) with the fluences as high as those at which (according to the results of measurements of the capacitance–voltage (*C*–*V*) characteristics) an insulator layer is formed whose thickness is comparable to that of a lightly doped epitaxial layer (26 μm). Similar exponential temperature dependences of variation in the resistance were previously observed for the SiC samples irradiated with protons and electrons and were attributed to pinning of the Fermi level [163, 206]. It was assumed that this type of variation in the resistance of irradiated SiC samples was caused by annealing of radiation defects formed in the cascades of atomic collisions. In the case of irradiation of SiC with Kr ions with low fluences (10^{10} cm^{-2}), a portion of so-called negative annealing was observed in the temperature dependence of resistance (Fig. 33, curve *3*). The presence of a similar portion in the case of annealing of the SiC samples irradiated with high fluences of ions and neutrons was attributed previously to the formation of thermally unstable clusters. In this case,

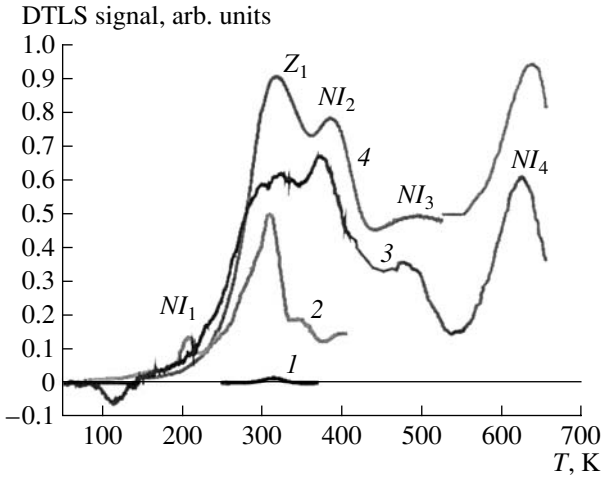

Fig. 32. The *C*-DLTS spectra of CVD 4*H*-SiC layers as measured both for initial 4*H*-SiC layers (curve *1*) and after irradiation with neutrons, Kr ions, and Bi ions (curves *3*, *2*, and *4*, respectively). Spectra *1* and *2* were measured using the Schottky barriers at temperatures no higher than 400 K, while spectra *3* and *4* were measured using p^+–*n* junctions doped with Al by ion implantation at temperatures as high as 700 K [214].

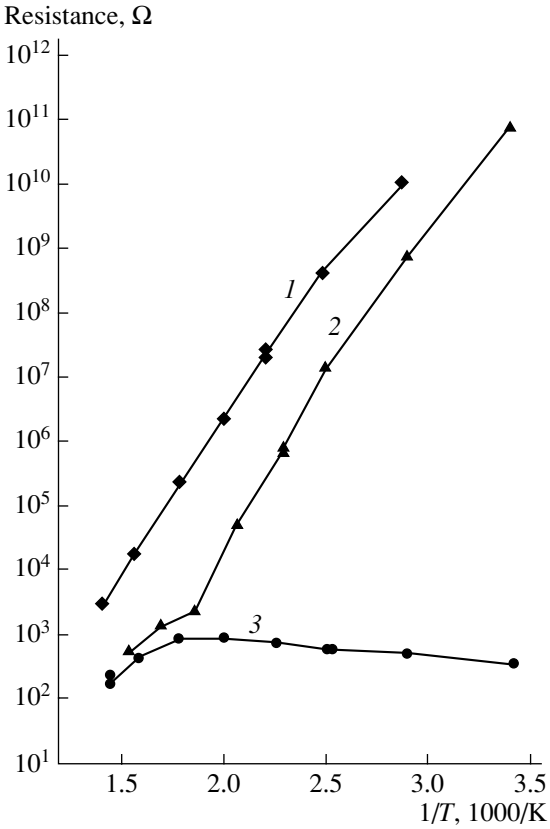

Fig. 33. Temperature dependences of resistance of CVD 4*H*-SiC layers irradiated with neutrons (curve *2*) and Bi and Kr ions (curves *1* and *3*) [214].

the sizes, concentration, and thermal stability of these vacancy-type clusters depended on the type and fluence of the incident particles and also on the doping level and the degree of purity of the initial material [206].

The structural features of the defect formation in the case of irradiation of SiC with high-energy Bi ions were considered in more detail for high-purity epitaxial *n*-4*H*-SiC CVD layers; the SEM, XRT, XRD, TEM, PL, and cathodoluminescence measurements were used [215]. The 26-μm-thick CVD *n*-4*H*-SiC layers that had the charge-carrier concentration of 5×10^{15} cm^{-3} were grown on the low-resistivity substrates and were irradiated with 710-MeV Bi ions with fluences of 1.4×10^9–10^{13} cm^{-2} and were then annealed at 500°C. According to the SEM data, irradiation with Bi ions with a fluence of 5×10^{10} cm^{-2} gave rise to a thin near-surface damaged layer with the thickness ≤1 μm and to accumulation of radiation defects in the epitaxial CVD layer with the thickness of 3–4 μm in the vicinity of the boundary

Table 2. Parameters of the defect centers detected in 4*H*-SiC before and after irradiation with neutrons and Kr and Bi ions

Irradiation	Center	$E_c - E_0$, eV	σ_n, cm^2	N, cm^{-3}
Initial sample	Z_1	0.63 ± 0.01	10^{-14}	2×10^{13}
Neutrons with the fluence of 3.1×10^{14} cm^{-2}	NI_1	0.37 ± 0.01	10^{-16}	5.5×10^{13}
	Z_1	0.69 ± 0.01	10^{-14}	5.5×10^{14}
	NI_2	0.74 ± 0.03	5×10^{-15}	5.8×10^{14}
	NI_3	0.92 ± 0.1	5×10^{-15}	~2×10^{14}
	NI_4	1.56 ± 0.02	5×10^{-13}	8×10^{14}
$^{84}Kr^+$, fluence 10^{10} cm^{-2}	NI_1	0.43 ± 0.01	4×10^{-15}	5×10^{13}
	Z_1	0.66 ± 0.02	10^{-14}	2.5×10^{14}
$^{209}Bi^+$, fluence 1.4×10^6 cm^{-2}	Z_1	0.68 ± 0.01	10^{-14}	5.3×10^{14}
	NI_2	0.74 ± 0.03	10^{-14}	2.8×10^{14}
	NI_3	0.92 ± 0.1	5×10^{-15}	~10^{14}
	NI_4	1.47 ± 0.04	5×10^{-13}	4×10^{14}

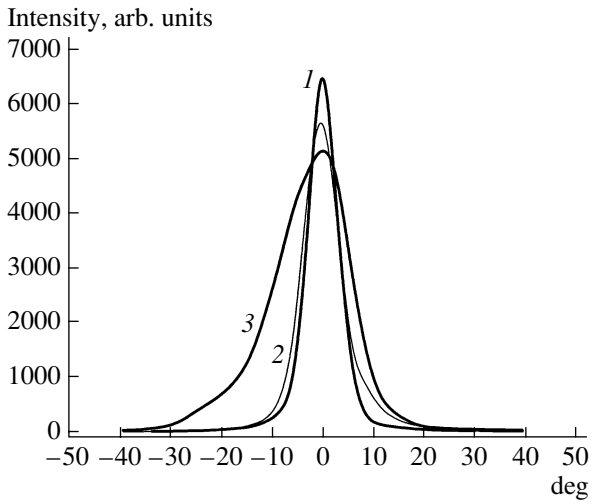

Fig. 34. Spectra of X-ray diffraction measured at the (0008) reflection for initial CVD 4*H*-SiC layer (curve *1*) and after irradiation of this layer with 710-MeV Bi with the fluence of 10^{10} cm^{-2} (curve *2*) and 10^{12} cm^{-2} (curve *3*). The thin line represents the result of calculation using the TRIM software package [215].

with the substrate. The XRD data obtained for different reflections also indicated that the distribution of radiation defects along the ions' tracks was nonuniform. The XRD data for the (0008) reflection detected a broadening of the rocking curves after irradiation of the sample as a result of an increase in the fluence (Fig. 34). At the same time, the half-widths of the rocking curves obtained for the (0004) reflection before and after irradiation of these samples were not different from each other for all fluences used. This finding indicates that there is a low concentration of defects in the initial portion of the ion's range (at the depth of the layer ≤5 μm for the (0004) reflections) and there is a drastic increase in the concentration of defects in the end portion of the range of Bi ions (at a depth of ~25 μm for the (0008) reflection), which is consistent with the SEM data. Taking into account the nonuniform distribution of primary radiation defects over the range of the Bi ions, which was established based on the SEM and XRD data and was calculated using the TRIM software package (Fig. 34), the TEM and microcathodoluminescence measurements were preceded by consecutive thinning of the CVD layer to the thickness of 5 μm with respect to the substrate. According to the TEM data, a damaged near-surface layer with the thickness of ≤0.1 μm was formed at the surface of the epitaxial CVD SiC layer irradiated with Bi ions with the fluence of 5×10^{10} cm^{-2} (Fig. 35). The pronounced pattern of a perfect lattice with atomic planes perpendicular to the *c* direction was then observed; these atomic planes were also pronounced in the middle part of the ions' range (Fig. 35a). Accumulation of radiation defects was also detected in the CVD layer at the end of the range of the Bi ions at a distance of 3–4 μm from the boundary with the substrate (Fig. 35b). In this case, a broad band of linear defects decorated with clusters and grouped in the base planes were observed; at the same time, amorphous portions were not detected. The likely formation of clusters in the case of irradiation with heavy Xe ions was mentioned in [206], while the cluster formation at the end of the ion range was revealed by the method of positron annihilation in the case of irradiation of the CVD epitaxial *n*-6*H*-SiC layers with protons [156]. Annealing of irradiated samples at a temperature of 500°C brought about a transformation of the defect structure in the epitaxial layer. Separate linear defects coalesced in continuous planes. A fragment of the irradiated and annealed portion of the CVD layer at a distance of approximately 1 μm from the boundary with the substrate is shown in Fig. 35c. A broad band with the peak at ~2.7 eV appeared in the PL spectrum of the SiC CVD layer after irradiation with Bi ions; this band is referred to as the D_1 spectrum [165]. A broadening of the D_1 spectral band to the end of the range of Bi ions with simultaneous decrease in the signal intensity was observed in the cathodoluminescence spectra measured over the depth of the irradiated CVD layer using a oblique section. This observation indicates that various types of defects with different levels appear as a result of irradiation; some of these defects can act as centers of nonradiative recombination.

Thus, the studies of SiC irradiated with ions revealed characteristic special features of the radiation-defect formation inherent in other semiconductors irradiated with ions. Simple vacancies V_C and V_{Si} in various charge states and with annealing temperatures of approximately 150°C are formed within the starting portion of the ion range. Clusters with vacancies and divacancies annealed out at temperatures higher than 1300°C are formed at the end of the projected ion range (R_p). As in the case of irradiation with electrons and neutrons, irradiation with ions introduces similar defect-related energy levels into the SiC band gap; the number of these levels increases as the ion mass is increased. At critical radiation doses that lead to the onset of amorphization of implanted layers, the conversion of polytypes 4*H*-SiC and 6*H*-SiC to the polytype 3*C*-SiC or the formation of stacking faults are possible as a result of high-temperature annealing. The formation of the defect structure in SiC is independent of the processes related to relaxation of ionization energy losses in the tracks of high-energy ions at a level as high as 34 keV/nm and is governed by radiation defects produced as a result of elastic-scattering processes.

Heating of the target in the course of irradiation brings about a decrease in the concentration of simple defects as a result of their annealing and transformation into divacancies and defect clusters and also an increase in the critical dose of amorphization. The lowest concentration of radiation defects is generated at the sample's temperature of 400°C during irradiation.

5. IRRADIATION OF SiC DEVICES WITH HIGH-ENERGY PARTICLES

As shown above, studies of the effect of irradiation with various high-energy particles on the SiC properties were mainly concerned with gaining insight into the nature of defect formation. However, it is no less important to study the radiation defects formed under the effect of radiation on fabricated device structures, since these studies yield information about the mechanisms of failures and threshold levels of radiation that bring about variations in the characteristics and degradation of devices, and also make it possible to develop models of their behavior under irradiation.

5.1. Irradiation of Device Structures

Earlier studies concerned with gaining insight into the effect of irradiation with high-energy particles on the characteristics of SiC devices were carried out using the structures based on the Lely *n*-6*H*-SiC crystals with high concentration of both electrons ($N_d - N_a > 10^{17}$ cm^{-3}) and defects. Therefore, the results obtained using this material can be considered only in retrospect. The first studies concerned with gaining insight into the electrical characteristics of rectifiers based on the Lely 6*H*-SiC crystals that had concentrations of uncompensated donors of ~10^{18} cm^{-3} and were irradiated with fast neutrons or γ-ray photons from the ^{60}Co source showed that the mobility and concentration of charge carriers decreased compared to those in the initial material [23]. Rectifiers were irradiated with reactor neutrons with fluences as high as 10^{17} cm^{-2} and fluence rates of 5×10^9–5×10^{11} cm^{-2} s^{-1} and also with γ-ray photons with the dose of 10^{11} cm^{-2} and the dose rates of 1.5×10^{10}–1.5×10^{12} cm^{-2} s^{-1}. Appreciable changes in the forward current–voltage (*I–V*) characteristics attributed to an increase in the SiC resistivity were observed after irradiation with neutrons with fluences of 3×10^{13} cm^{-2}, while the reverse characteristics were not changed even after irradiation with the fluence of 10^{17} cm^{-2}. Irradiation of the samples with γ-ray photons in the aforementioned range of fluences did not affect the shape of the *I–V* characteristics. It was shown that annealing of irradiated samples at temperatures as high as 320°C brought about a decrease in the resistance of the irradiated structures and partial recovery of forward *I–V* characteristics. In comparison with the Si-based diodes irradiated with neutrons, it was concluded that SiC is a material with a higher radiation resistance. As a result of studying the variation in the lattice parameters and the density of hexagonal 6*H*-SiC caused by irradiation with reactor neutrons with fluences as high as ~10^{20} cm^{-2} with subsequent annealing at temperatures as high as 1200°C, it was concluded that a rapid annealing of radiation defects can be expected at a temperature of 500°C [216].

Based on these data, the diode structures formed in the 6*H*-SiC Lely crystals were studied [217] as neutron counters for measuring the distribution of high-intensity fluxes of high-energy particles in a reactor at 500°C. Diodes were irradiated with neutron fluences as

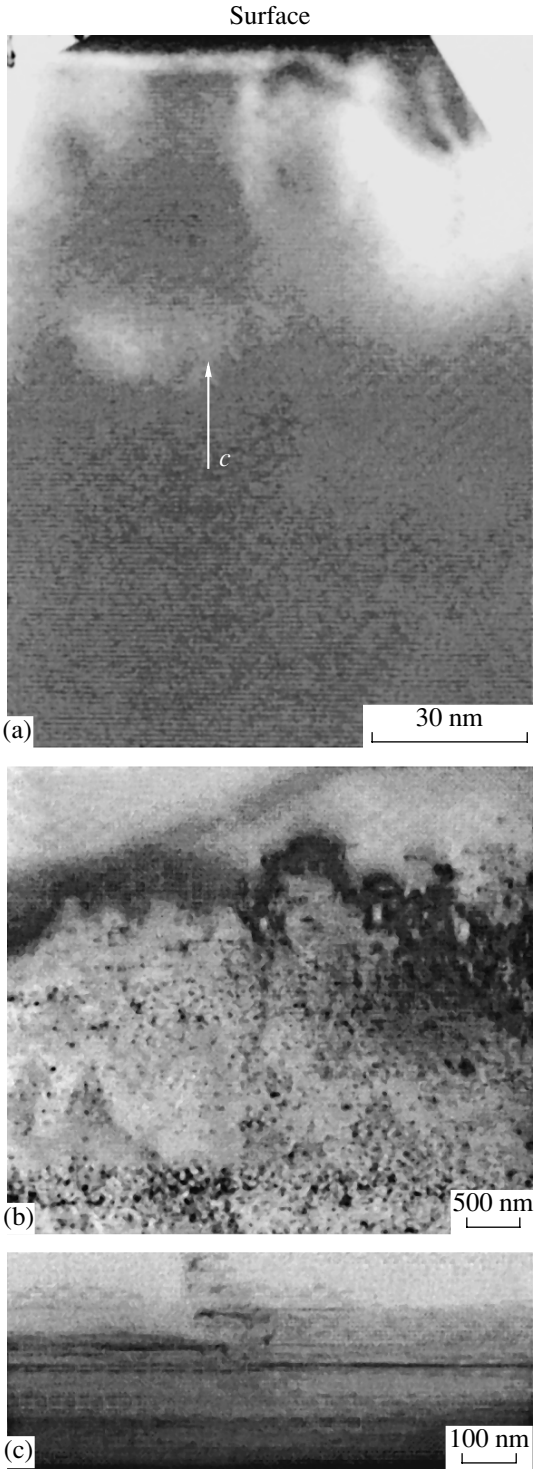

Fig. 35. TEM images of cross section of epitaxial CVD *n*-4*H*-SiC layer irradiated with Bi ions (710 MeV, 5×10^{10} cm^{-2}); the images were obtained (a) near the layer's surface, (b) at the end of the range of Bi ions, and (c) after annealing at a temperature of 500°C [215].

high 10^{17} cm^{-2} with the rate of 2×10^{12} cm^{-2} s^{-1} and were then annealed at 500°C. Variations in the *I–V* characteristics as the resistance of the structures increased were observed after irradiation with the neutron fluence of 10^{14} cm^{-2}; however, the diodes retained the rectifying properties even after irradiation with a fluence of 10^{17} cm^{-2}. These properties were partially recovered after annealing at a temperature of 500°C, which made it possible to conclude that devices based on SiC feature a high radiation resistance at elevated temperatures and can operate in severe-radiation channels of nuclear reactors.

The effect of neutron radiation on the electroluminescent characteristics of light-emitting diodes (LEDs) based on SiC was studied in the case where these diodes were irradiated at 300 K with thermal neutrons with the energy higher than 10 keV and the fluence of 10^{15} cm^{-2}. The LED *p–n* structures were formed by diffusion of Al or B into the Lely 6*H*-SiC crystals with the charge-carrier concentration of ~10^{18} cm^{-3} [218]. The LED properties were studied in the temperature range of 76–300 K after these LEDs were irradiated. It was shown that irradiation reduced the EL intensity owing to a decrease in the nonradiative lifetime of minority charge carriers. At the same time, the exposure to neutrons gave rise to radiative centers. It was believed [218] that, at low forward voltages (lower than the contact potential difference), radiation almost did not affect the processes in the space-charge region and the EL efficiency was independent of the radiation dose. These facts made it possible to conclude [218] that it is promising to use SiC-based LEDs under exposure to neutrons. Similar data on the absence of the effect of neutron radiation on the EL characteristics of the Al- and B-doped diffusion p–n–n^+ structures formed in the Lely SiC crystals were reported by Ryzhikov et al. [219]. The *I–V* characteristics of the EL diodes were studied before and after irradiation of these diodes with neutrons (at 300 K) with the energy higher than 0.1 MeV and doses of 10^{13}–10^{15} cm^{-2}. If the neutron fluences did not exceed 3×10^{13} cm^{-2}, no changes in the intensity and spectrum of EL were observed; the *I–V* characteristics also remained unchanged. An increase in the dose to 10^{14}–10^{15} cm^{-2} brought about a degradation of the *I–V* characteristic and EL, which was attributed [219] to the formation of shunts in the active region of the structures due to cluster formation and capture of holes by these clusters.

The effect of neutron radiation on the lifetimes of charge carriers was also not observed in the case where the *p–n*-6*H*-SiC epitaxial structures formed in the Lely crystals by liquid-phase epitaxy were irradiated with 1-MeV neutrons with fluences of 5×10^{13}–5×10^{14} cm^{-2} [220]. However, significant changes in the rectifying characteristics of the diodes were observed as a result of irradiation: the resistance of the samples increased and the forward *I–V* characteristics degraded. Irradiation did not appreciably affect the reverse *I–V* characteristics; a decrease in the reverse currents was observed for some of the samples. Annealing of irradiated samples at temperatures as high as 700 K brought about partial recovery of the diodes' rectifying properties. It was believed [220] that irradiation with neutrons did not affect the lifetimes of holes and reduced the leakage currents for the irradiation conditions under consideration. A decrease in the leakage currents in the *I–V* characteristics was also observed in the case where the diode 6*H*-SiC structures based on the CVD and sublimation *p–n* junctions with various concentrations of charge carriers in the base *n*-type region (4×10^{15}–4×10^{16} cm^{-3}) and the hole concentration in the *p*-type region ($N_a - N_d = 10^{19}$ cm^{-3}) [221] were irradiated with 0.9-MeV electrons (with a dose of 1.6×10^{16} cm^{-2}) and 8-MeV protons (with a fluence of 5.4×10^{15} cm^{-2}). A decrease in the leakage currents in the *I–V* characteristic as a result of irradiation was attributed [221] to healing of the shunts that were present in the initial structures owing to structural inhomogeneities.

New data were obtained in the case where diode structures with the Schottky barrier that were formed on sublimation *n*-6*H*-SiC epitaxial layers with the charge-carrier concentration of 10^{16}, 3×10^{16}, and 10^{17} cm^{-3} were irradiated with neutrons with the fluence of 4×10^{15} cm^{-2} accompanied by γ-ray radiation in a pulsed reactor [222, 223]. After irradiation, the shape of the *I–V* characteristics did not change for the structures where the doping level of the epitaxial layer was 10^{17} cm^{-3}. For the structures with $N_d - N_a = (1$–$3) \times 10^{16}$ cm^{-3}, irreversible changes in the characteristics were observed, so that diodes lost their rectifying properties. It was shown that even annealing of these degraded structures at a temperature as high as 600°C did not result in the recovery of the *I–V* characteristic. No effect of the accompanying γ-ray radiation on the *I–V* characteristic was observed. The charge-carrier concentration $\leq 8 \times 10^{16}$ cm^{-3} was considered as critical for transition to the insulator state in the case of irradiation with the neutron fluence of 4×10^{15} cm^{-2}, which is consistent with the data reported in [224], in which case the transistor structures formed in the *n*-6*H*-SiC epitaxial layers with the charge-carrier concentration of 3×10^{16} cm^{-3} were irradiated with reactor neutrons. The radiation-induced degradation of the *I–V* characteristics for the diode structures with the disappearance of rectifying properties was related [222, 223] to the introduction of radiation defects with deep levels located at $E_c - 0.35$ eV and $E_c - 0.6/0.8$ eV and with high annealing temperatures. These centers were also observed in *n*-6*H*-SiC after irradiation with reactor neutrons with the fluences of 5×10^{13}–10^{15} cm^{-2} and were found to be thermally stable at annealing temperatures as high as 1400 and 900°C, respectively [130]. It is important that the degradation of the characteristics was found to be more pronounced if the doping level of the material was lower.

This conclusion was verified by the results obtained by irradiating the diode structures formed in high-

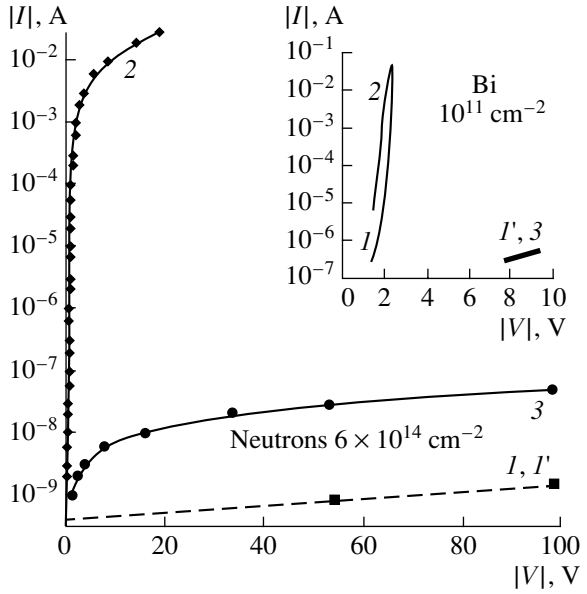

Fig. 36. The forward (*1*, *2*) and reverse (*1'*, *3*) *I–V* characteristics of p^+–*n*–n^+ structures based on 4*H*-SiC and obtained by ion implantation. The inset shows similar characteristics after irradiation with neutrons and Bi ions. Curves *1* and *1'* were measured at $T = 293$ K, while curves *2* and *3* were measured at $T = 650$ and 428 K (Bi) [226].

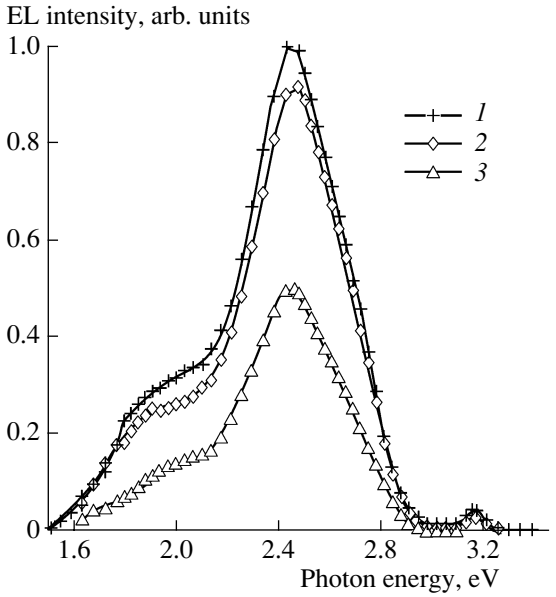

Fig. 37. Spectra of injection electroluminescence (EL) of p^+–*n*–n^+ structures based on 4*H*-SiC and obtained by ion-implantation doping with Al. Curve *1* corresponds to EL at a forward current of 100 mA before irradiation; curve *2* was measured after irradiation with γ-ray photons; and curve *3* corresponds to EL after irradiation with the fluence of 1.2×10^{14} cm^{-2} of neutrons [227].

purity *n*-4*H*-SiC CVD epitaxial layers with $N_d - N_a = (5–8) \times 10^{15}$ cm^{-3} with reactor neutrons with fluences of $(1.2–6.2) \times 10^{14}$ cm^{-2} and with accompanying γ-ray photons with the dose of $(2.3–8.6) \times 10^4$ rad [225]. The Schottky diodes and the p^+–*n* junctions ion-implantation-doped with Al formed in the CVD layers were irradiated. According to the DLTS measurements, an increase in the neutron fluence brought about an increase in the types and concentrations of the acceptor-type defects [131]. It was shown that an increase in the neutron fluence to 6.2×10^{14} cm^{-2} leads to complete degradation of the *I–V* characteristics for the diodes when the resistance of the structures became as high as ~50 GΩ. However, in contrast to the data reported in [222, 223], as a result of heating of the diode structures in the course of measurements of the *I–V* and *C–V* characteristics, the concentrations of some defects decreased or these defects completely disappeared, which brought about a partial recovery of the rectifying properties of the diodes (Fig. 36) [226]. The effect of accompanying γ-ray radiation on the *I–V* characteristics was not observed. Recovery of degraded *I–V* characteristics as a result of heating to 428 K was also observed for the above-described structures irradiated with 710-MeV Bi ions with the fluence of 10^{11} cm^{-2} (see the inset in Fig. 36) [226]. These data (in combination with the results reported in [216, 217, 220]) indicate that the radiation resistance of the devices based on SiC is high at elevated temperatures.

For p^+–*n* junctions doped with Al by ion implantation and formed in high-purity CVD layers, the effect of accompanying γ-ray radiation on the recombination parameters of the forward *I–V* characteristics and the EL intensity at 300 K [227] was not detected in the case of irradiation with neutrons [225]. However, an increase in the neutron-radiation fluence brought about an increase in the recombination current. This current increased by two orders of magnitude at the maximum fluence of 6.2×10^{14} cm^{-2}. Variations in the EL spectrum (Fig. 37) were also detected after irradiation with neutrons. As the neutron fluence was increased, the intensities of the blue defect-related EL (at the photon energy of 2.45 eV) and the edge excitonic EL (at 3.16 eV) decreased; the latter EL disappeared at the maximum fluence. These changes in the EL spectrum as a result of irradiation with neutrons were attributed [227] to a decrease in the lifetime of nonequilibrium charge carriers. An analysis of forward portions of the *I–V* characteristics showed that the estimated lifetime of nonequilibrium charge carriers decreased by two orders of magnitude as a result of irradiation with the maximum fluence of 6.2×10^{14} cm^{-2}. Heat treatment of the samples in the temperature range of 350–650°C did not recover the recombination-related *I–V* characteristics and the lifetimes of nonequilibrium charge carriers as measured after irradiation with the maximum neutron fluence. At the same time, the resistance of the structure and rectifying characteristics of the diodes were recovered [225]. An irreversible decrease in the lifetime of minority charge carriers as a result of irradiation of diode structures based on 6*H*-SiC with 8-MeV protons

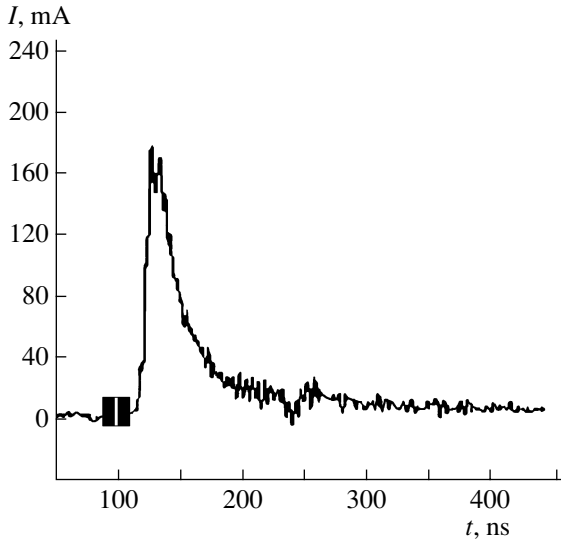

Fig. 38. The recovery time for p^+–n–n^+ structures based on 4*H*-SiC and doped with Al by ion implantation; the measurements were carried out after irradiation with high-power short (22 ns) X-ray pulses with the energy of 3×10^{10} rad/s [226].

with fluences of $(0.3–5.4) \times 10^{14}$ cm^{-2} was also reported previously [228]. The junctions were formed by sublimation epitaxy with the charge-carrier concentration of $N_d - N_a = 4 \times 10^{16}$ cm^{-3} in the base region. The lifetimes of minority charge carriers decreased by two orders of magnitude at the maximum fluence of protons. Annealing of the samples in the temperature range of 300–800 K did not affect the lifetimes, which decreased as a result of irradiation. It was concluded that it was possible to control the variation in the lifetime of nonequilibrium charge carriers in the case of irradiation with protons.

A decrease in the lifetime of nonequilibrium charge carriers was also observed in the case of irradiation of *p*–*i*–*n* diodes based on 4*H*-SiC with 400-keV He ions with the doses of $(0.1–2.0) \times 10^{14}$ cm^{-2} [229]. The diodes were formed on the basis of epitaxial *n*-4*H*-SiC 16.5-μm-thick CVD layers with $N_d - N_a = 4 \times 10^{15}$ cm^{-3} and a thin epitaxial CVD p^+-type layer with the charge-carrier concentration of 2×10^{18} cm^{-3}. The projected range of He ions was 1.15 μm; i.e., electrical characteristics varied in the base region of the diodes. It was shown that irradiation with ions under the above-mentioned conditions did not affect the reverse *I*–*V* characteristics of the diodes. In the forward direction, the resistance of the structure increased insignificantly as the radiation dose was increased, which was attributed to the introduction of radiation defects. Irradiation affected appreciably the switching characteristics of the diode. An increase in radiation dose brought about a decrease in both the recovery currents (from 3.09 to 2.18 A) and the switching time of the *p*–*i*–*n* diode (from 16.6 to 9.14 ns). The observed improvement in the characteristics of bipolar devices as a result of irradiation with He ions reduced the switching losses, which is especially important at high frequencies. Since no effect of temperature on the lifetime of nonequilibrium charge carriers was observed (this lifetime decreased as a result of irradiation), one can expect the high-frequency characteristics of SiC devices to be improved at elevated operation temperatures.

The effect of γ-ray radiation on the characteristics of SiC devices was considered in the above as accompanying the effect of irradiation with neutrons; however, some publications were concerned with irradiation with γ-ray photons separately. For example, it was shown that irradiation with γ-ray photons (from a ^{60}Co source) with the dose of 1–10 Mrad did not affect the forward *I*–*V* characteristics of *p*–*i*–*n* diodes formed on epitaxial 4*H*-SiC layers [230]. However, irradiation profoundly affected the reverse *I*–*V* characteristics of the diodes. Reverse currents increased (in comparison with the initial values in unirradiated samples) after irradiation with γ-ray photons with the dose as high as 4 Mrad.

There are also a small number of publications concerned with the effect of irradiation with X-ray photons on the characteristics of the device SiC structures. Recently, the kinetics of SiC-based diode structures (the p^+–n junctions doped with Al using ion implantation) was studied under the effect of high-power pulses of X-ray radiation in the nanosecond range with the dose rate of 3×10^{10} rad/s [226]. It was shown that the recovery time for the diode structures was ~25 ns of the duration of an X-ray pulse was 22 ns (Fig. 38). In this case, the ionization current generated as a result of irradiation was lower by an order of magnitude than that in the Si-based structures. This finding indicates that the devices based on SiC are resistant to short high-power radiation pulses.

For the devices whose structure involves the SiO_2 layers (JFETs and MOSFETs), the radiation resistance in the case of irradiation with high-energy particles is limited by radiation-induced changes at the SiC/SiO_2 interface, rather than in the SiC bulk [231–234].

5.2. Irradiation of Detectors

Detectors of nuclear particles make it possible to determine most directly and explicitly the radiation resistance of the material from which these detectors are fabricated. The detectors are most sensitive to a wide set of properties: degradation of the carriers' transport parameters and origination of their inhomogeneities, temporal stability of the value (and sign) of the volume charge of impurities, the presence of deep-level centers, and the generation rate of charge carriers with involvement of these centers.

The effect of irradiation with α particles on the lifetime of charge carriers in epitaxial CVD *n*-4*H*-SiC layers with the charge-carrier concentration of 2.2×10^{15} cm^{-3} was analyzed by measuring the detector characteristics of the Au-barrier Schottky diodes formed on

the above layers [235]. The detectors were irradiated with α particles with energies of 5.48 and 2 MeV in air from a ^{241}Am source. An analysis of the dependence of the charge-collection efficiency (CCE) on the reverse voltage applied to the diode, the efficiency of the collection of the EBIC (electron-beam-induced current) signal in relation to the electron's energy, and also the DLTS and ICTS data, made it possible to conclude that the structural defects introduced by irradiation reduced the lifetime of minority charge carriers (holes). It has recently become possible to compensate the efficiency of a decrease in the charge-carrier lifetime in the course of irradiation of detectors with α particles with the energies of 3.9 and 5.5 MeV from a ^{238}Pu source by increasing the detector operation temperature to 170°C [193]. The detectors were formed by ion-implantation doping of the *n*-4*H*-SiC CVD layers (with the charge-carrier concentration of 6×10^{14} cm^{-3}) with Al. It was shown that an increase in the temperature of detectors in the course of measurements brought about an increase in the CCE and an improvement in the energy resolution due to an increase in the diffusion length of holes L_p with the increase in temperature by a factor of 1.4 [28].

The effect of irradiation with 8.6-MeV electrons with fluences of $(0.5–9.48) \times 10^{14}$ cm^{-2} on the value of CCE for the detectors formed as Au Schottky barriers in epitaxial *n*-4*H*-SiC layers with the charge-carrier concentration of 2×10^{15} cm^{-3} was considered in [114]. Spectral detector characteristics were measured in the case of irradiation of the structures with 4.14-MeV α particles. The *C–V* characteristics of the Schottky barriers indicated that irradiation of the diodes with the maximum electron dose brought about a decrease in the concentration of uncompensated donors by a factor of 10. However, even in the case of these significant variations in the conductivity of epitaxial layers, the devices retained their detecting properties and featured 100% CCE at the reverse voltages higher than 160 V. Heating of the samples to 400 K led to partial recovery of the $N_d - N_a$ concentration in epitaxial layers.

The effect of irradiation with ions on the detector characteristics of SiC structures was considered theoretically and experimentally on the basis of the data on the ion-beam induced current (IBIC) obtained in the case of irradiation with 2-MeV protons with fluences as high as 4×10^{10} cm^{-2} of Schottky diodes formed on 4*H*-SiC epitaxial layers with the charge-carrier concentration of 5×10^{14} cm^{-3} [236]. It was experimentally established that the amplitude of the CCE signal decreased by 30% at a depth of 7 μm from the surface after irradiation of the diode structures with protons with the maximum fluence of 4×10^{10} cm^{-2}. The concentrations of radiation defects at a depth of 7 μm below the surface were at a minimum, while the diffusion lengths of charge carriers were at a maximum, according to the calculated vacancy profiles and energy losses for 2-MeV protons; these losses have a maximum at a depth of 32 μm. According to theoretical estimations, the diffusion lengths of charge carriers and the values of CCE had the smallest values at this depth.

The diode and triode structures formed in the epitaxial layers of *p*-6*H*-SiC and *p*-4*H*-SiC with the concentrations $N_a - N_d = (0.7–5) \times 10^{15}$ cm^{-3} also retained their detector characteristics after irradiation with 8-MeV protons with the fluences of $2 \times 10^{13}–2 \times 10^{14}$ cm^{-2} [160]. The detectors' characteristics were measured at the initial portion of the proton range using the 3.5-MeV α particles (the range of these particles was ~10 μm). It was shown that, even in the case of irradiation with maximum fluences of protons, the detectors were still able to perform spectrometry of α particles. It is noteworthy that, in this case, the energy resolution was ≤10% for triode structures and ~3% for diode structures.

The effect of irradiation with protons on the detector characteristics was also studied using the p^+–*n*–n^+ structures formed by ion implantation of Al into the 55-μm-thick *n*-4*H*-SiC CVD layers with the charge-carrier concentration of ~10^{14} cm^{-3} [237]. The detectors were irradiated with 8-MeV protons with a fluence of 3×10^{14} cm^{-2}. The characteristics of these detectors were tested using the 5.4-MeV [alpha] particles of natural decay (the range was ~20 μm). In the case of the above fluence of protons, the concentration of the primary radiation defects was $\sim 1.2 \times 10^{17}$ cm^{-3}, which exceeded by three orders of magnitude the initial value for uncompensated donors. The analysis of the detector characteristics made it possible to conclude that radiation defects were distributed uniformly in the bulk and that there was no accumulation of centers for the charge-carrier capture since the maximum of the vacancy profile was located in the substrate deep below the epitaxial-layer region. The introduction of the aforementioned amount of defects brought about a pronounced compensation of conductivity of the epitaxial layer, which made it possible to measure the detector characteristics in two modes of connection, i.e., in the reverse and forward directions. It was shown that an increase in the proton fluence from 10^{14} to 3×10^{14} cm^{-2} brought about a decrease in the value of CCE and the energy resolution by the factors of 1.75 and 1.5, respectively. In addition, in the case of irradiation with the fluence of 3×10^{14} cm^{-2}, the polarization voltage was observed, which indicated that the radiation defects related to the space charge were accumulated. This detrimental factor calls into question the use of an irradiated structure as a nuclear-radiation detector.

The characteristics of detectors formed as Au Schottky barriers in the *n*-4*H*-SiC layers with the charge-carrier concentration of $3 \times 10^{13}–10^{15}$ cm^{-3} were studied by Nava et al. [238] after irradiation with various high-energy particles. The detector structures were irradiated with 24-GeV protons with the fluence of 10^{14} cm^{-2}, ^{60}Co γ-ray photons with the dose as high as 40 Mrad, and 8-MeV electrons with the dose of 9.4×10^{14} cm^{-2}. The irradiated structures were tested using α particles

with the energies of 2, 4.14, and 5.48 MeV. A complete collection of ionization charge was obtained with CCE of 100% after all types of radiation. It was established that the hole lifetime decreased in the neutral region of the layer of the charge-carrier generation from the value of 300 ns for the unirradiated sample to 3 ns after all types of irradiation. The diffusion lengths L_p of the charge carriers decreased as the dose of incident particles was increased [239]. A decrease in the value of L_p as the dose of incident particles was increased was attributed to the generation of new recombination centers and to an increase in the concentration of already existing defects in the initial samples.

It is of special interest to study the characteristics of SiC detectors irradiated with high-energy particles with high fluences (~10^{16} cm^{-2}) that exceed by more than an order of magnitude those planned for the experiments at the CERN next-generation accelerators in 2007. These high fluences of protons with energies of 8 MeV (the fluence 8×10^{15} cm^{-2}) and 1000 MeV (the fluence 3×10^{14} cm^{-2}) were used to irradiate the detectors formed on the basis of p^+–n–n^+ structures and Schottky diodes in the 6*H*-SiC films with concentrations of 9×10^{16} and 5×10^{14} cm^{-3}, respectively [240, 241]. The effect of proton radiation was studied by the method of α spectrometry with the particles' energy of 5.77 MeV. It was shown that even in the case of introduction of high concentrations of radiation defects (~10^{17} cm^{-3}), which exceeded by two orders of magnitude the charge-carrier concentration in the initial samples, irradiation with protons did not lead to complete degradation of the detectors; they were still able to detect fast ions. A similar conclusion was reached in the case where the detectors in the form of Au Schottky barriers on epitaxial 4*H*-SiC layers with charge-carrier concentrations of $(4–5) \times 10^{14}$ cm^{-3} were irradiated with 24-GeV protons with the fluence of 1.4×10^{16} cm^{-2} and with 1-MeV neutrons with the fluences of 3×10^{13}–7×10^{15} cm^{-2} [242]. The initial and irradiated detectors were tested in vacuum using 5.486-MeV α particles from a ^{241}Am source or in air using β particles from a ^{90}Sr source. It was shown that, at the fluence of incident particles of 3×10^{15} cm^{-2}, the detectors' capacitance was independent of voltage since the initial material was compensated by the introduction of radiation defects. However, even when irradiated with maximum fluences, the detectors featured values of CCE of 25–30% after irradiation with protons, and 18% after irradiation with neutrons according to the results of testing of the detectors with α and β particles.

Thus, the reported data show that it is possible to recover the rectifying diodes' characteristics degraded as a result of irradiation with high-energy particles by heating the diodes to 500°C. The obtained results confirm that the devices based on SiC (in particular, detectors) have a high radiation resistance at high fluences of radiation.

6. CONCLUSIONS

One can come to the following conclusions by analyzing the above-reported results of studies concerned with irradiation of both SiC and devices based on this compound with high-energy particles.

(I) The effects of irradiation with all types of high-energy particles (from electrons to heavy (^{209}Bi) ions) introduce into SiC a wide variety of primary and secondary defects in different charge states that govern the mobilities of these defects and also the positions of the defects' energy levels in the band gap. V_C vacancies with higher mobility and complexes involving these vacancies are annealed out at lower temperatures as compared to the defects based on V_{Si} vacancies.

(II) As the mass of incident particles is increased, the number of the types of the defects, their concentrations and, especially, their sizes, increase, which brings about an increase in the temperature of both the appearance of complex defects and their annealing. An increase in the mass of incident particles reduces the threshold dose for transition to the amorphous state with simultaneous increase in the annealing temperature for the defects.

(III) An increase in both the dose of incident particles and the generation rate of radiation defects brings about an increase in the variety of defects and their sizes and concentrations until the leveling-off state is attained, which leads to the formation of tails in the density of states in the vicinity of the edges of the band gap, and to the band-gap decrease.

(IV) An increase in the energy of incident particles brings about a decrease in the concentration of introduced radiation defects and an increase in the critical radiation dose that leads to degradation of the SiC-based devices.

(V) The energy required for displacement of C atoms in SiC is lower than that for displacement of Si atoms; however, both energies decrease as the mass and dose of incident particles are increased.

(VI) The deep-level radiation defects that appear in the case of irradiation of SiC with all studied types of particles and exhibit the highest thermal stability are those with the levels E_c – 0.35/0.43 eV (the E_1/E_2 centers), E_c – 0.6/0.74 eV (the Z_1/Z_2 centers), E_c – 1.0/1.2 eV (the *R* centers), and E_c – 1.5/1.6 eV (the *EH*6/7 centers).

(VII) Heating of SiC in the course of irradiation brings about a decrease in the generation rate for radiation defects and an increase in the critical radiation dose that leads to amorphization; the most pronounced effect is observed at a temperature of 400°C.

(VIII) The effect of irradiation with high-energy particles can be used for controlled variation in the electrical parameters of SiC (transmutation, polytype transformations, and insulating layers) by analogy with other semiconductors.

(IX) High radiation resistance of SiC is verified; however, the reported results are so diverse that it is difficult to favor any particular polytype.

(X) The SiC detectors retain their detecting properties after irradiation with ultrahigh fluences of high-energy particles; heating of detectors in the course of their testing brings about an improvement in the detectors' spectrometric characteristics.

(XI) It can be stated that the optimal operation temperature of SiC-based devices is 400–500°C, in which situation an active annealing of simple defects occurs and the rate of formation of complex defects stable at high temperatures is low.

(XII) It is shown that the radiation- and time-related operation life of SiC devices can be increased under the conditions of irradiation at elevated temperatures.

ACKNOWLEDGMENTS

I thank G.N. Violina for her valuable comments during discussion of the subject of this review.

This study was supported in part by the Russian Foundation for Basic Research, the project no. 05-02-08012.

REFERENCES

1. C. Lind and D. C. Bardwell, J. Franklin Inst. **196**, 521 (1923).
2. M. S. Livingston and H. A. Bethe, Rev. Mod. Phys. **9**, 245 (1937).
3. M. Burton and G. K. Rollefson, *Photochemistry* (Prentice-Hall, New York, 1939).
4. S. S. Bhatnagar, K. G. Mathar, and K. L. Buthiraja, Z. Phys. Chem. (Leipzig) **163A**, 8 (1933).
5. A. Smits, Z. Phys. Chem. (Leipzig) **152A**, 432 (1930).
6. N. F. Mott and H. S. W. Massey, *The Theory of Atomic Collisions*, 3rd ed. (Clarendon, Oxford, 1965; Mir, Moscow, 1969).
7. E. P. Wigner, J. Appl. Phys. **17**, 857 (1946).
8. F. Seitz, Discuss. Faraday Soc. **5**, 271 (1949).
9. F. Keywell, Phys. Rev. **97**, 1611 (1955).
10. G. H. Kinchin and R. S. Pease, Prog. Phys. **18**, 1 (1955) [Usp. Fiz. Nauk **60**, 590 (1956).
11. D. E. Harrison, Phys. Rev. **102**, 1473 (1956).
12. N. Bohr, *The Penetration of Atomic Particles through Matter*, 3rd ed. (Munksgaard, Copenhagen, 1960; Inostrannaya Literatura, Moscow, 1960).
13. G. J. Dienes and G. H. Vineyard, *Radiation Effects in Solids* (Interscience, New York, 1957; Inostrannaya Literatura, Moscow, 1960).
14. V. S. Vavilov and N. A. Ukhin, *Radiation Effects in Semiconductors and Semiconductor Devices* (Atomizdat, Moscow, 1969) [in Russian].
15. *Problems in Radiation Technology of Semiconductors*, Ed. by L. S. Smirnov (Nauka, Novosibirsk, 1980) [in Russian].
16. V. S. Vavilov, B. M. Gorin, N. S. Danilin, A. E. Kiv, Yu. A. Nurov, and V. I. Shakhovtsov, *Radiation Methods in Solid-State Electronics* (Radio i Svyaz', Moscow, 1990) [in Russian].
17. V. M. Gusev, K. D. Demakov, M. G. Kasaganova, et al., Fiz. Tekh. Poluprovodn. (Leningrad) **9**, 1238 (1975) [Sov. Phys. Semicond. **9**, 820 (1975)].
18. E. V. Kalinina, N. K. Prokof'eva, A. V. Suvorov, et al., Fiz. Tekh. Poluprovodn. (Leningrad) **12**, 2305 (1978) [Sov. Phys. Semicond. **12**, 1372 (1978)].
19. G. Lindstrom, M. Moll, and E. Fretwurst, Nucl. Instrum. Methods Phys. Res. A **426**, 1 (1999).
20. *Properties of Advanced Semiconductor Materials: GaN, AlN, InN, BN, SiC, SiGe*, Ed. by M. E. Levinshtein, S. L. Rumyantsev, and M. S. Shur (Wiley, New York, 2001).
21. A. L. Barry, B. Lehman, D. Fritsch, and D. Brauning, IEEE Trans. Nucl. Sci. **38**, 1111 (1991).
22. A. A. Lebedev, A. M. Ivanov, and N. B. Strokan, Fiz. Tekh. Poluprovodn. (St. Petersburg) **38**, 129 (2004) [Semiconductors **38**, 125 (2004)].
23. L. W. Aukerman, H. C. Corton, R. K. Willardson, and V. E. Bryson, in *Silicon Carbide*, Ed. by J. R. O'Connor and J. Smiltens (Pergamon, Oxford, 1959), p. 388.
24. R. V. Babcock and H. C. Chang, *Neutron Dosimetry* (International Atomic Energy Agency, Vienna, 1963), Vol. 1, p. 613.
25. P. C. Capera, P. Malinaric, R. B. Campbell, and J. Ostroski, IEEE Trans. Nucl. Sci. **11** (6), 262 (1964).
26. G. F. Kholuyanov and B. V. Gavrilovskiĭ, Fiz. Tekh. Poluprovodn. (Leningrad) **2**, 573 (1968) [Sov. Phys. Semicond. **2**, 472 (1968)].
27. J. J. Sumakeris, M. K. Das, Seoyong Ha, et al., Mater. Sci. Forum **483–485**, 155 (2005).
28. N. B. Strokan, A. M. Ivanov, E. V. Kalinina, et al., Fiz. Tekh. Poluprovodn. (St. Petersburg) **39**, 382 (2005) [Semiconductors **39**, 364 (2005)].
29. P. A. Ivanov, M. E. Levinshteĭn, T. T. Mnatsakanov, et al., Fiz. Tekh. Poluprovodn. (St. Petersburg) **39**, 897 (2005) [Semiconductors **39**, 861 (2005)].
30. *Advances in Silicon Carbide Processing and Applications*, Ed. by S. E. Saddow and A. Agarwal (Artech House, Boston, 2005).
31. L. S. Stil'bans, *Physics of Semiconductors* (Sovetskoe Radio, Moscow, 1967), p. 167 [in Russian].
32. V. S. Balandovich and G. N. Violina, Cryst. Lattice Defects Amorphous Mater. **13**, 189 (1987).
33. J. Schneider and K. Maier, Physica B (Amsterdam) **185**, 199 (1993).
34. A. I. Girka, V. A. Kuleshin, A. D. Mokroshin, et al., Fiz. Tekh. Poluprovodn. (Leningrad) **23**, 2159 (1989) [Sov. Phys. Semicond. **23**, 1337 (1989)].
35. H. Inui, H. Mori, and H. Fujuta, Philos. Mag. B **61**, 107 (1990).
36. N. Son, E. Sörman, W. Chen, et al., Phys. Rev. B **55**, 2863 (1997).
37. H. Itoh, T. Ohshima, M. Yoshikawa, et al., Phys. Status Solidi A **162**, 173 (1997).
38. A. Kawasuso, H. Itoh, D. Cha, and S. Okada, Mater. Sci. Forum **264–268**, 611 (1998).
39. A. Kawasuso, F. Redmann, R. Krause-Rehberg, et al., J. Appl. Phys. **90**, 3377 (2001).

40. A. Kawasuso, F. Redmann, R. Krause-Rehberg, et al., Phys. Status Solidi B **223**, R8 (2001).
41. T. Staab, L. M. Torpo, M. J. Puska, and R. M. Nieminen, Mater. Sci. Forum **353–356**, 533 (2001).
42. A. Kawasuso, F. Redmann, R. Krause-Rehberg, et al., Appl. Phys. Lett. **79**, 3950 (2001).
43. G. Brauer, W. Anward, E.-M. Nicht, et al., Phys. Rev. B **54**, 2512 (1996).
44. E. Sörman, N. T. Son, W. M. Chen, et al., Phys. Rev. B **61**, 2613 (2000).
45. Mt. Wagner, N. Q. Thinh, N. T. Son, et al., Mater. Sci. Forum **389–393**, 501 (2002).
46. A. Kawasuso, M. Yoshikawa, M. Maekawa, et al., Mater. Sci. Forum **433–436**, 477 (2003).
47. C. Seitz, A. A. Rempel, A. Mageri, et al., Mater. Sci. Forum **433–436**, 289 (2003).
48. N. T. Son, P. N. Hai, Mt. Wagner, et al., Semicond. Sci. Technol. **14**, 1141 (1999).
49. V. Ya. Bratus, I. N. Makeeva, S. M. Okulov, et al., Mater. Sci. Forum **353–356**, 517 (2001).
50. D. Cha, H. Itoh, N. Morishita, et al., Mater. Sci. Forum **264–268**, 615 (1998).
51. H. Itoh, A. Yedono, T. Ohshima, et al., Appl. Phys. A: Mater. Sci. Process. **65**, 315 (1997).
52. S. Kanazawa, M. Okada, T. Nozaki, et al., Mater. Sci. Forum **389–393**, 521 (2002).
53. N. T. Son, P. N. Hai, A. Shuja, et al., Mater. Sci. Forum **338–342**, 821 (2000).
54. N. T. Son, P. N. Hai, and E. Janzén, Phys. Rev. B **63**, R201201 (2001).
55. A. Gali, B. Aradi, P. Deak, et al., Phys. Rev. Lett. **84**, 4926 (2000).
56. V. Ya. Bratus, T. T. Petrenko, H. J. von Bandeleben, et al., Appl. Surf. Sci. **184**, 229 (2001).
57. N. T. Son, P. N. Hai, and E. Janzén, Phys. Rev. Lett. **87**, 045502 (2001).
58. T. Umeda, J. Isoya, N. Morishita, et al., Phys. Rev. B **69**, R121201 (2004).
59. L. Torpo, M. Marlo, T. E. M. Staab, and R. M. Nieminen, J. Phys.: Condens. Matter **13**, 6203 (2001).
60. V. Ya. Bratus, T. T. Petrenko, S. M. Okulov, and T. L. Petrenko, Phys. Rev. B **71**, 125202 (2005).
61. Z. Zolnai, N. T. Son, B. Magnusson, et al., Mater. Sci. Forum **457–460**, 473 (2004).
62. V. S. Vaĭner and V. S. Il'in, Fiz. Tverd. Tela (Leningrad) **23**, 3659 (1981) [Sov. Phys. Solid State **23**, 2126 (1981)].
63. N. T. Son, B. Magnusson, and E. Janzén, Appl. Phys. Lett. **81**, 3945 (2002).
64. M. Bockstedte and O. Pankratov, Mater. Sci. Forum **338–342**, 949 (2000).
65. S. Dannefaer, V. Avalos, M. Syvajarvi, and R. Yakimova, Mater. Sci. Forum **433–436**, 173 (2003).
66. S. Dannefaer and D. Kerr, Diamond Relat. Mater. **13**, 157 (2004).
67. S. Dannefaer, V. Avalos, and R. Yakimova, Mater. Sci. Forum **483–485**, 481 (2005).
68. V. B. Pinheiro, T. Lingner, F. Caudepon, et al., Mater. Sci. Forum **457–460**, 517 (2004).
69. M. Boskstedle, M. Heid, A. Mattausch, and O. Pankratov, Mater. Sci. Forum **433–436**, 471 (2003).
70. Th. Lingner, S. Greulich-Weber, J.-M. Spaeth, et al., Phys. Rev. B **64**, 245212 (2001).
71. W. J. Choyke and Lyle Patrik, Phys. Rev. B **4**, 1843 (1971).
72. E. Rauls, U. Gerstmann, M. V. B. Pinheiro, et al., Mater. Sci. Forum **483–485**, 465 (2005).
73. E. Rauls, Th. Frauenheim, A. Gali, and P. Deak, Phys. Rev. B **68**, 155208 (2003).
74. L. Torpo, R. M. Nieminen, K. E. Laasonen, and S. Poykko, Appl. Phys. Lett. **74**, 221 (1999).
75. H. J. von Bandeleben, J. I. Cantin, L. Henry, and M. F. Barthe, Phys. Rev. B **62**, 10841 (2000).
76. H. J. von Bandeleben, J. I. Cantin, P. Baranov, and E. M. Mokhov, Mater. Sci. Forum **353–356**, 509 (2001).
77. X. Kerbiriou, M.-F. Barthe, S. Esnouf, et al., in *Proceedings of International Conference on Silicon Carbide and Related Materials, ICSCRM2005* (Pittsburg, USA, 2005), No. 63, p. 43.
78. H. J. von Bandeleben and J. I. Cantin, Appl. Surf. Sci. **184**, 237 (2001).
79. B. Aradi, A. Gali, P. Deak, et al., Phys. Rev. B **63**, 245202 (2001).
80. A. A. Rempel, W. Sprengel, K. Blaurock, et al., Phys. Rev. Lett. **89**, 185501 (2002).
81. M.-F. Barthe, L. Henry, S. Arpiainen, and G. Blondiaux, Mater. Sci. Forum **483–485**, 473 (2005).
82. S. Arpiainen, K. Saarinen, P. Hautojärvi, et al., Phys. Rev. B **66**, 075206 (2002).
83. J. W. Steeds, S. Furkert, J. M. Hayes, and W. Sullivan, Mater. Sci. Forum **457–460**, 561 (2004).
84. T. Egilsson, J. P. Bergman, I. G. Ivanov, et al., Phys. Rev. B **59**, 1956 (1999).
85. G. A. Evans, J. W. Steeds, L. Ley, et al., Phys. Rev. B **66**, 035204 (2002).
86. J. W. Steeds, G. A. Evans, S. Furkert, et al., Mater. Sci. Forum **433–436**, 305 (2003).
87. J. M. Perlado, L. Malerba, A. Sanchez-Rubio, and T. Diaz de la Rubia, J. Nucl. Mater. **276**, 235 (2000).
88. F. Gao, E. J. Bylaska, W. J. Weber, and L. R. Corrales, Nucl. Instrum. Methods Phys. Res. B **180**, 286 (2001).
89. A. Mattausch, M. Bockstedle, and O. Pankratov, Mater. Sci. Forum **353–356**, 323 (2001).
90. W. Sullivan, J. W. Steeds, H. J. von Bandeleben, and J.-L. Cantin, in *Proceedings of International Conference on Silicon Carbide and Related Materials, ICSCRM2005* (Pittsburg, USA, 2005), No. 66.
91. W. Windl, T. J. Lenosky, J. D. Kress, and A. F. Voter, Nucl. Instrum. Methods Phys. Res. B **141**, 61 (1998).
92. R. Devanathan and W. J. Weber, J. Nucl. Mater. **278**, 258 (2000).
93. L. Malerba and J. M. Perlado, Phys. Rev. B **65**, 045202 (2002).
94. F. Gao, W. J. Weber, and R. Devanathan, Nucl. Instrum. Methods Phys. Res. B **191**, 487 (2002).
95. *Problems in Radiation Technology of Semiconductors*, Ed. by L. S. Smirnov (Nauka, Novosibirsk, 1980), p. 256 [in Russian].

96. In-Tae Bae, M. Ishimaru, and Y. Hirotsu, Mater. Sci. Forum **389–393**, 467 (2002).
97. R. Devanathan, W. J. Weber, and F. Gao, J. Appl. Phys. **90**, 2303 (2001).
98. J. W. Steeds, F. Carosella, G. A. Evans, et al., Mater. Sci. Forum **353–356**, 381 (2001).
99. S. C. Sridhara, P. O. A. Persson, F. H. C. Carlsson, et al., Mater. Res. Soc. Symp. Proc. **640**, H6.5.1 (2001).
100. W. Sullivan and J. W. Steeds, in *Proceedings of International Conference on Silicon Carbide and Related Materials, ICSCRM2005* (Pittsburg, USA, 2005), No. 45, p. 40.
101. V. S. Ballandovich, Fiz. Tekh. Poluprovodn. (St. Petersburg) **33**, 1314 (1999) [Semiconductors **33**, 1188 (1999)].
102. T. Dalibor, G. Pensl, H. Matsunami, et al., Phys. Status Solidi A **162**, 199 (1997).
103. G. Pensl and W. J. Choyke, Physica B (Amsterdam) **185**, 264 (1993).
104. C. Hemmingsson, N. T. Son, O. Kordina, et al., J. Appl. Phys. **84**, 704 (1998).
105. C. Hemmingsson, N. T. Son, and E. Janzén, Appl. Phys. Lett. **74**, 839 (1999).
106. M. Gong, S. Fung, C. D. Beling, and Z. You, J. Appl. Phys. **85**, 7604 (1999).
107. C. Hemmingsson, N. T. Son, O. Kordina, et al., J. Appl. Phys. **81**, 6155 (1997).
108. C. G. Hemmingsson, N. T. Son, A. Ellison, et al., Phys. Rev. B **58**, R10119 (1998).
109. J. P. Doyle, M. K. Linnarsson, P. Pellegrino, et al., J. Appl. Phys. **84**, 1354 (1998).
110. A. Kawasuso, M. Weidner, F. Redmann, et al., Mater. Sci. Forum **389–393**, 489 (2002).
111. L. Storasta, A. Henry, J. P. Bergman, and E. Janzén, Mater. Sci. Forum **457–460**, 469 (2004).
112. T. A. G. Eberlein, R. Jones, and P. R. Briddon, Phys. Rev. Lett. **90**, 225502 (2003).
113. I. Pintilie, L. Pintilie, K. Irmscher, and B. Thomas, Appl. Phys. Lett. **81**, 4841 (2002).
114. A. Castaldini, A. Cavallini, L. Rigutti, and F. Nava, Appl. Phys. Lett. **85**, 3780 (2004).
115. A. Castaldini, A. Cavallini, L. Rigutti, et al., J. Appl. Phys. **98**, 053706 (2005).
116. G. Alfieri, E. V. Monakhov, B. G. Svensson, and M. K. Linnarsson, J. Appl. Phys. **98**, 043518 (2005).
117. M. Gong, S. Fung, C. D. Beling, and Z. You, J. Appl. Phys. **85**, 7120 (1999).
118. B. E. Watt, Phys. Rev. **87**, 1037 (1953).
119. *Neutron Transmutation Doping in Semiconductors*, Ed. by E. Meese (Plenum, New York, 1979).
120. V. Nagest, J. W. Farmer, R. F. Davis, and H. S. Kong, Appl. Phys. Lett. **50**, 1138 (1987).
121. L. A. de Balona and J. H. N. Loubser, J. Phys. C **3**, 2344 (1989).
122. T. Wimbauer, B. K. Meyer, A. Hofstaetter, et al., Phys. Rev. **56**, 7384 (1997).
123. A. A. Lepneva, E. N. Mokhov, V. G. Oding, and A. S. Tregubova, Fiz. Tverd. Tela (Leningrad) **33**, 2217 (1991) [Sov. Phys. Solid State **33**, 1250 (1991)].
124. S. Kanazawa, I. Kimura, M. Okada, et al., Mater. Sci. Forum **338–342**, 825 (2000).
125. Th. Lingner, S. Greulich-Weber, and J.-M. Spaeth, Phys. Rev. B **64**, 245212 (2001).
126. S. B. Orlinski, J. Schmidt, E. N. Mokhov, and P. G. Baranov, Phys. Rev. B **67**, 125207 (2003).
127. I. V. Ilyin, M. V. Muzafarova, E. N. Mokhov, et al., Physica B (Amsterdam) **340–342**, 128 (2003).
128. I. V. Ilyin, M. V. Muzafarova, E. N. Mokhov, et al., Mater. Sci. Forum **483–485**, 489 (2005).
129. Lyle Patrick and W. J. Choyke, J. Phys. Chem. Solids **34**, 565 (1973).
130. X. D. Chen, S. Fung, C. C. Ling, et al., J. Appl. Phys. **94**, 3004 (2003).
131. E. V. Kalinina, G. F. Kholuyanov, D. V. Davydov, et al., Fiz. Tekh. Poluprovodn. (St. Petersburg) **37**, 1260 (2003) [Semiconductors **37**, 1229 (2003)].
132. S. Kanazawa, M. Okada, J. Ishii, et al., Mater. Sci. Forum **389–393**, 517 (2002).
133. T. Troffer, C. Peppermuller, G. Pensl, et al., J. Appl. Phys. **80**, 3739 (1996).
134. S. Greulich-Weber, M. Freege, J.-M. Spaeth, et al., Solid State Commun. **93**, 393 (1995).
135. A. Gali, P. Deak, P. R. Briddon, and W. J. Choyke, Phys. Rev. B **61**, 12 602 (2000).
136. S. Tamura, T. Kimoto, H. Matsunami, et al., Mater. Sci. Forum **338–342**, 849 (2000).
137. F. H. C. Carlsson, L. Storasta, B. Magnusson, et al., Mater. Sci. Forum **353–356**, 555 (2001).
138. C. Seitz, A. Magerl, R. Hock, et al., Mater. Res. Soc. Symp. Proc. **640**, H6.4.1 (2001).
139. P. G. Baranov, I. V. Ilyin, E. N. Mokhov, et al., Mater. Sci. Forum **433–436**, 503 (2003).
140. L. L. Snead, S. J. Zinkle, J. C. Hay, and M. C. Osborne, Nucl. Instrum. Methods Phys. Res. B **141**, 123 (1998).
141. N. Bohr and J. Lindhard, Mat. Fys. Medd. K. Dan. Vidensk. Selsk. **28** (7), 17 (1954).
142. M. I. Markovich, É. N. Vologdin, and P. T. Barmin, in *Physical Foundations of Radiation Technology of Solid-State Electronic Devices*, Ed. by A. F. Lubchenko (Naukova Dumka, Kiev, 1978), p. 151 [in Russian].
143. V. V. Kozlovskiĭ, *Modification of Semiconductors by Proton Beams* (Nauka, St. Petersburg, 2003) [in Russian].
144. V. M. Kulakov, E. A. Ladygin, V. I. Shakhovtsov, et al., in *Effect of Penetrating Radiation on Electronic Devices*, Ed. by E. A. Ladygin (Sovetskoe Radio, Moscow, 1980), p. 34 [in Russian].
145. J. F. Zeigler, J. P. Biersack, and U. Littmamark, *The Stopping and Range of Ions in Solids* (Pergamon, Oxford, 1985).
146. H. Itoh, M. Yoshikawa, I. Nashiyama, et al., IEEE Trans. Nucl. Sci. **37**, 1732 (1990).
147. H. Itoh, M. Yoshikawa, I. Nashiyama, et al., J. Electron. Mater. **21**, 707 (1992).
148. H. J. von Bandeleben, J. L. Cantin, I. Vickridge, and G. Battistig, Phys. Rev. B **62**, 10126 (2000).
149. M. M. Anikin, A. S. Zubrilov, A. A. Lebedev, et al., Fiz. Tekh. Poluprovodn. (Leningrad) **25**, 479 (1991) [Sov. Phys. Semicond. **25**, 289 (1991)].

150. L. Storasta, F. H. C. Carisson, S. G. Shidhara, et al., Mater. Sci. Forum **353–356**, 431 (2001).
151. M. L. David, G. Alfieri, E. V. Monakhov, et al., Mater. Sci. Forum **433–436**, 371 (2003).
152. D. M. Martin, H. Kontegaard Nielsen, P. Lévêque, and A. Hallén, Appl. Phys. Lett. **84**, 1704 (2004).
153. A. Galeckas, H. Kontegaard Nielsen, J. Linnros, et al., Mater. Sci. Forum **483–485**, 327 (2005).
154. W. Puff, A. G. Balogh, and P. Mascher, Mater. Sci. Forum **338–342**, 965 (2000).
155. W. Puff, A. G. Balogh, and P. Mascher, Mater. Sci. Forum **338–342**, 969 (2000).
156. D. T. Britton, M.-F. Barthe, C. Corbel, et al., Appl. Phys. Lett. **78**, 1234 (2001).
157. M.-F. Barthe, P. Desgardin, L. Henry, et al., Mater. Sci. Forum **389–393**, 493 (2002).
158. D. V. Davydov, A. A. Lebedev, V. V. Kozlovski, et al., Physica B (Amsterdam) **308–310**, 641 (2001).
159. E. V. Bogdanova, V. V. Kozlovskiĭ, D. S. Rumyantsev, et al., Fiz. Tekh. Poluprovodn. (St. Petersburg) **38**, 1211 (2004) [Semiconductors **38**, 1176 (2004)].
160. N. B. Strokan, A. M. Ivanov, N. S. Savkina, et al., Fiz. Tekh. Poluprovodn. (St. Petersburg) **38**, 841 (2004) [Semiconductors **38**, 807 (2004)].
161. V. A. Kozlov, V. V. Kozlovskiĭ, A. N. Titkov, et al., Fiz. Tekh. Poluprovodn. (St. Petersburg) **36**, 1310 (2002) [Semiconductors **36**, 1227 (2002)].
162. A. A. Lebedev, A. I. Veĭnger, D. V. Davydov, et al., Fiz. Tekh. Poluprovodn. (St. Petersburg) **34**, 897 (2000) [Semiconductors **34**, 861 (2000)].
163. A. A. Lebedev, A. I. Veĭnger, D. V. Davydov, et al., Fiz. Tekh. Poluprovodn. (St. Petersburg) **34**, 1058 (2000) [Semiconductors **34**, 1016 (2000)].
164. N. N. Gerasimenko, in *Proceedings of 1st Moscow International Physical School of Institute of Theoretical and Experimental Physics* (Zvenigorod, 1998), p. 173.
165. L. Patrick and W. J. Choyke, Phys. Rev. B **5**, 3253 (1972).
166. A. Uedono, H. Itoh, T. Ohshima, et al., Jpn. J. Appl. Phys., Part 1 **36**, 6650 (1997).
167. H. Wirth, W. Anwand, G. Brauer, et al., Mater. Sci. Forum **264–268**, 729 (1998).
168. W. Anwand, G. Brauer, P. G. Coleman, et al., Appl. Surf. Sci. **149**, 148 (1999).
169. S. G. Sridhara, D. G. Nizhner, R. P. Devaty, et al., Mater. Sci. Forum **264–268**, 493 (1998).
170. M. Gong, C. V. Reddy, C. D. Beling, et al., Appl. Phys. Lett. **72**, 2739 (1998).
171. Y. Pasaud, W. Skorupa, and J. Stoemenos, Nucl. Instrum. Methods Phys. Res. B **120**, 181 (1996).
172. N. Chechenin, K. Bourdelle, A. Suvorov, and A. Kastilio-Vitlosh, Nucl. Instrum. Methods Phys. Res. B **65**, 341 (1992).
173. W. Jiang, W. J. Weber, S. Thevuthasan, and D. E. McCready, Nucl. Instrum. Methods Phys. Res. B **148**, 557 (1999).
174. W. Jiang, S. Thevuthasan, W. J. Weber, and R. Grötzschel, Nucl. Instrum. Methods Phys. Res. B **161–163**, 501 (2000).
175. N. Q. Khanh, Z. Zolnai, T. Lohner, et al., Nucl. Instrum. Methods Phys. Res. B **161–163**, 424 (2000).
176. A. Kawasuso, M. Weidner, F. Redmann, et al., Physica B (Amsterdam) **308–310**, 660 (2001).
177. M. Weidner, T. Frank, G. Pensl, et al., Physica B (Amsterdam) **308–310**, 633 (2001).
178. D. Åberg, A. Hallén, and B. G. Svensson, Physica B (Amsterdam) **273–274**, 672 (1999).
179. Th. Frank, G. Pensl, Song Bai, et al., Mater. Sci. Forum **338–342**, 753 (2000).
180. X. D. Chen, C. C. Ling, S. Fung, et al., Mater. Sci. Soc. Symp. Proc. **815**, J5.5.1 (2004).
181. C. C. Ling, X. D. Chen, G. Brauer, et al., J. Appl. Phys. **98**, 043508 (2005).
182. Th. Frank, M. Weidner, H. Itoh, and G. Pensl, Mater. Sci. Forum **353–356**, 439 (2001).
183. Y. Tanaka, N. Kobayashi, H. Okumura, et al., Mater. Sci. Forum **338–342**, 909 (2000).
184. A. Ruggiero, S. Libertino, M. Mauceri, et al., Mater. Sci. Forum **457–460**, 493 (2004).
185. A. Ruggiero, M. Zimbone, F. Roccaforte, et al., Mater. Sci. Forum **483–485**, 485 (2005).
186. F. Roccaforte, F. Giannazzo, C. Bongiorno, et al., Mater. Sci. Forum **483–485**, 729 (2005).
187. F. Gao, W. J. Weber, and W. Jiang, Phys. Rev. B **63**, 214106 (2001).
188. J. Slotte, K. Saarinen, M. S. Janson, et al., J. Appl. Phys. **97**, 033513 (2005).
189. A. Uedono, S. Tanigawa, T. Frank, et al., J. Appl. Phys. **87**, 4119 (2000).
190. S. Nakashima, T. Mitani, J. Senzaki, et al., J. Appl. Phys. **97**, 123507 (2005).
191. M. Bockstedle, A. Mattausch, and O. Pankratov, Mater. Sci. Forum **457–460**, 715 (2004).
192. M. Laube, F. Schmid, G. Pensl, et al., J. Appl. Phys. **92**, 549 (2002).
193. E. Kalinina, N. Strokan, A. Ivanov, et al., in *Proceedings of 6th European Conference on Silicon Carbide and Related Materials, ECSCRM2006* (Newcastle, UK, 2006).
194. M. S. Janson, J. Slotte, A. Yu. Kuznetsov, et al., J. Appl. Phys. **95**, 57 (2004).
195. M. S. Janson, A. Hallén, P. Godignon, et al., Mater. Sci. Forum **338–342**, 889 (2000).
196. W. Jiang and W. J. Weber, Phys. Rev. B **64**, 125206 (2001).
197. J. Wong-Leung, M. S. Janson, and B. G. Svensson, J. Appl. Phys. **93**, 8914 (2003).
198. F. H. C. Carlsson, S. G. Sridhara, A. Hallén, et al., Mater. Sci. Forum **433–436**, 345 (2003).
199. W. Anwand, G. Brauer, P. G. Coleman, et al., Appl. Surf. Sci. **149**, 140 (1999).
200. J. Slotte, K. Saarinen, A. Yu. Kuznetsov, and A. Hallén, Physica B (Amsterdam) **308–310**, 664 (2001).
201. Y. Zhang, W. J. Weber, W. Jiang, et al., J. Appl. Phys. **93**, 8914 (2003).
202. E. Wendler, A. Helf, and W. Wesch, Nucl. Instrum. Methods Phys. Res. B **141**, 105 (1998).
203. A. Yu. Kuznetsov, J. Wong-Leung, A. Hallén, et al., J. Appl. Phys. **94**, 7112 (2003).

204. V. A. Skuratov, A. E. Efimov, and D. L. Zagorskiĭ, Fiz. Tverd. Tela (St. Petersburg) **44**, 165 (2002) [Phys. Solid State **44**, 171 (2002)].

205. A. I. Girka, A. Yu. Dadyk, A. D. Mokrushin, et al., Sov. Tech. Phys. Lett. **15**, 24 (1989).

206. A. I. Girka, A. D. Mokrushin, E. N. Mokhov, et al., Zh. Éksp. Teor. Fiz. **97**, 578 (1990) [Sov. Phys. JETP **70**, 322 (1990)].

207. L. Liszkay, K. Havancsak, M.-F. Barthe, et al., Mater. Sci. Forum **363**, 123 (2001).

208. M. Levalois, I. Lhermitte-Sebire, P. Marie, et al., Nucl. Instrum. Methods Phys. Res. B **107**, 239 (1996).

209. I. Lhermitte-Sebire, J. L. Chermant, M. Levalois, et al., Philos. Mag. A **69**, 237 (1994).

210. K. Yasuda, M. Takeda, H. Masuda, and A. Yoshida, Phys. Status Solidi A **71**, 549 (1982).

211. D. V. Kratic, M. D. Vlajic, and R. A. Verrall, Key Eng. Mater. **122–124**, 387 (1996).

212. S. J. Zinkle, J. W. Jones, and V. A. Skuratov, Mater. Res. Soc. Symp. Proc. **650**, R3.19.1 (2001).

213. E. Kalinina, G. Kholujanov, G. Onushkin, et al., Mater. Sci. Forum **433–436**, 467 (2003).

214. E. V. Kalinina, G. F. Kholuyanov, G. A. Onushkin, et al., Fiz. Tekh. Poluprovodn. (St. Petersburg) **38**, 1223 (2004) [Semiconductors **38**, 1187 (2004)].

215. E. V. Kalinina, V. A. Skuratov, A. A. Sitnikova, et al., Fiz. Tekh. Poluprovodn. (St. Petersburg) **41**, 392 (2007) [Semiconductors **41**, 376 (2007)].

216. W. Primak, L. H. Fuchs, and P. P. Day, Phys. Rev. **103**, 1184 (1956).

217. M. Heerschap and R. de Coninck, in *Semiconductor Counters for Radiations*, Ed. by G. L. Smolyan (Gosatomizdat, Moscow, 1962), p. 238 [in Russian].

218. C. E. Barnes, Appl. Phys. Lett. **20**, 86 (1972).

219. I. V. Ryzhikov, I. L. Kasatkin, and E. F. Uvarov, Élektron. Tekh., Ser. 2: Poluprovodn. Prib., No. 4(147), 9 (1981).

220. V. V. Evstropov and A. M. Strel'chuk, Fiz. Tekh. Poluprovodn. (St. Petersburg) **30**, 92 (1996) [Semiconductors **30**, 52 (1996)].

221. A. M. Strel'chuk, V. V. Kozlovski, A. A. Lebedev, and N. Yu. Smirnova, Mater. Sci. Forum **483–485**, 1001 (2005).

222. A. V. Afanas'ev, V. A. Il'in, and A. A. Petrov, Peterb. Zh. Élektron., Nos. 3–4, 12 (2000).

223. A. Yu. Nikiforov, A. V. Afanas'ev, V. A. Il'in, et al., in *Radiation Resistance of Electronic Systems: Stability-2001* (Paims, Moscow, 2001), Vol. 4, p. 145.

224. A. Yu. Nikiforov, P. A. Ivanov, and V. V. Luchinin, in *Radiation Resistance of Electronic Systems: Stability-2002* (Paims, Moscow, 2002), Vol. 5, p. 167.

225. A. Yu. Nikiforov, E. V. Kalinina, V. V. Luchinin, et al., in *Radiation Resistance of Electronic Systems: Stability-2002* (Paims, Moscow, 2002), Vol. 5, p. 169.

226. E. Kalinina, A. Strel'chuk, A. A. Lebedev, et al., in *Proceedings of International Conference on Silicon Carbide and Related Materials, ICSCRM2005* (Pittsburg, USA, 2005).

227. A. Strel'chuk, E. Kalinina, A. O. Konstantinov, and A. Hallén, Mater. Sci. Forum **483–485**, 993 (2005).

228. A. Strel'chuk, V. V. Kozlovski, N. S. Savkina, et al., in *Proceedings of EMRS* (Strasburg, 1998).

229. Y. Tanaka, K. Kojima, K. Takao, et al., Mater. Sci. Forum **483–485**, 985 (2005).

230. M. Wolborski, M. Bakowski, and W. Klamra, Mater. Sci. Forum **457–460**, 1487 (2004).

231. J. M. McGarrity, C. J. Scozzie, J. Blackburn, and W. M. DeLancey, in *Proceedings of IEEE Nuclear Science Symposium and Medical Imaging Conference* (1995), Record 1, p. 114.

232. T. Ohshima, K. K. Lee, A. Ohi, et al., Mater. Sci. Forum **389–393**, 1093 (2002).

233. K. K. Lee, T. Ohshima, and H. Itoh, IEEE Trans. Nucl. Sci. **50**, 194 (2003).

234. J. N. Merrett, J. R. Williams, J. D. Cressler, et al., Mater. Sci. Forum **483–485**, 885 (2005).

235. F. Nava, P. Vanni, G. Verzellesi, et al., Mater. Sci. Forum **353–356**, 757 (2001).

236. A. Lo Giudice, P. Olivero, F. Fizzotti, et al., Mater. Sci. Forum **483–485**, 389 (2005).

237. A. M. Ivanov, A. A. Lebedev, and N. B. Strokan, Fiz. Tekh. Poluprovodn. (St. Petersburg) **40**, 1259 (2006) [Semiconductors **40**, 1227 (2006)].

238. F. Nava, E. Vittone, P. Vanni, et al., Nucl. Instrum. Methods Phys. Res. A **505**, 645 (2003).

239. G. Bertuccio, S. Binetti, S. Caccia, et al., Mater. Sci. Forum **483–485**, 1015 (2005).

240. N. B. Strokan, A. A. Lebedev, A. M. Ivanov, et al., Fiz. Tekh. Poluprovodn. (St. Petersburg) **34**, 1443 (2000) [Semiconductors **34**, 1386 (2000)].

241. A. M. Ivanov, N. B. Strokan, D. V. Davydov, et al., Fiz. Tekh. Poluprovodn. (St. Petersburg) **35**, 495 (2001) [Semiconductors **35**, 481 (2001)].

242. S. Sciortino, F. Hartjes, S. Lagomarsino, et al., Nucl. Instrum. Methods Phys. Res. A **552**, 138 (2005).

Translated by A. Spitsyn